The VLT/NaCo large program to probe the occurrence of exoplanets and brown dwarfs in wide orbits I. Sample definition and characterization

S. Desidera, E. Covino, S. Messina, J. Carson, J. Hagelberg, J. E. Schlieder, K. Biazzo, J. M. Alcala, G. Chauvin, Arthur Vigan, et al.

A&A 573, A126 (2015)
DOI: 10.1051/0004-6361/201323168

Astronomy & Astrophysics

The VLT/NaCo large program to probe the occurrence of exoplanets and brown dwarfs in wide orbits

I. Sample definition and characterization⋆,⋆⋆,⋆⋆⋆

S. Desidera[1], E. Covino[2], S. Messina[3], J. Carson[4,5], J. Hagelberg[6], J. E. Schlieder[5], K. Biazzo[3], J. M. Alcalá[2], G. Chauvin[7], A. Vigan[8], J. L. Beuzit[7], M. Bonavita[1], M. Bonnefoy[5], P. Delorme[7], V. D'Orazi[9,1], M. Esposito[10,2], M. Feldt[5], L. Girardi[1], R. Gratton[1], T. Henning[5], A. M. Lagrange[7], A. C. Lanzafame[3,11], R. Launhardt[5], M. Marmier[6], C. Melo[12], M. Meyer[13], D. Mouillet[7], C. Moutou[8], D. Segransan[6], S. Udry[6], and C. M. Zaidi[7]

[1] INAF – Osservatorio Astronomico di Padova, Vicolo dell'Osservatorio 5, 35122 Padova, Italy
e-mail: silvano.desidera@oapd.inaf.it
[2] INAF – Osservatorio Astronomico di Napoli, Salita Moiariello 16, 80131 Napoli, Italy
[3] INAF – Osservatorio Astrofisico di Catania, via S. Sofia 78, 95123 Catania, Italy
[4] Department of Physics & Astronomy, College of Charleston, 58 Coming St. Charleston, SC 29424, USA
[5] Max-Planck-Institut für Astronomie, Königstuhl 17, 69117 Heidelberg, Germany
[6] Geneva Observatory, University of Geneva, Chemin des Maillettes 51, 1290 Versoix, Switzerland
[7] Institut de Planétologie et d'Astrophysique de Grenoble, UJF, CNRS, 414 rue de la piscine, 38400 Saint-Martin d'Hères, France
[8] Aix-Marseille Université, CNRS, LAM (Laboratoire d'Astrophysique de Marseille) UMR 7326, 13388 Marseille, France
[9] Department of Physics and Astronomy, Faculty of Science, Macquarie University, Sydney NSW, 2109, Australia
[10] Instituto de Astrofisica de Canarias, C/ Via Lactea, s/n, 38205 La Laguna, Tenerife, Spain
[11] Universitá di Catania, Dipartimento di Fisica e Astronomia, via S. Sofia 78, 95123 Catania, Italy
[12] European Southern Observatory, Casilla 19001 Santiago 19, Chile
[13] Institute for Astronomy, ETH Zurich, Wolfgang-Pauli Strasse 27, 8093 Zurich, Switzerland

Received 2 December 2013 / Accepted 22 April 2014

ABSTRACT

Context. Young, close stars are ideal targets for searching planets using the direct imaging technique. The determination of stellar parameters is crucial for the interpretation of imaging survey results, particularly since the luminosity of substellar objects has a strong dependence on system age.
Aims. We have conducted a large program with NaCo at the VLT to search for planets and brown dwarfs in wide orbits around 86 stars. A large fraction of the targets observed with NaCo were poorly investigated in the literature. We performed a study to characterize the fundamental properties (age, distance, and mass) of the stars in our sample. To improve target age determinations, we compiled and analyzed a complete set of age diagnostics.
Methods. We measured spectroscopic parameters and age diagnostics using dedicated observations acquired with FEROS and CORALIE spectrographs at La Silla Observatory. We also made extensive use of archival spectroscopic data and the results that are available in the literature. Additionally, we exploited photometric time-series, which are available in ASAS and Super-WASP archives, to derive a rotational period for a large fraction of our program stars.
Results. We provided updated characterization of all the targets observed in the VLT NaCo Large program, a survey designed to probe the occurrence of exoplanets and brown dwarfs in wide orbits. The median distance and age of our program stars are 64 pc and 100 Myr, respectively. Nearly all the stars have masses between 0.70 and 1.50 $M_{\odot}$, with a median value of 1.01 $M_{\odot}$. The typical metallicity is close to solar with a dispersion that is smaller than that of samples usually observed in radial velocity surveys. Several stars are confirmed or proposed here to be members of close young moving groups. Eight spectroscopic binaries are identified.

Key words. stars: fundamental parameters – stars: rotation – stars: activity – stars: pre-main sequence – binaries: general – stars: kinematics and dynamics

1. Introduction

High-angular resolution deep imaging in the near-infrared maximizes the capability to detect faint circumstellar bodies amid the large brightness of the central star (Absil & Mawet 2010). The first detections of comoving companions with planetary mass were obtained using deep VLT/NaCo infrared imaging with contrasts up to 6–8 mag at >0.5 arcsec separation around very young objects, such as 2MASS J1207334−393254 (Chauvin et al. 2004) and AB Pic (Chauvin et al. 2005).

⋆ Based on observations collected at La Silla and Paranal Observatory, ESO (Chile) using FEROS, HARPS, and NaCo; with the CORALIE echelle spectrograph mounted on the 1.2 m Swiss telescope at La Silla Observatory; and on the All Sky Automated Survey (ASAS) photometric data.
⋆⋆ Tables 1–4, 6, 8 and Appendices are available in electronic form at http://www.aanda.org
⋆⋆⋆ Tables 9–12 and D.1 are only available at the CDS via anonymous ftp to cdsarc.u-strasbg.fr (130.79.128.5) or via http://cdsarc.u-strasbg.fr/viz-bin/qcat?J/A+A/573/A126

After these earliest discoveries, improvements in data acquisition and data analysis techniques (e.g. the introduction of angular differential imaging, Marois et al. 2006) allowed the detection of the first objects that were likely formed in protoplanetary disks, such as the four-planet system orbiting HR 8799 (Marois et al. 2008, 2010) and the giant planet orbiting at 8 AU from the well known star-disk system β Pic (Lagrange et al. 2010). In the last year, several additional discoveries of directly-imaged planets have been reported (Rameau et al. 2013; Kuzuhara et al. 2013; Currie et al. 2014).

Several surveys were also carried out with published detection limits for hundreds of objects (e.g., Masciadri et al. 2005; Lafrenière et al. 2007; Chauvin et al. 2010). These observations allowed a first estimate of the frequency of giant planets in wide orbits (Nielsen & Close 2010). There are exciting prospects for the detection of planets of lower masses (below 1 M_J), and of smaller semimajor axes, thanks to the availability of new instrumentation, such as SPHERE at VLT (Beuzit et al. 2010), GPI at Gemini-South (Macintosh et al. 2008), SCExAO at Subaru (Martinache & Guyon 2009), and LBTI (Hinz et al. 2008; Esposito et al. 2011).

As the luminosity of substellar objects is strongly dependent on age (Burrows et al. 1997; Baraffe et al. 2003), the determination of the mass of a detected planet, or the derivation of detection limits in terms of planetary mass, requires a careful evaluation of the stellar age. Other parameters, such as stellar mass, metallicity, distance to the system, multiplicity, and membership to associations are also required for a proper interpretation of the results in terms of both positive detections and statistics of the whole survey. Such comprehensive knowledge allows for meaningful comparisons with the outcomes of other planet-search projects using different techniques (e.g., Fischer & Valenti 2005; Mayor et al. 2011) and outcomes from planet formation models (Mordasini et al. 2009, 2012; Boss 1997; Vorobyov et al. 2013).

The determination of stellar age is a challenging task, especially for isolated field objects (Soderblom 2010). A variety of indicators can be used, such as isochrone fitting, lithium content, chromospheric and coronal emission, stellar rotation, and kinematics. The various indicators have complementary sensitivities for stars of different spectral types and different ages. Furthermore, some diagnostics like those related to rotation and magnetic activity might give spuriously young ages as in the case of tidally-locked binaries. Therefore, the best results are obtained from a complete examination of all possible indicators and by a careful and suitable combination of their results.

The NaCo Large Programme (NaCo-LP, PI. J.L. Beuzit) is a coordinated European effort, aimed at conducting an homogeneous and systematic study of the occurrence of extrasolar giant planets (EGPs) and brown dwarfs (BDs) in wide orbit (5–500 AU) around young, close stars. First epoch observations were performed in 2009–2010 and the follow-up observations for the confirmation of physical association of the candidates to their central stars were completed in March 2013. First results include the characterization of the debris disk around HD 61005 (Buenzli et al. 2010) and the study of the astrophysical false alarm represented by the white dwarf around HIP 6177, which mimics a substellar object at near-infrared (NIR) wavelengths (Zurlo et al. 2013).

The goal of this paper is to provide detailed stellar characterization of the targets of the NaCo-LP, based on high-resolution spectroscopic data acquired for this purpose, and the spectroscopic and photometric data available from public archives, complemented by information from the literature. The companion paper (Chauvin et al. 2015) presents the deep imaging observations and their results. Results from the NaCo-LP sample are merged with those of other surveys of comparable depth to produce a comprehensive statistical analysis of the occurrence of giant planets in wide orbits around FGK stars (Vigan et al., in prep.) and a complementary study of the brown dwarf population (Reggiani et al., in prep.).

The layout of this paper is the following. In Sect. 2, we introduce the target sample while we present the spectroscopic dataset and describe the data reduction procedures in Sect. 3. In Sect. 4, we present the spectroscopic analysis performed to determine radial and projected rotational velocities to measure the lithium line 6707.8 Å strength and to derive effective temperature. In Sect. 5, we present the analysis of photometric time series to derive the rotation period; in Sect. 6, we examine magnetic activity diagnostics Ca II H and K and X-ray emission. In Sect. 7, we report the presence of possible stellar companions; we analyze the kinematic parameters supporting the membership to known nearby associations in Sect. 8. We evaluate distances and metallicities of the targets and infer stellar masses and ages in Sect. 9. In Sect. 10, we summarize our results. In Appendix A, we report the compilation of data available in the literature for our targets and in Appendix B, we describe individual targets. In Appendix C, we provide our calibration of choromospheric emission for FEROS spectra; while the details of our search for rotation period on photometric time series are presented in Appendix D.

2. Sample selection

The target selection was based on an initial compilation of about one thousand young nearby stars, based on various literature sources and dedicated observations and assembled in preparation for the SPHERE GTO survey (Mouillet et al. 2010). The youth diagnostics include high lithium content, Ca II H and K line chromospheric emission, Hα emission, X-ray activity, rotation rate, and kinematics. From that list, objects that were within a distance horizon of 100 pc, were younger that 200 Myr[1], and had a magnitude limit of approximately $R < 9.5$ were selected[2]. Furthermore, known spectroscopic and close visual (separation <6 arcsec) binaries were rejected, to have a sample as free as possible from dynamical perturbations to planets in wide orbits and to avoid potential problems with the quality of adaptive optics (AO) wavefront sensing, as posed by the presence of a close stellar companion. For spectroscopic binaries, there are no technical difficulties for AO observations, as the components are not spatially resolved, but we decided, nevertheless, to focus our attention on single stars and on individual components of wide binaries. This allows us to get more statistically significant inferences and to have a sample more suited for comparison with the frequency of giant planets in wide orbits, as derived from radial velocity (RV) surveys. The study of the frequency of circumbinary planets is deferred for a separate study (Bonavita et al., in prep.).

The resulting list was cross-correlated with that of recent direct imaging surveys achieving similar sensitivities to our project. The 90 objects that were already observed with adequate depth were excluded and the final sample of the NaCo-LP is formed by about 110 targets that were never observed

[1] Three objects slightly older than 200 Myr were observed in the July 2010 run because of the lack of suitable targets in the original target list.

[2] More precisely, the sample selection is based on the expected sensitivity limits for the SPHERE adaptive optics sensor, which also depends on the color of the star.

with deep imaging instruments. Eighty-six of these originally selected 110 stars were observed at the telescope and form the sample studied in this paper (Table 9). The remaining 25 were not observed due to weather or technical losses. The previously published wide companions of the targets were also considered in our study even when they were not observed as part of NaCo-LP because of the constraints they provided on the parameters of the system (e.g., age, and distance). The pending statistical analysis on the frequency of planetary-mass objects in wide orbits will be based on the whole sample of about 200 objects, which combines targets observed by NaCo-LP and observational results from the literature (Vigan et al., in prep.).

Final values for the stellar parameters derived in this paper might lie outside of the original selection criteria due to the availability of new observational determinations, improvements in adopted calibrations, or a better understanding of the physical nature of the systems being investigated.

3. Spectroscopic data

For the spectroscopic characterization of our targets, we used data acquired with several instruments. Some of the spectra were specifically acquired by us to characterize the targets. Other spectra were accessed through the NaCo-LP collaboration and from public archives.

3.1. FEROS spectra

High-resolution spectra were collected using FEROS as part of preparatory observations for the SPHERE GTO survey. Observations were performed during several runs from November 2008 to March 2010 as part of Max Planck Institut für Astronomie (MPIA) observing time. The OBJ+SKY mode of FEROS was preferred to avoid contamination by Th-Ar lines, as we are more interested in having clean spectra for stellar characterization purposes rather than attaining the highest RV precision. Integration times were selected to obtain a signal-to-noise ratio of about 100 for stars brighter than $V \sim 9$. In addition, we exploited FEROS spectra that are available from the ESO public data archive[3]. These latter data were taken with various FEROS instrument set-ups and have a variety of signal-to-noise ratios. Altogether, we considered 77 spectra for 64 stars in this paper.

The FEROS spectra extend between 3600 Å and 9200 Å with a resolving power $R = 48\,000$ (Kaufer et al. 1999). All the data were reduced using a modified version of the FEROS-DRS pipeline (running under the ESO-MIDAS context FEROS), which yields the wavelength-calibrated, merged, and normalized spectrum. The reduction steps were the following: bias subtraction and bad-column masking; definition of the echelle orders on flat-field frames; subtraction of the background diffuse light; order extraction; order-by-order flat-fielding; determination of wavelength-dispersion solution by means of ThAr calibration-lamp exposures; order-by-order normalization; rebinning to a linear wavelength-scale with barycentric correction; and merging of the echelle orders.

We also considered FEROS spectra of our targets obtained by Torres et al. (2006), that were reduced with the instrument pipeline and kindly provided to us by the SACY team. We refrained from systematically repeating the measurement of the spectroscopic parameters, but we considered the SACY spectra for in-depth evaluation of individual cases (e.g., suspected spectroscopic binaries), as reported in Appendix B.

[3] archive.eso.org

3.2. HARPS spectra

For our investigation, we also considered the spectra obtained with HARPS at the ESO 3.6 m telescope in La Silla (Mayor et al. 2003) as part of planet search surveys by the Geneva team (Mayor et al. 2011) and the Lagrange et al. (2009) RV survey of early-type stars. We also retrieved additional HARPS spectra available in the ESO archive. Most of these come from the RV survey for planets around young stars by Guenther & Esposito (2007) with a few individual spectra from other projects. Overall, we have considered HARPS spectra for 13 objects with the number of spectra per object ranging from 1 to 77.

3.3. CORALIE spectra

Observations of 11 targets were performed with the CORALIE spectrograph at the *Euler* 1.2 m telescope in La Silla from January 2012 to August 2013 with the main goal of checking the binarity of the objects in our sample through RV determination and line profile evaluation. The spectra were reduced with the instrument on-line pipeline. Spectra of six additional stars observed as part of the CORALIE exoplanet search survey (Udry et al. 2000) were also considered in our analysis.

3.4. Other data

Two spectra of HIP 46634 (kindly provided by the SOPHIE Consortium) obtained with the SOPHIE spectrograph at the Haute Provence 1.93 m telescope were considered to derive the star's activity level. We also analyzed the CES spectra of the components of HD 16699 A and B obtained by Cutispoto et al. (1999; kindly provided by L. Pastori) to understand the origin of discrepancies between results from the literature and results from our own analysis, which turned out to be due to an exchange of binary system components (see Appendix B for details).

4. Determination of spectroscopic parameters

We exploited the FEROS, HARPS, and CORALIE spectra to measure several spectroscopic parameters that are useful for stellar characterization and age determination. Our determinations (i.e., heliocentric RV, $v \sin i$, effective temperature, lithium equivalent width, S-index, and $\log R_{\rm HK}$) are listed in Tables 1–4 for the different datasets, and the procedure to measure them are described below. The final adopted values, including literature measurements, are listed in Table 10 for RV and Table 11 for the other spectroscopic parameters.

4.1. Projected rotational velocity and radial velocity

4.1.1. FEROS

The heliocentric RV and the projected rotational velocity ($v \sin i$) were determined by cross-correlating the object spectra with low-$v \sin i$ template spectra (HD 80170, K5 III-IV, and $RV \sim 0\,{\rm km\,s^{-1}}$), as obtained with the same instrument and reduced in the same way. The normalized target spectra were preliminarily rebinned to a logarithmic wavelength scale and split into six wavelength-ranges that were free of emission lines and of telluric absorptions (see Esposito et al. 2007). A Gaussian profile was fitted to the peak of the cross-correlation function (CCF), computed in each of the six distinct spectral ranges. The resulting RV values were averaged with appropriate weights

(Schisano et al. 2009). The projected rotational velocity $v \sin i$ was derived from the full width half maximum (FWHM) of the cross-correlation peak in each of the six ranges above. The relation FWHM-$v \sin i$ was obtained by convolving the template spectra with rotational profiles of $v \sin i$ from 1 to 100 km s^{-1}. Our measurements of heliocentric RV and $v \sin i$ are listed in Table 1.

4.1.2. HARPS and CORALIE

The RV and FWHM of CCF are directly delivered by the instrument pipelines, which are based on the Weighted CCF technique (Pepe et al. 2002). For moderately fast rotators, the correlation was performed by increasing the width of the region used in the CCF fit according to the line width. For some very fast rotators ($v \sin i \sim 50$ km s^{-1}) observed with CORALIE, we simply measured the positions of a few very strong lines in the spectra to derive the RVs. For fast-rotating A and F type stars observed with HARPS, we also obtained differential RV using the SAFIR code (Galland et al. 2005), which is optimized for this kind of analysis. The transformation between FWHM and $v \sin i$ was performed as described in Santos et al. (2002). Spectroscopic parameters derived from CORALIE and HARPS spectra are listed in Tables 2–4.

4.2. Lithium equivalent width

The equivalent width (EW) measurements of the Li 6707.8 Å resonance line were obtained by a Gaussian fit, and the results are reported in Tables 1 and 4 for FEROS and HARPS spectra respectively. The listed EW does not include corrections for blends with close lines, which occur for stars with significant rotation. Typical measurement errors are of the order of ≤5 mÅ, while they are up to ∼50 mÅ for fast rotators.

4.3. T_{eff} determinations

The determinations of the spectroscopic effective temperature in Tables 1 and 4 for FEROS and HARPS spectra, respectively, were obtained through the method based on EW ratios of spectral absorption lines. These were acquired by means of the ARES[4] automatic code (Sousa et al. 2007) using the calibration for FGK dwarf stars by Sousa et al. (2010). The quoted errors are the internal ones and do not include calibration uncertainties. When multiple spectra are available, we list the mean values and the error of the mean, which are below 10 K and well below systematics. For rotational velocity above ≈20 km s^{-1}, the number of measured line-ratios drops drastically with correspondingly larger errors due to increased line blending. The temperature determinations become less reliable for $v \sin i$ larger than 30 km s^{-1} (Desidera et al. 2011). For five stars with both FEROS and HARPS spectra available, the spectroscopic temperatures resulting from the two instruments are fully consistent (mean difference $\Delta T_{\rm eff(FEROS-HARPS)} = -4$ K with an rms dispersion of 34 K). Four stars have more than ten spectra with HARPS, enabling an estimate of the intrinsic variability of effective temperature, which results in 20–50 K rms. In some cases, as shown in Fig. 1 for HIP 32235, temperature variations show significant correlations with chromospheric activity. This is due to large spots covering the stellar photosphere when the star is active. This issue is further examined in a forthcoming study (Messina et al., in prep.). Larger temperature variations (≥100 K) are expected to be present for the stars in our sample with very high levels of magnetic activity and photometric variability (see, e.g., Frasca et al. 2005).

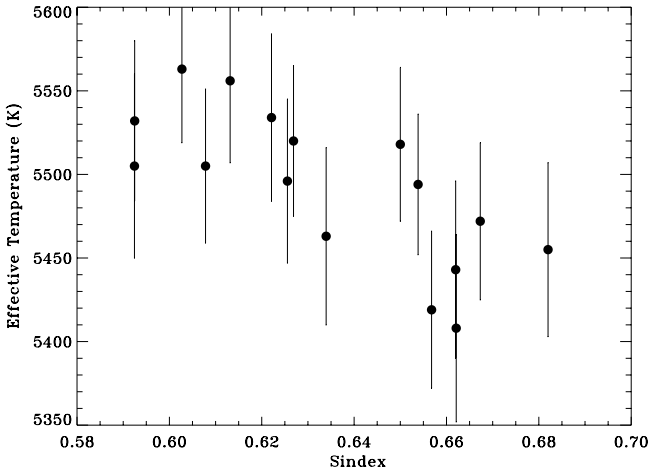

Fig. 1. Variations in effective temperature as measured by applying ARES on HARPS spectra of HIP 32235. The temperature is displayed as a function of S index chromospheric emission.

Photometric temperatures were obtained from $B-V$, $V-I$, and $V-K$ colors using the calibrations by Casagrande et al. (2010; adopting metallicity from the literature when available (see Sect. 9.2) and assuming solar metallicity otherwise). The comparison between photometric and spectroscopic temperatures (Fig. 2) shows that stars with faster rotation show larger dispersion, as expected for an increasing role of line blending. Large scatter is also observed for F-type stars. This is likely due to the moderately fast rotation of most of these stars in our sample and also due to an effective temperature, which is close to the limit of the Sousa et al. (2010) calibration or even beyond it in some cases. The available spectral types further support the photometric temperatures in these discrepant cases.

When considering only stars with $v \sin i \leq 15$ km s^{-1} and FEROS spectra (24 stars), the mean difference (photometric minus spectroscopic temperatures) is −52 K with an rms dispersion of 111 K. A systematic trend, with the spectroscopic temperature being warmer, appears to be present below 5300 K, while results for solar-type stars agree very well (mean difference −2 K with rms dispersion of 79 K for 16 stars with $v \sin i < 15$ km s^{-1} and $T_{\rm eff} > 5400$ K).

Small amounts of interstellar or circumstellar absorption might be present in some individual cases, therefore biasing the photometric temperature, but this is not a general explanation for the systematic offset observed for the coolest stars. A similar discrepancy in effective temperature for cool stars was observed by Sousa et al. (2008), when comparing their spectroscopic temperatures with those based on the infrared flux method as implemented by Casagrande et al. (2006). This was interpreted by Sousa et al. (2008) as being due to the increasing errors in the spectroscopic analysis at cooler temperatures, as the analysis is differential with respect to the Sun.

Considering the additional uncertainties that are specific to active young stars, such as photometric and spectroscopic variability, the effects of magnetic activity on the stellar atmospheric structure, and a slightly lower gravity for the youngest stars, we consider the agreement between photometric and spectroscopic temperature satisfactory. A full understanding of the

[4] http://www.astro.up.pt/~sousasag/ares/

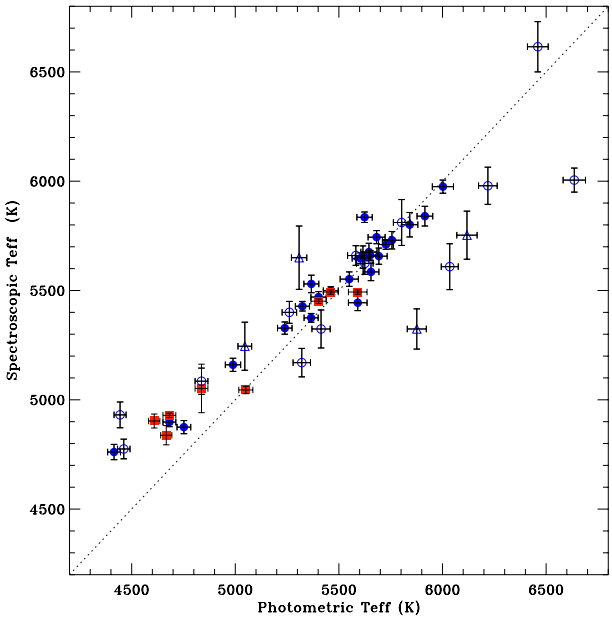

Fig. 2. Spectroscopic vs. photometric effective temperatures. Blue filled circles: stars with FEROS spectra and $v \sin i < 15$ km s^{-1}; blue empty circles: stars with FEROS spectra and $15 < v \sin i < 30$ km s^{-1}; blue empty triangles: stars with FEROS spectra and $v \sin i > 30$ km s^{-1}; red filled squares: stars with HARPS spectra.

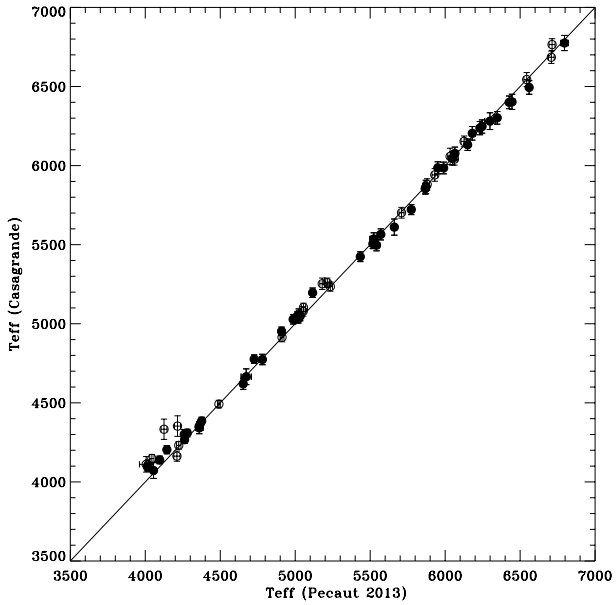

Fig. 3. Comparison between photometric effective temperatures obtained using Casagrande et al. (2010) calibration for $B - V$, $V - I$, and $V - K$ color to the effective temperatures of the 5–30 Myr stars considered in Pecaut & Mamajek (2013; their Table 9, BT-Settl models). Close visual binaries and spectroscopic binaries are plotted as open circles; single stars and components of wide binaries are filled circles.

contribution of these source of errors on spectroscopic and photometric temperatures is beyond the scope of this paper.

The temperature calibration by Casagrande et al. (2010) is mostly based on old stars. Its application to our sample should then be checked. Pecaut & Mamajek (2013) have recently developed an effective temperature scale which is optimized for 5–30 Myr old stars, and then applicable to a significant fraction of our targets. We considered the stars in their Table 9 with an effective temperature range between 4000 to 7000 K and compared to the effective temperatures derived from Casagrande et al. (2010) calibration using $B - V$, $V - I$ and $V - K$ colors. The results are shown in Fig. 3. These results show that there is no significant offset between the two temperature scales (mean difference of +3 K and median –3 K for single stars) with a scatter of 34 K with a possible trend vs temperature. We also compared the effective temperatures for Sco-Cen members from Pecaut et al. (2012) and find comparable results.

Therefore, the differences of effective temperatures from colors (at least for the combination of colors we used) are quite small. This is consistent with the difference of 40 K with respect to Casagrande et al. (2011) for six stars in common as quoted in Pecaut & Mamajek (2013). The difference is instead much larger for temperatures derived from spectral types.

There is another concern in the application of Pecaut & Mamajek (2013) relations to our sample stars: if the origin for the differences in temperature scale of main sequence and pre-main sequence stars is linked to the lower stellar gravity at the youngest age, its use should be limited to stars younger than about 30 Myr (and possibly even younger for F-G stars). If instead this is due to the effects of phenomena related to the magnetic activity, as plages and star spots (see their Sect. 5), then the calibration should be applied also to stars up to 100–120 Myr old, which have similar activity levels of β Pic and Tuc-Hor MGs members, and old tidally-locked binaries.

Henceforth, we adopt the photometric temperatures using the Casagrande et al. (2010) scale, as these are homogeneously available for all targets and are likely more accurate than the spectroscopic temperature for cool stars and objects with high $v \sin i$, as discussed above.

5. Rotational periods

5.1. Data

In the present study, we use photometric time-series data to investigate the variability of our targets and, specifically, to infer their rotational periods, brightest (least spotted) magnitudes, and levels of magnetic activity at a photospheric level.

The photometric data were retrieved mainly from three public archives: the All Sky Automated Survey (ASAS[5], Pojmanski 1997, 2002), the Wide Angle Search for Planets (SuperWASP[6], Pollacco et al. 2006; Butters et al. 2010), and the HIPPARCOS catalog[7] (Perryman et al. 1997).

5.1.1. The ASAS photometry

The ASAS project monitors all stars brighter than $V = 14$ mag at declinations $\delta < +28°$ with a typical sampling of 2 days. Since the ASAS archive contains data from 1997 to date, the time-series that it provides are particularly suitable for investigating variability over different time scales, specifically for probing the activity-induced rotational modulation. The ASAS program provides aperture photometry through five apertures. For each star in our sample, we adopted the aperture that gave the highest photometric precision (i.e., the minimum average magnitude uncertainty), which is the range 0.02–0.03 mag for target stars under analysis.

[5] www.astrouw.edu.pl/asas/
[6] www.wasp.le.ac.uk/public/
[7] vizier.u-strasbg.fr/viz-bin/VizieR?-source=I%2F239

5.1.2. The SuperWASP photometry

The public SuperWASP light curves are available for a time interval from 2004 to 2008 for both the northern and southern observatories. Although temporal and spatial coverage are irregular, SuperWASP stars at the most favorable sky declinations have observation sequences up to nine hours long with a sampling of about ten minutes, making the data more sensitive than that of ASAS for revealing periods <1 d. Our analysis is based on the processed flux measurements obtained through the application of the SYSREM algorithm (Tamuz et al. 2005). The typical photometric accuracy for the targets under study is on the order of 0.01–0.02 mag. Owing to differences with respect to the standard Johnson *V*-band ASAS photometry, we decided to analyze the SuperWASP dataset independently without merging it with ASAS data. SuperWASP observations from 2004 to 2005 were collected without a filter with the spectral transmission being defined by the optics, detector, and atmosphere. In the subsequent years, observations were collected through a wide-band filter (400–700 nm).

5.1.3. The HIPPARCOS photometry

For a limited number of targets, HIPPARCOS photometry was also available. However, owing to very irregular sampling and low photometric precision, we were able to derive rotation periods for only a handful of these stars.

5.1.4. Data from the literature

For all of our targets, we searched the literature for published period determinations. We focused on published measurements that used the same time-series as our own measurements, which includes the ASAS Catalogue of Variable Stars (ACVS), and the search for variable stars from SuperWASP (Norton et al. 2007). We also retrieved 17 rotation periods from Messina et al. (2010, 2011), and 22 rotation periods from other sources (see Appendix B). For most of the published periods, we were able to confirm the values with our own analyses. We relied solely on literature values for only HIP 46637 and HIP 71908.

5.2. Photometry rotation period search

We used the Lomb-Scargle periodogram method (Press et al. 1992; Scargle 1982; Horne & Baliunas 1986) and the Clean algorithm (Roberts et al. 1987) to search for the rotation periods. As demonstrated in Messina et al. (2010, 2011), the most accurate approach to infer the rotation period of late-type stars from the light rotational modulation is to perform the period search on the whole time-series and on associated time segments when a sufficiently long time-series is available (generally longer than one observing season). This approach not only speeds up the period detection process but also prevents other phenomena, such as the growth and decay of active regions, whose typical timescales are longer than the period of the rotational modulation from distorting period determinations.

For the present investigation, we had at our disposal the ASAS time-series up to 10 yr long and the SuperWASP time-series up to 4 yr long. We therefore segmented both datasets into sub-time-series, with each series corresponding typically to one yearly observation season. This approach was unsuitable for HIPPARCOS data, owing to low and uneven sampling; in this case, the analysis was only performed on the whole time-series.

A detailed description of the period search method is given in Messina et al. (2010). We briefly recall here that the false alarm probability (FAP) associated with the period determination is computed by using Monte Carlo bootstrap methods on 1000 simulated light curves; the FAP is the probability that a peak of a given height in the periodogram is caused simply by statistical variations, which is due to Gaussian noise. For each complete time-series and for each time segment, a corresponding FAP was computed. Only periods with FAP $\leq 1\%$ were retained for subsequent analysis. The uncertainty associated with each period was computed from the FWHM of the main power peak in the window function, following the methods of Lamm et al. (2004).

5.3. Period results

The results of our period search are summarized in Table 11, where we list the rotation period, its uncertainty, and a flag on the confidence level of the determination for each target. On a sample of 99 targets, we were able to determine the rotation period for 70 objects. Specifically, 27 periods are determined in this study for the first time, while the remaining 43 are retrieved from the literature (17 out of 43 from Messina et al. 2010, 2011). For 25 out of these 43 targets, we were able to retrieve either ASAS or SuperWASP photometry, carry out our independent analysis, and confirm the literature values. As described in Messina et al. (2011), periods derived in at least five segments or fewer than five segments with an independent confirmation from the literature, and that are consistent with $v \sin i$, are referred to as *confirmed periods* (C). Periods derived from fewer than five time segments but are consistent with $v \sin i$, and that produce mean sinusoidal fit residuals smaller than the light-curve amplitude in at least five segments, are referred to as *likely periods* (L). Periods derived from fewer than five segments that produce mean sinusoidal fit residuals that are lower than the light-curve amplitude in fewer than five segments, or with only 1–2 determinations in the literature, or that are inconsistent with $v \sin i$, are referred to as *uncertain periods* (U). We have 40 *confirmed* periods, 14 *likely* periods, 14 *uncertain*, periods, and two taken from the literature alone.

We could not determine the rotation periods for 29 out of 99 stars in our sample. Sixteen of the 29 stars with unknown periods have spectral types earlier than F8. These stars are expected to have very shallow external convection zones and, consequently, very low activity levels. Therefore, any eventual rotational modulation is unlikely to be detected by analysis of ground-based data[8]. In the case of HIP 71908 (F1Vp), a low-amplitude (~5 mmag) modulation was detected by space-based observations (Bruntt et al. 2009). The remaining 13 stars, although of late spectral type, exhibited non-periodic variability. In several cases, they are members of binary systems which are not spatially resolved in ASAS and Super-WASP images; ASAS and Super-WASP have pixel scales of 15.5 and 13.7 arcsec respectively (Pojmański 2001). Individual cases are discussed in Appendix B. A summary of the results of our period search for the individual seasons and additional details are provided in Appendix D.

[8] An exception is represented by HD 32981 (F8V). F-type stars occasionally exhibit spots sufficiently large enough to induce light modulation with amplitude of a few hundredths of a magnitude (see, e.g., García-Alvarez et al. 2011), thus enabling detection from ground-based observatories.

6. Activity diagnostics

Magnetic activity and related phenomena are known to depend on rotational period and also on stellar age for stars of spectral types from mid-F to mid-M. In this section, we consider indicators of chromospheric and coronal activity.

6.1. Ca II H and K emission

Chromospheric emission in CaII H and K lines was determined by measuring the S-index on the FEROS spectra, as described in Desidera et al. (2006). Details on the calibration of our instrumental S-index into the standard Mt. Wilson scale are provided in Appendix C. The procedures adopted for HARPS and CORALIE are described in Lovis et al. (2011) and Marmier (2012), respectively. The activity measurements obtained with the three instruments are presented in Tables 1, 2, and 4. Most of the measurements obtained with FEROS are single-epoch, while those from the CORALIE planet search and some of those from HARPS archive are multi-epoch over months or years, which then partially average the variability of the chromospheric emission on timescales of the rotation period and the activity cycle of the star. The activity measurement of HIP 46634 was obtained by the SOPHIE Consortium by following the procedures described in Boisse et al. (2010). When available, we also considered additional data from the literature (Appendix A).

6.2. X-ray emission

The target list was cross-correlated with the ROSAT all-sky survey (RASS) catalog (Voges et al. 1999, 2000), adopting a matching radius of 30 arcsec. The X-ray fluxes were derived using the calibration by Hünsch et al. (1999). For wide multiple systems that were unresolved by ROSAT (see Table 6), a suitable correction to the flux was included on the basis on the bolometric flux ratio of the components. In a couple of cases (HD 16699 A and B; HIP 72399/72400), the availability of XMM observations at higher spatial resolution enabled us to identify the main source of the X-ray emission in a binary system. For the systems HIP 35564 and HIP 25434/6, whose primaries are early-F stars, we assumed that the whole X-ray emission comes from the secondary. However, this assumption is uncertain, as both primaries are spectroscopic binaries and then the additional late-type star might contribute significantly to the integrated X-ray flux.

The hardness-ratios HR1 $= (B - A)/(B + A)$ and HR2 $= (D-C)/(D+C)$, where A, B, C and D are the integrated counts in the energy range 0.11–0.41 keV, 0.52–2.01 keV, 0.52–0.90 keV, and 0.91–2.01 keV, respectively, are plotted in Fig. 4. The two stars TYC 7743-1091-1 and TYC 6781-0415-1 are found to be hard X-ray sources with HR1 close to 1. Three stars, HIP 71933, TYC 6818-1336-1 and TYC 5736-0649-1, are moderately hard sources (HR1 $\sim$ 0.4–0.6). The hardness-ratios can be used to derive clues on stellar age, as the members of young moving groups 10–30 Myr old typically have soft X-ray emission, while hard emission is observed for classical T Tauri stars (Neuhaeuser et al. 1995; Kastner et al. 2003). Hard X-ray emission might in principle be due to interstellar or circumstellar absorption (Kastner et al. 2003), but the aforementioned hard X-ray sources are likely to exhibit emission due to flare activity (see Stelzer et al. 2000, and references therein).

For stars which are not detected by ROSAT, upper limits on X-ray luminosity were derived by considering the integration time of the nearest X-ray source in the ROSAT Faint Source Catalog.

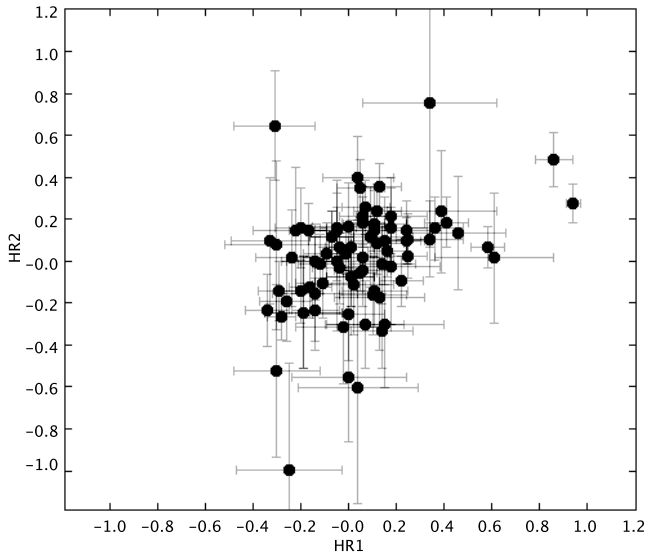

Fig. 4. Hardness-ratios diagram for the NaCo-LP targets. The two sources with HR1 closest to 1 are TYC 7743-1091-1 and TYC 6781-0415-1.

To estimate the ratio of X-ray to bolometric luminosity $R_X = \log(L_X/L_{bol})$, we derived the luminosities of the targets using the apparent V magnitude, the bolometric correction from Flower (1996) and the distances derived in Sect. 9.1. We converted the bolometric magnitude, defined as $M_{bol} = V + BC_V + 5\log\pi + 5$ to $L/L_\odot$ by using $M_{bol\odot} = 4.73$, as recommended by Torres (2010). The interstellar extinction was assumed to be negligible since all targets are relatively nearby, except for a few individual cases where evidence of modest reddening existed (see Sect. 9.1 and Appendix B). X-ray luminosities and $\log(L_X/L_{bol})$ are listed in Table 11.

6.3. Correlations of activity indicators and rotation

Coronal and chromospheric emissions are in general expected to show correlation with the rotation period, as their origin is tied to the rotation itself (see, e.g., Pizzolato et al. 2003). On the other hand, at very fast rotational velocities and activity levels, correlations are no longer observed, as the star enters the so-called "saturated regime". To evaluate the status of our targets and also to check for peculiar discrepant cases that might distort the observed quantities (e.g., aliases of the true rotation period), we evaluate here the correlation between activity and rotation. Figure 5 shows the correlation between $\log R_{HK}$ vs. $\log L_X/L_{bol}$ for the stars in our sample. A similar slope is observed for the whole range of emission levels.

Figure 6 shows the Rossby number (used here to take the dependence of the rotation period on color into account, Noyes et al. 1984) vs. $\log R_{HK}$ and $\log L_X/L_{bol}$. The change in slope due to the saturation effects is clearly seen in the $\log L_X/L_{bol}$ plot.

We also compared the measured rotation period with the expected one based on the Ca II H and K and X-ray coronal emission and calibrations by Mamajek & Hillenbrand (2008). In the first case (Fig. 7; upper panel), the correlation between the predicted and observed rotation period is low for stars with fast rotation. This effect was also noted by Mamajek & Hillenbrand (2008), who propose that this may be explained by 1) a larger intrinsic variability compared to stars with slower rotation rates; 2) a sparseness of activity measurements; and 3) a spread in convective turnover times due to a mixing of main sequence and

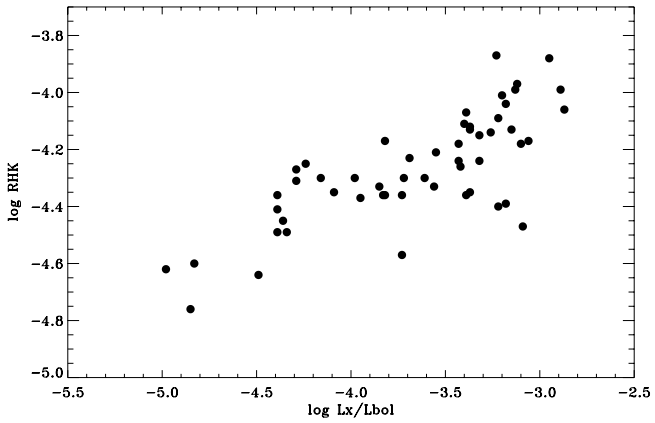

Fig. 5. $\log R_{\rm HK}$ vs. $\log L_{\rm X}/L_{\rm bol}$ for the stars in our sample.

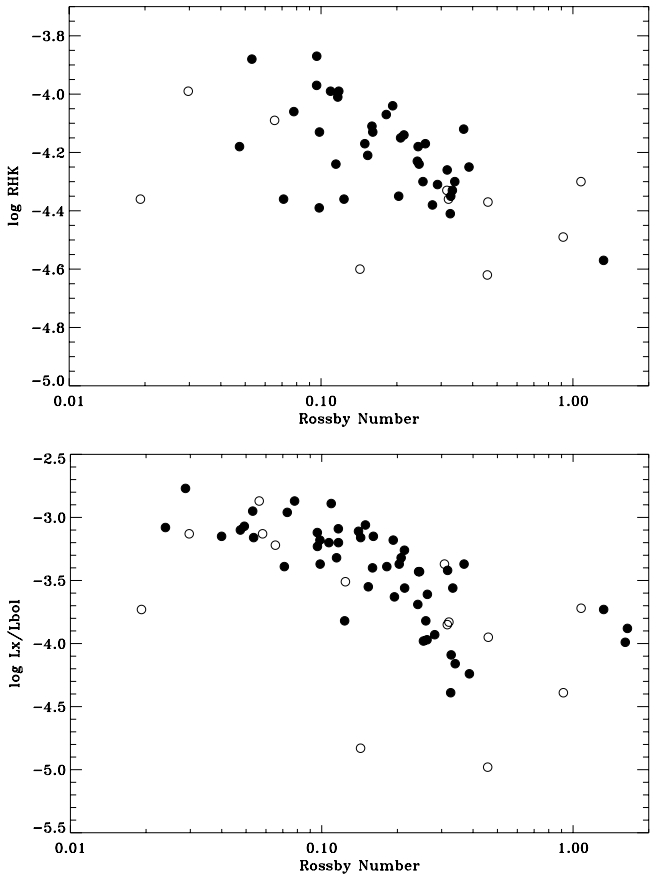

Fig. 6. $\log R_{\rm HK}$ and $\log L_{\rm X}/L_{\rm bol}$ (upper and lower panels respectively) vs. Rossby number for the stars in our sample. Filled circles represent stars with *confirmed* or *likely* rotation period. Empty circles represent stars with an *uncertain* rotation period.

pre-main sequence stars. One should also consider that a proper calibration of the S index into the standard Mt. Wilson scale is challenging at high activity levels due to the paucity of suitable calibrators and the presence of intrinsic variability of the chromospheric emission. Therefore, mixing results from independent sources (as done here) might result in an increased scatter. Furthermore, for projected rotational velocities larger than about 40 km s^{-1}, the emission of the Ca II H and K cores is spread out beyond the ∼1 Å window typically used for the measurement of the S-Index (Desidera et al. 2006). X-ray derived periods (Fig. 7; lower panel) can be derived only for stars outside the saturated

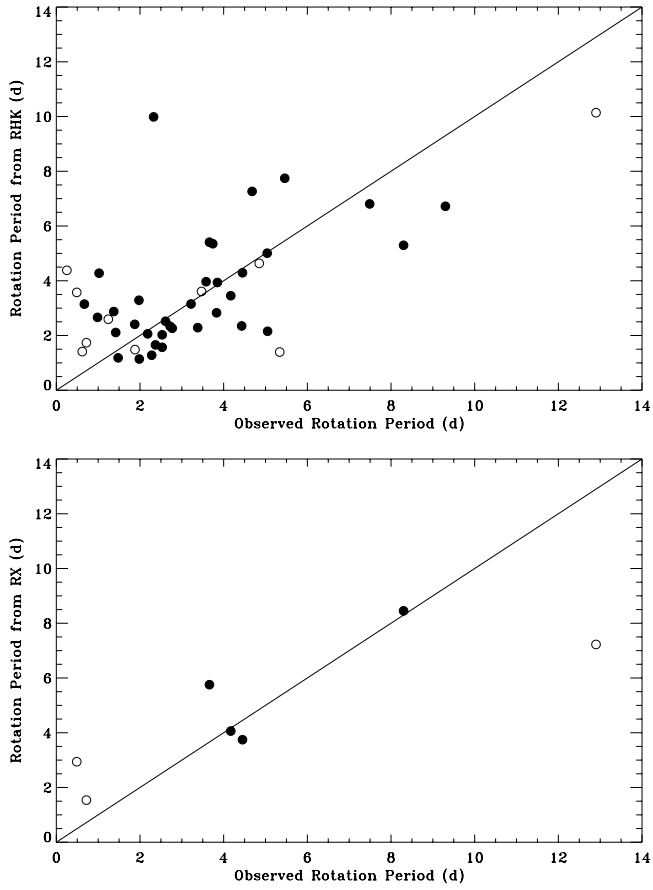

Fig. 7. Observed rotation period vs. the expected rotation period from the value of $\log R_{\rm HK}$ (*upper panel*) and $R_{\rm X}$ (*lower panel*), as derived by using the Mamajek & Hillenbrand (2008) calibrations. Filled circles represent stars with *confirmed* or *lilely* rotation period. Empty circles represent stars with *uncertain* rotation period. The outlier in the upper panel is represented by HIP 79958. As the measured rotation period appears to be robust, the discrepancy may be due to poor sampling of H and K variability or due to calibration issues resulting from the low temperature of the star. See Appendix B for further details.

regime (Mamajek & Hillenbrand 2008). The plot shows the expected correlation for unsaturated stars.

6.4. Ultraviolet flux

Ultraviolet NUV and FUV magnitudes from the GALEX satellite (Martin et al. 2005) were checked to identify or confirm WD companions (see Zurlo et al. 2013, for the case of HIP 6177) and to indirectly evaluate the level of magnetic activity when direct measurements were not available. The GALEX magnitudes were available for 34 objects in our sample. With the exception of HIP 6177, we did not identify additional objects with peculiar FUV and NUV fluxes.

7. Multiplicity, close companions, and discs

We summarize here the evidence for additional stellar companions at either wide or close separations. A complete census of stellar multiplicity is important for several reasons. For instance, the presence of a close companion can bias the derivation of stellar parameters, as is the case for photometric distance. A wide companion may also be used to provide additional diagnostics to constrain the properties of the target. More generally, knowledge

Table 5. Close visual binaries discovered or confirmed by NaCo-LP AO observations.

Target	Sep (mas)	Sep (AU)	ΔH (mag)
TYC 0603-0461-1	74 ± 14	4.3	0.1 ± 0.2
HIP 6177	1566 ± 6	52.6	7.1 ± 0.2
HIP 8038	437 ± 7	12.8	2.5 ± 0.2
TYC 8484-1507-1	60 ± 14	3.6	0.2 ± 0.2
TYC 9181-0466-1	1891 ± 7	146.9	1.5 ± 0.2
TYC 8927-3620-1	87 ± 14	7.1	0.5 ± 0.2
TYC 9231-1566-1	1975 ± 7	193.6	3.0 ± 0.2
TYC 8989-0583-1	2584 ± 8	169.0	2.6 ± 0.2
TYC 9010-1272-1	262 ± 8	24.0	1.0 ± 0.2
TYC 7835-2569-1	901 ± 7	63.3	0.1 ± 0.2
TYC 6786-0811-1	120 ± 10	9.4	0.3 ± 0.2
HIP 80290	3340 ± 2	278.2	1.9 ± 0.2
HIP 94235	506 ± 7	31.0	3.8 ± 0.3
HD 199058	471 ± 7	31.1	2.5 ± 0.2
HIP 107684	326 ± 7	29.4	2.8 ± 0.3
HIP 108422	170 ± 7	9.9	3.0 ± 0.2

Notes. We list the name of the star, the projected separation measured with NaCo (from the companion paper Chauvin et al. 2015) in mas and in AU and the magnitude difference in H band.

of target environment is important for the proper interpretation of the astrophysical results of our NaCo imaging program and for comparisons with other surveys. Beside stellar multiplicity, the presence of disks is also relevant in this context. There are four stars with resolved debris disks in our sample: HIP 11360, HD 61005, HIP 76829, and HIP 99273. They are discussed in Appendix B.

7.1. Visual binaries

Several new close binaries were discovered as part of the NaCo-LP. The details of their discovery are reported in the companion paper presenting the direct imaging results (Chauvin et al. 2015). We summarize here their properties, as the binarity has to be considered to correct photometric distances and temperatures; binarity is also relevant for a proper interpretation of the age indicators. Three close binaries were previously known: HIP 108422 (Chauvin et al. 2003, physical association confirmed by our NaCo observations), TYC 7835-2569-1 (Brandner et al. 1996), and TYC 6786-0811-1 (Köhler et al. 2000). Three of the newly discovered companions are proposed members of the AB Dor moving group (MG) and one belongs to the ϵ Cha group. These discoveries contribute to the census of stellar multiplicity at young ages in loose associations (Duchêne & Kraus 2013).

Several targets have wide companions (defined here as those with projected separation larger than 6 arcsec) whose presence and association either were already established in the literature or are proposed here. They are listed in Table 6. These wide companions are outside NaCo's field of view, so they did not impact target selection. To estimate the reliability of these wide pairs as true bound systems, we followed the methods of Lépine & Bongiorno (2007) to calculate the separation, projected separation (assuming identical distance as the brighter companion), and proper motion difference for all candidate wide binaries. We used relations in Dupuy & Liu (2012) and Lépine & Bongiorno (2007) to place statistical constraints on the likelihood that binary pairs are real and physically bound. From the fractional proper motion difference of the components, $fr_\mu = \Delta_\mu / avg_\mu$, where Δ_μ is the proper motion difference and avg_μ is the average proper motion of the components, Dupuy & Liu (2012) show that a $fr_\mu \leq 0.2$ indicates that the pair is likely physically bound. We also used the statistic Δ_X from Lépine & Bongiorno (2007), which uses a power law to describe the relationship between separation, Δ_μ, and avg_μ. If $\Delta_X < 1.0$, the pair is likely bound. This statistic is calibrated only for stars with 150 mas/yr $< \mu <$ 450 mas/yr. Thus, it could be less useful for stars with smaller proper motion where the relationship may not follow a power law.

The analysis shows that most of the wide pairs in Table 6 are likely bound. Measured parameters such as age, distance, and moving group membership can therefore be shared between the components. All stars for which $\Delta_X > 1.0$ are stars that have $avg_\mu < 150$ mas/yr, implying that this statistic is less useful. For these stars, the fr_μ is probably a better indication of a physically bound nature, although it is not as strong a constraint as Δ_X. Finally, we note that several of the proposed binaries are actually hierarchical multiples, as revealed by imaging of tight visual companions and observed RV variations (see Appendix B).

7.2. Spectroscopic and astrometric binaries

We summarize the presence of spectroscopic binarity among our targets in Table 7 by considering both RV variability and the presence of multiple components in the spectra (SB2). Two critical issues prevent firm conclusions in some specific cases. 1) For single-epoch spectra, line-profile analysis of young, active stars often reveals deformation due to star spots crossing the stellar disk. It is difficult to distinguish between such effects and the presence of a companion. 2) The evaluation of the significance of the proposed RV variations depends on the adopted error bars, which are often not available in the literature data. Furthermore, there are cases where significant RV variations of amplitudes up to a few km s^{-1}, can be caused by stellar or circumstellar phenomena, such as variable obscuration from a circumstellar disk (see, e.g., Schisano et al. 2009, for the case of T Cha) or stellar oscillations in the case of early-type stars. A couple of suspected astrometric binaries is also included in Table 7.

8. Kinematics and membership to nearby associations

8.1. Kinematic parameters and space velocities

Proper motions were taken from Tycho2 (Høg et al. 2000) and van Leeuwen (2007) when available. For HIP 46634/7 and HIP 58240/1, we adopted instead the original HIPPARCOS values Perryman et al. (1997; see Sect. 9.1). For HIP 25434/6, we adopted the long term proper motion from Tycho2 as there are indications that the HIPPARCOS astrometry is biased by the presence of an additional component (see Appendix B). Absolute RVs were derived from our own spectra and extensive literature compilation (see Table 10). A minimum error bar of 0.5 km s^{-1} was adopted to take the uncertainties in the absolute RV and the uncertainties in the zero-point systematics between different instruments into account. The determination of distances is discussed in Sect. 9.1.

The space positions, space velocities, and their uncertainties were derived using relations from Johnson & Soderblom (1987). In these calculations, we have used the J2000 transformation matrix, which have been taken from the introduction of the HIPPARCOS catalog, to convert to Galactic coordinates.

Table 7. Spectroscopic and astrometric binaries in the NaCo-LP sample.

Target	Remarks
confirmed SB	
TYC 5839-0596-1	SB2
HIP 3924	SB2
HIP 72399	SB1
TYC 7835-2569-1	SB2 + close VIS
HIP 35564	SB1
HIP 36414	SB1
TYC 7188-575-1	SB1
TYC 5206-0915-1	SB1
suspected SB	
TYC 7796-2110-1	SB2?
TYC 9010-1272-1	SB2? + close VIS
TYC 8128-1946-1	RV Var ?
HIP 71933	RV var ?; astr. acceleration
TYC 6815-0874-1	SB2 ?
HIP 13008	astrom. acceleration
TYC 9245-0617-1	RV var

Notes. See notes in Appendix B for further details.

8.2. Membership to nearby associations

Table 8 presents the list of moving groups, associations, and solar-neighborhood open clusters considered in our kinematic analysis. Adopted parameters are described for each group. If the uncertainties in the U, V, and W space velocities of the associations were quoted in the literature, we included those in the analysis. If no uncertainties were quoted, we used a conservative uncertainty estimate of ± 1 km s^{-1} for moving groups and ± 2 km s^{-1} for open clusters. We considered the young, nearby population to be represented by stars within the U, V, and W boundaries defined by Zuckerman & Song (2004), which are also shown in Fig. 10. Zuckerman & Song (2004) noted that the majority of solar-neighborhood stars within ~60 pc that are younger than 50 Myr have kinematic parameters within these boundaries. However, it should be considered that old stars in the same kinematic space outnumber true young stars. Therefore, independent indicators of youth are required for a firm inference on stellar age. HIP 71908 is an example of a moderately old star with kinematics similar to those of young stars (see Appendix B). The adopted ages are presented in Sect. 8.3.

We then calculated the significance in the difference (Sig D) among U, V, and W galactic velocities, which are calculated for each NaCo-LP target and each association in the above list. As an example, the Sig D for the U velocity is defined as

$$\mathrm{SigD}_U = \frac{(U_{\mathrm{star}} - U_{\mathrm{group}})}{\sqrt{(\mathrm{d}U_{\mathrm{star}})^2 + (\mathrm{d}U_{\mathrm{group}})^2}}. \quad (1)$$

The SigD value represents how many sigma that separates the space velocity of the target from that of the group being considered. In our analyses of NaCo-LP targets, we considered U, V, and W space velocities to be consistent with membership if it had a SigD ≤ 2.0 in each of the U, V, and W velocities. This is only one indication that a star may belong to a given association, but it serves as a first step in the process to define bona fide membership. We further checked the moving group membership by calculating Bayesian membership probabilities using the online tools BANYAN I and II (Malo et al. 2013; Gagné et al. 2014). The online versions of these tools use only the available kinematics for this star as input and do not consider the star's age (e.g. CMD position). We used all available kinematic information for each star as input (coordinates, our adopted proper motions, radial velocities, and distances). In several cases, the two versions of BANYAN yielded highly discrepant results. This is likely caused by changes to the prior, the *UVWXYX* distributions, and the definition of the Galactic field between the first and second iterations of BANYAN (Gagné et al. 2014). A detailed comparison of the differences between the two tools is beyond the scope of this paper. We indicate the targets where discrepancies arise along with further details regarding target ages and group membership in Appendix B.

In most cases, we confirm the membership assignments by Torres et al. (2008) and Malo et al. (2013), and we identify some possible additional members. Discrepancies for individual cases are mostly due to differences in the kinematic data (e.g., RV in the case of HIP 11360). Different membership criteria adopted in the various studies also play a role. A large number of the NaCo-LP targets are found to be kinematically consistent with the young, nearby population.

8.3. Absolute ages of nearby moving groups

Our age determination is mostly based on comparison of indirect indicators as measured for individual NACO-LP targets to those of members of groups and clusters, such as β Pic, Tucana, Columba, Carina, AB Dor, Pleiades, and Hyades. While the age ranking of these groups is mostly defined, the absolute values of their ages is widely debated in the literature. A full assesment of the issue of the absolute ages is beyond the scope of this paper but we present the motivation of our adopted ages for the youngest groups for which members are found within the NACO-LP sample. For some of the groups considered below (β Pic, IC 2391, Pleiades) we anticipate that there is a systematic discrepancy between ages obtained using the lithium depletion boundary of low-mass stars with respect to isochrone fitting with the first method yielding older ages. This trend is common to several other open clusters (e.g., Dobbie et al. 2010).

8.3.1. β Pic, ϵ Cha, and Sco-Cen groups

The most widely adopted age for the β Pic is 12 Myr, based on the isochrone fitting by Zuckerman et al. (2001; 12^{+8}_{-4} Myr) and the kinematic traceback analysis by Ortega et al. (2002) and Song et al. (2003). Torres et al. (2008) adopted instead 10 Myr. Very recently, a significantly older age (21 ± 4 Myr) has been derived by Binks & Jeffries (2014) using the lithium depletion boundary of low-mass stars. An age around 20 Myr is only marginally compatible with the isochrone fitting results by Zuckerman et al. (2001).

The kinematic traceback age nominally have a small error bar (about 1 Myr) but is based on the list of members known in 2002–2004. The current enlarged list of members and the improvement in the kinematic parameters, due to the release of the revised HIPPARCOS parallaxes by van Leeuwen (2007), additional RV data, and more complete census of multiplicity, indicate the need of updating the analysis. The study by Mamajek et al. (in prep., preliminary results presented in Soderblom et al. 2013) claims that the group was not smaller in the past, ruling out a 12 Myr age at >3 sigma.

An older age for β Pic would allow us to reconcile the result by Song et al. (2012) that stars in LCC and UCL are slightly

younger than those of β Pic MG (from the comparison of lithium EW as a function of color) to the absolute ages of UCL and LCC of 16 and 17 Myr respectively, which are derived using an isochrone fitting, which includes the recent work by Pecaut et al. (2012).

Performing an isochrone fitting to β Pic MG members with a trigonometric parallax, adopting the photometric temperatures as in Sect. 4.3, and using Bressan et al. (2012) models as described in Sect. 9.3 yields an age of 16 ± 2 Myr (internal error only) midway between the original 12 Myr estimate and the recent estimate based on lithium depletion boundary. To check the reliability of our result, we considered the F-type stars in the Sco-Cen region that were recently studied by Song et al. (2012) and we got very similar results, with our ages being older by about 1 Myr.

Considering the uncertianties related to the various techniques, we adopt 16±6 Myr as our age for the β Pic MG. This estimate has the additional advantage of being homogeneous with the age determination from isochone fitting performed for our program stars in Sect. 9.3. For the Sco-Cen subgroups, the ages by Pecaut et al. (2012) were adopted with lower limits at the ages proposed by Song et al. (2012) for UCL and LCC and by Preibisch et al. (2002) and Preibisch & Mamajek (2008) for US.

In our sample, there are also two members of the ϵ Cha group. Torres et al. (2008) adopt an age of 6 Myr. As we adopt older ages for young groups, such as β Pic MG and Upper Scorpius, an upward revision of the age of this group is also possible. The analysis by da Silva et al. (2009) based on lithium shows that ϵ Cha is younger than TW Hya, which is younger than β Pic MG. Therefore, we adopt 10 Myr as the age for the ϵ Cha group, allowing for the younger age proposed by Torres et al. (2008) as lower limit.

8.3.2. Tucana, Columba, Carina, and Argus

The most widely adopted age for Tucana, Columba, and Carina is 30 Myr (Zuckerman & Song 2004; Torres et al. 2008). Argus and IC 2391 open cluster are considered to be slightly older (35–40 Myr). The absolute age of the IC 2391 open cluster was estimated to be 40 Myr by using a isochrone fitting (Platais et al. 2007) and 50 Myr using the lithium depletion boundary (Barrado y Navascués et al. 2004). The very recent determination of the lithium depletion boundary for Tucana from Kraus et al. (2014) yields an age of about 40 Myr. Our isochrone fitting yields an age of 35 Myr for the members of these latter groups, which are compatible with the previously adopted age.

Considering that Tucana, Columba, and Carina appear to be younger than Argus based on Li EW vs. effective temperature graph and Li depletion boundary (da Silva et al. 2009; Kraus et al. 2014) and the absolute age determination of IC 2391 appears sound within 10 Myr, there are only limited margins for any upward revision of age of these groups with respect to the values adopted in Torres et al. (2008). Additional evidence for a young age of the Columba association comes from the interferometric measurements of the proposed member HR 8799 (Zuckerman et al. 2011), where the radius of the star is consistent with an age ~30 Myr (Baines et al. 2012)[9]. Dynamical stability studies of the planetary system that orbits HR 8799 provide additional indirect evidence for a young system age. An older stellar age implied larger planet masses that would lead to a dynamically unstable system (Currie et al. 2011; Sudol & Haghighipour 2012; Esposito et al. 2013).

[9] See Hinz et al. (2010) for a different view on Columbs membership.

Therefore, we adopt a value of 30 Myr for Tucana, Columba, and Carina and 45 Myr for Argus (the mean between isochrone and lithium depletion boundary ages).

8.3.3. AB Dor moving group

The age of AB Dor MG is highly debated in the literature, ranging from 50 Myr in the first paper that presented the association (Zuckerman et al. 2004) to about 150 Myr. Janson et al. (2007) found an age of 50–100 Myr for the AB Dor quadruple system, while Guirado et al. (2011) favor an age of 40–50 Myr from the size of AB Dor A derived through interferometric measurements. Luhman et al. (2005) suggest a link to the Pleaides open cluster with a common origin and a similar age. Torres et al. (2008) and da Silva et al. (2009) adopt 70 Myr, which is equal to their adopted age for the Pleiades. Barenfeld et al. (2013) cast doubt of the existence of the group as a whole, finding that only half of the proposed members might share a common origin and setting an age lower limit at 110 Myr from the position of K dwarfs on color-magnitude diagram. Messina et al. (2010) noted the similar distribution of rotation periods among AB Dor and Pleiades members, while that of the α Per open cluster is clearly different, indicating its younger age. On the other hand, the comparison of Li EW of AB Dor and Pleiades members show that the median values for AB Dor are above those of Pleiades for $B - V$ between 0.7 to 0.9 (Fig. 10), suggesting a slightly younger age for AB Dor. X-ray luminosity is also slightly larger for AB Dor members on average. Adopting 125 Myr as an absolute age for the Pleiades (Stauffer et al. 1998), we assume 100 Myr as the age for AB Dor MG in the following, with the caveat that stars with slightly different ages but sharing kinematics may be mixed in the adopted target list.

9. Fundamental parameters

9.1. Photometric and trigonometric distances

Our adopted distances are based on trigonometric parallaxes from van Leeuwen (2007) when available. For multiple systems where separate parallaxes were available, their weighted average was adopted. For HIP 25434/6, HIP 46634/7 and HIP 58240/1, the weighted averages of parallaxes from the original HIPPARCOS catalog were adopted, as they lead to more consistent positions in the color-magnitude diagrams. However, formal parallax errors for these pairs may be underestimated. For TYC 8484-1507-1, TYC 8128-1946-1, and TYC 9339-2158-1, we used the trigonometric parallaxes of their bound wide companions in our analysis, though these companions were not a part of our target sample. For TWA 21, the parallax is from Weinberger et al. (2013).

For stars without trigonometric parallax, photometric distances were obtained using BVIJHK photometry (Table 9). Reference sequences at various ages were built using members of moving groups with available trigonometric parallaxes. Target distance was then derived based on the multiband photometry, adopted age, and the reference calibration. Typical scatter in these standard relations implies errors of about 15–20% in the photometric distances (Fig. 8). The presence of known companions was taken into account by including correction to the unresolved photometry when applicable. Interstellar reddening was checked by comparing photometric temperature, spectroscopic temperatures when available, and spectral types from the literature. In a few cases of stars with a distance close or slightly above 100 pc, the presence of small amounts of reddening

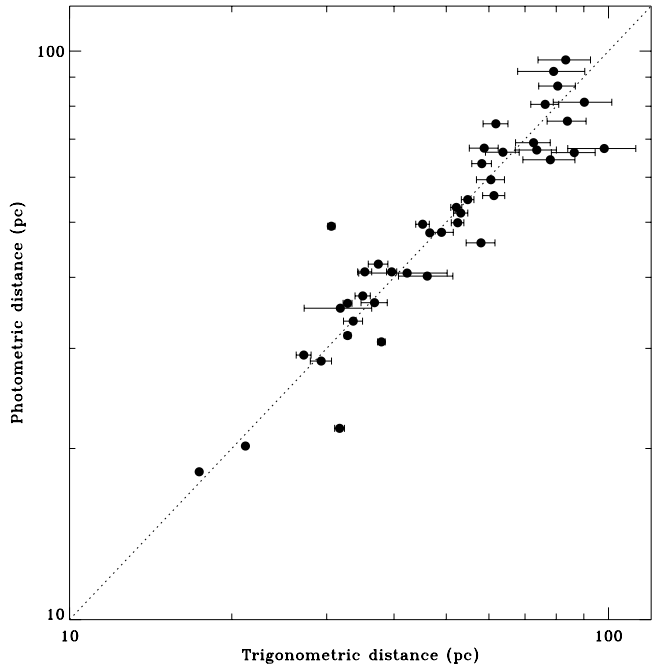

Fig. 8. Comparison of trigonometric and photometric distances for the stars in the sample with available trigonometric parallax. The rms scatter in the difference is 17%.

($E(B-V) \leq 0.1$ mag) was suggested. Photometric distances have larger errors for very young stars (age 5–20 Myr). In these instances, the absolute magnitude and derived distances depend sensitively on the adopted ages; the derived values would be systematically underestimated for unidentifed cases of evolved RS CVn variables.

9.2. Metallicity

Metallicity has been found to have a strong correlation with planet frequency at least for RV detections of giant planets around solar type stars (Fischer & Valenti 2005). Whether the planet metallicity connection extends from the separations accessible with RV surveys to those considered in direct imaging surveys is highly uncertain and depends on the main formation and migration mechanisms.

The determination of the metallicity of young stars, such as those in our sample, is made difficult by the high level of magnetic activity, the fast rotational velocities, and the possibility of veiling in the spectra. These phenomena cause larger errors in the abundance analysis with respect to older stars of similar spectral types. Differences in the atmospheric structure of young, active stars with respect to old, inactive main sequence stars might introduce spurious effects (see, e.g., Padgett 1996).

In spite of these challenges, a number of studies have addressed the issue of the metallicity of close young stars with a rather general agreement on a typical solar or slightly subsolar metallicity and the lack of metal-rich very young stars (see, e.g., James et al. 2006; Santos et al. 2008; Biazzo et al. 2011).

The study of the chemical composition of several stars in young associations resulted in no significant scatter between the individual members (Viana Almeida et al. 2009; D'Orazi et al. 2009; De Silva et al. 2013). Therefore, mean values (derived from stars both inside and external to our sample) were adopted for all association members.

To have the largest number of associations analyzed in an homogeneous way, we adopted the metallicities by Viana Almeida et al. (2009) for β Pic, Tuc, Col, Car, AB Dor, and ϵ Cha MGs[10]. Metallicity of the Carina-Near MG is from Biazzo et al. (2012). Metallicity of the Her-Lyr MG is from Fuhrmann (2004).

A few other stars have spectroscopic metallicity determinations in the literature. Photometric metallicities based on Strömgren photometry were not considered, except for the few cases of moderately old stars, as the strong magnetic activity is known to bias toward lower values the metallicity derived from this method (Morale et al. 1996).

9.3. Isochrone fitting, stellar masses, and radii

Stellar masses and isochrone ages were derived through interpolation of stellar models by Bressan et al. (2012), which include pre- and post-main sequence evolutionary phases in a homogeneous way. We used the tool *param* (da Silva et al. 2006)[11], adapted to use the Bressan et al. (2012) stellar evolutionary models. *Param* performs a Bayesian determination of the most likely stellar intrinsic properties, weighting all the isochrone sections compatible with the measured parameters (metallicity, effective temperature, parallax, apparent magnitude) and their errors. It adopts a flat distribution of ages within a given interval, as a prior. We found that Bressan et al. (2012) models are very similar to those of Tognelli et al. (2011) and Dotter et al. (2008) at least for effective temperatures warmer than 4500–4000 K. Differences at $T_{\rm eff} < 4000$ K are not of concern for the analysis of the stars in our sample.

In most cases, isochrone fitting yields very poor constraints on stellar ages (e.g., errors of a few Gyrs), which is expected for stars close to the main sequence (Fig. 9). Tighter constraints are derived from indirect indicators, such as lithium and rotation-activity phenomena (see Sect. 9.4). The stellar masses and ages resulting from isochrone fitting within the whole range of input stellar parameters are correlated, with older ages yielding lower stellar masses. To infer the stellar masses corresponding to the plausible ages of our targets, we run the *param* interface a second time for these targets, by adopting the minimum and maximum ages from Table 10 and keeping fixed the other input parameters. Differences in stellar masses with respect to the unconstrained run are typically of about 0.02–0.04 $M_{\odot}$, with larger masses that occur when adopting the age limits from the indirect indicators. The *param* tool also provides the stellar radii, which were coupled with the measured $v \sin i$ to estimate the reliability of detected rotation periods (see Appendix B for discussion on individual objects). The isochrone ages of the few targets for which this method contributes significantly in the determination of stellar ages are listed in Table 10.

9.4. Stellar ages

Our approach to age determination is to consider all the indicators available to us to better understand the properties of each object and derive stellar age. The lesson we got from the case of HIP 6177 (Zurlo et al. 2013) is that significant discrepancies

[10] Viana Almeida et al. (2009) noted a trend of metallicity with effective temperatures, possibly due to the effects of stellar activity. Removing it by assuming that no correction is needed for a solar type star would increase the metallicities by about 0.1 dex. Since the origin of this trend is uncertain and the assumption of its null value for solar temperature is questionable, we do not apply such shifts.

[11] http://stev.oapd.inaf.it

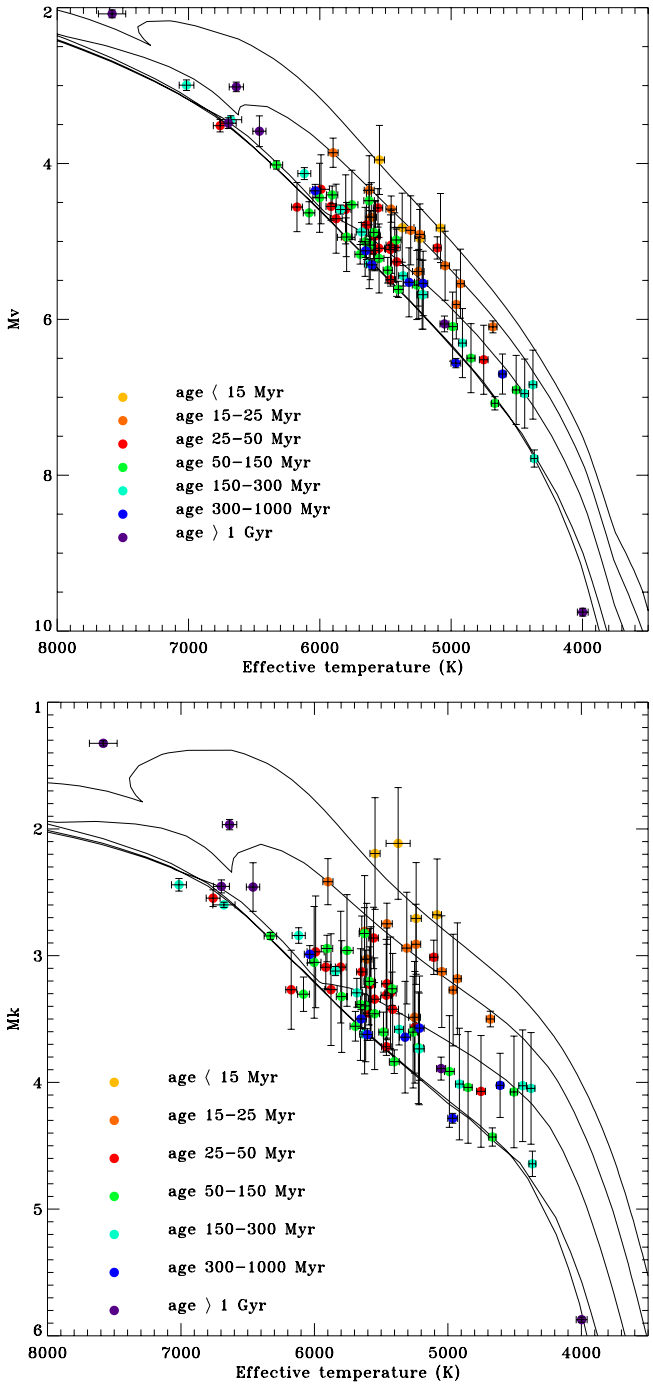

Fig. 9. HR diagram (*upper panel*: effective temperature vs. M_V; *lower panel*: effective temperature vs. M_K) for stars in the NaCo-LP sample. Stars with different ages are plotted with different colors. Overplotted are pre-main sequence, solar-metallicty isochrones for 5, 12, 30, 70, and 200 Myr (from Bressan et al. 2012). The two B-type stars HIP 10602 and HIP 12394 and the Li-rich giant HD 99409 are outside plot limits.

between age indicators may hide an astrophysical situation that is different from a normal young star (the expected typical target in our survey) and, therefore, requires an in-depth investigation.

In the previous sections, we provided several parameters (lithium EW, Ca II H and K emission, X-ray emission, rotation period), which are known to depend on stellar age. The stellar age from lithium was estimated for each target from a comparison of measured lithium EW with that of the confirmed members of young moving groups and clusters of similar color (Fig. 10). For Ca II H and K emission, X-ray emission, and rotation period, we adopted the age calibration by Mamajek & Hillenbrand (2008)[12]. Our target stars have colors extending outside some of the validity limits of these calibrations ($B-V$ between 0.5 to 0.9 for $\log R_{HK}$ and X-ray emission). As shown in Fig. 10, the results from known group members support the use of these relations for most of our target stars, even when they are slightly outside the formal boundaries, leaning toward the red side (from $B-V = 0.9$ up to $B-V = 1.2$–1.3). On the blue side, the situation is different, as both $\log R_{HK}$ and R_X become smaller when temperature increases at fixed age, due the vanishing of the stellar magnetic activity when the external convective zone of the star becomes too thin. Therefore, the extrapolation of the Mamajek & Hillenbrand (2008) calibrations would provide a significant overestimation of the stellar age[13]. The results of the age calibration are included in Table 12 as upper limits.

The measurement of stellar age from the rotation period (gyrochronology) is becoming increasingly popular, as it is not vulnerable to the time variability that characterizes the chromospheric and coronal emissions. However, it should be noted that a group of coeval young stars usually distributes along two sequences: that of very fast rotators ("C" sequence following the nomenclature by Barnes 2007) and that of slower rotators with the rotation period increasing with color ("I" sequence; Fig. 10). The gyrochronology calibration applies only to stars on the "I" sequence; for stars on the "C", its use is not appropriate and only supports a young age for the star.

Age from isochrone fitting has been derived in Sect. 9.3. As discussed above, isochrone fitting does not add tighter constraints on stellar age in most cases when compared to other methods, since the star position on the CMD is very close to the main sequence. For stars that are off of the main sequence, the use of other age indicators (e.g., lithium) allows us to conclusively discriminate between the case of young pre-main sequence stars and evolved post-main sequence stars and to assign corresponding ages. Position on the CMD is also affected by the presence of companions. Having sensitivity with NaCo imaging down to a few-AU separation for stellar companions and having checked for the presence of blended components in high resolution spectra for most of our target stars, we think that we have identified most cases of binary companions contributing significantly to the integrated flux of the system. However, the possibility of a few remaining cases cannot be excluded.

Finally, as discussed in Sect. 8.2, kinematic parameters alone cannot be considered as conclusive proof of a given stellar age value, as numerous old stars occupy the same kinematic space of young stars. Final assignment of membership to groups is based on both the kinematic analysis and the consistency of the age indicators with the age of the group. Ambiguous cases arise for stars where the other age indicators yield poor constraints, such as early F stars. The existence of space velocities firmly outside the kinematic space on which confirmed young stars are found (see for example the Montes et al. 2001 boundaries, also shown in Fig. 10) is considered a strong indication for an age older than about 500 Myr.

[12] There are some differences between our adopted ages for groups and clusters and those on which the Mamajek & Hillenbrand (2008) calibration is based, but they are mostly confined to the youngest groups (β Pic and Upper Scorpius), which is an age range where our age estimate is primarily based on other indicators.

[13] Actually; a result from Fig. 10 show that R_X is smaller for stars with $B-V \sim 0.5$ with respect to coeval stars with redder colors, indicating that the color dependence starts to become already important in the range of the Mamajek & Hillenbrand (2008) calibration.

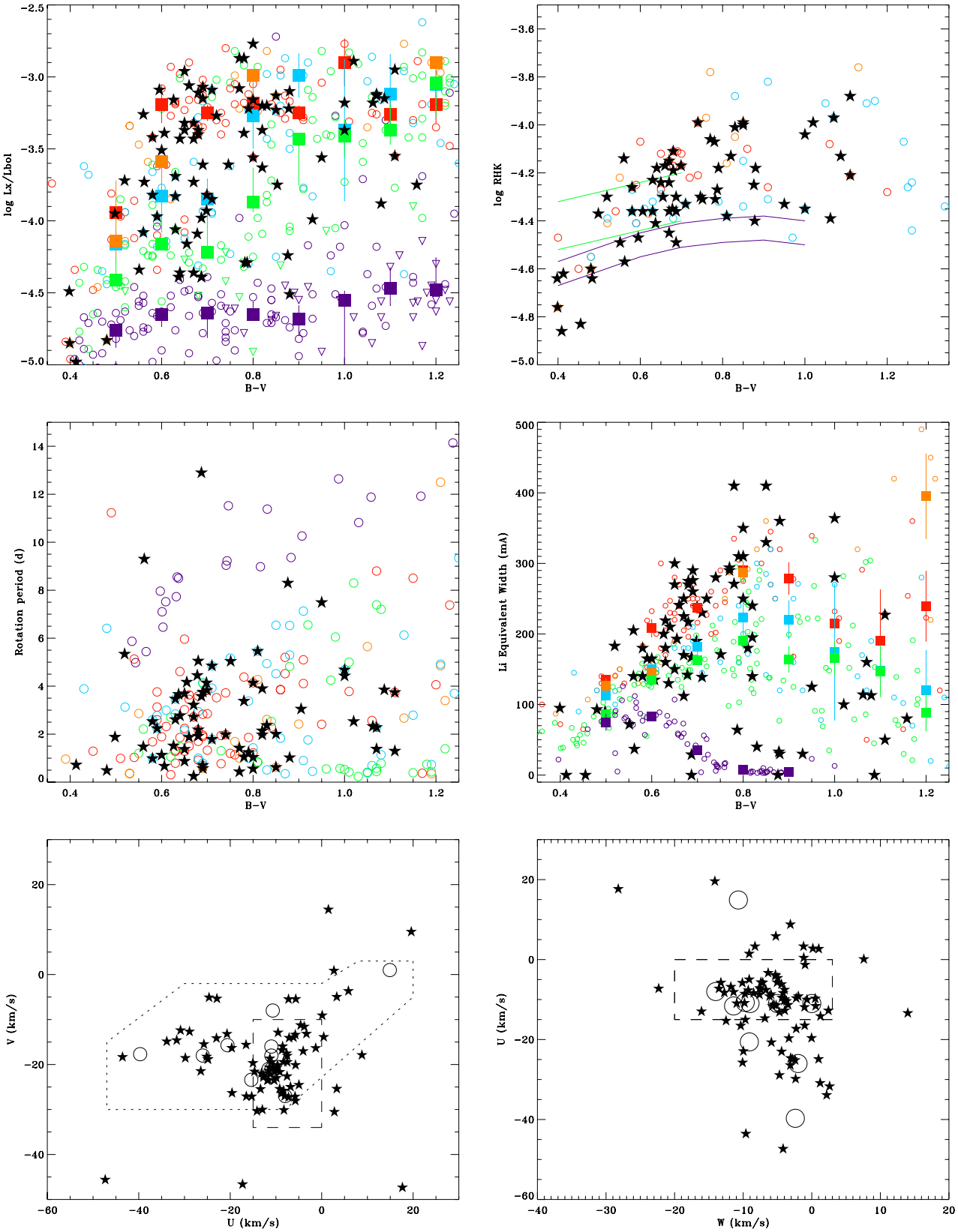

Fig. 10. Age indicators for the stars in the sample. *From top-left*: $R_X = \log L_X/L_{bol}$ vs. $B-V$; $\log R_{HK}$ vs. $B-V$; rotation period vs. $B-V$; lithium equivalent width vs. $B-V$; U vs. V space velocities; and U vs. W space velocities. In all the panels, the black stars represent the targets. In the R_X, $\log R_{HK}$, rotation period, and lithium plots, orange circles represent β Pic MG; red circles: Tucana-Columba-Carina MG; light blue circles: AB Dor MG; green circles: Pleiades OC; purple circles: Hyades OC. In the R_X vs. $B-V$ and EW Li vs. $B-V$ panels, the filled squares represent the median value of R_X and EW Li for the corresponding color bin. In the $\log R_{HK}$ plot, green and purple lines represent the locus populated by Pleiades and Hyades stars, respectivey. In the latter two panels, the positions of some young moving groups are marked as open circles. The dashed-line box in both panels is the locus of the Nearby Young Population as defined in Zuckerman & Song (2004). The dotted contours in the U vs. V plot show the locus of kinematically young stars proposed by Montes et al. (2001).

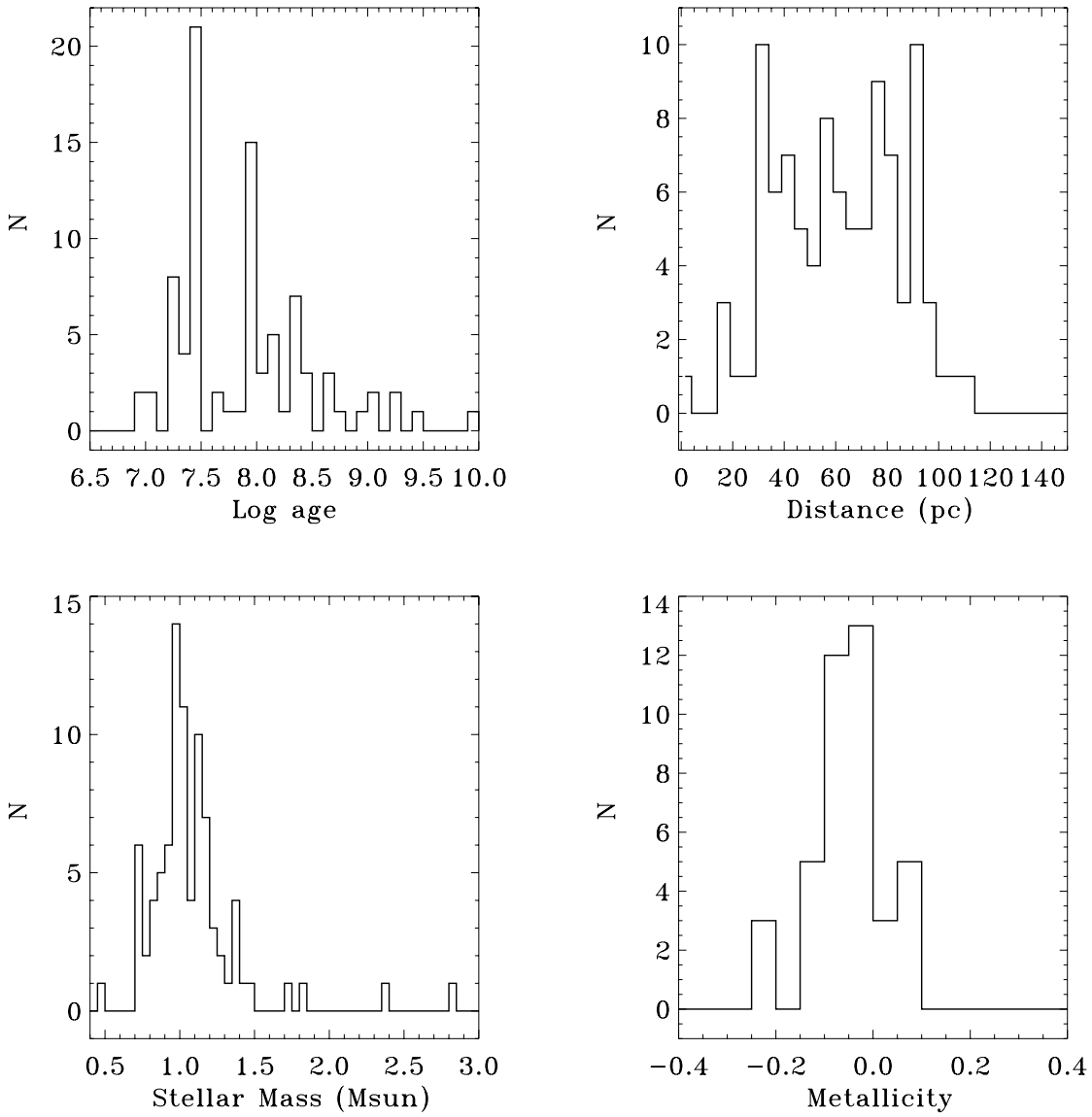

Fig. 11. Distribution of stellar age, distance, mass, and metallicity for the stars in the NaCo-LP sample.

The spread in rotation rates for coeval young stars (see, e.g., Messina et al. 2010), and the saturation of X-ray emission at fast rotation periods (Pizzolato et al. 2003) make the dependence of these indicators shallow for young ages (ages smaller than the Pleiades), as discussed in Soderblom et al. (2013), for example. As an example, β Pic, Tucana, Columba, and Carina and AB Dor members overlap on the $\log L_X/L_{bol}$ vs. $B-V$ diagram in Fig. 10. Therefore, the exact numerical values resulting from age calibrations cannot be taken at face value, but the consistency of activity and rotation is a strong indication of youth unless fast rotation is due to alternative causes (see below). For such candidate young stars, lithium EW, kinematics, and isochrone fitting in a few cases are more robust indicators of the stellar age.

Special care is required for close spectroscopic binaries. Tidal locking represents a viable alternative to young age for explaining the fast rotational velocity and high levels of chromospheric and coronal activity[14]. In these cases, indicators such as rotation period, and coronal emission, and chromospehric emission are not considered for age determination, and we rely only on indicators that are not directly linked to rotation, such as lithium, kinematics, and isochrone fitting. For the spectroscopic binaries in our sample, the orbital period is typically not available, as the binarity was identified with just a handful of RV measurements, or even one single spectrum in the case of SB2. Therefore, we cannot conclusively infer the tidal locking nature of active binary stars like TYC 7188-575-1 and TYC 5206-0915-1. Furthermore, the lack of an RV orbital solution prevents the determination of a system RV, adding uncertainties on the space velocities and effectively making them useless in some cases. Lithium EW is available in most cases, and age estimates for candidate tidally-locked binaries are primarily based on this diagnostic. However, it is possible that lithium abundance is also affected in close binaries, as it is often observed in RS CVn systems (Pallavicini et al. 1992).

By applying these techniques, we derived ages for our target stars. The ages from individual indicators and the final adopted values are given in Table 10. Most of them are confirmed to be young. Besides the tidally-locked systems and the star rejuvenated by the progenitor of its WD companion

[14] It should be noted that the two explanations are not mutually exclusive. There are cases of close tidally locked binaries that are found to be young based on lithium EW, membership to groups, or presence of disks (e.g., V4046 Sgr).

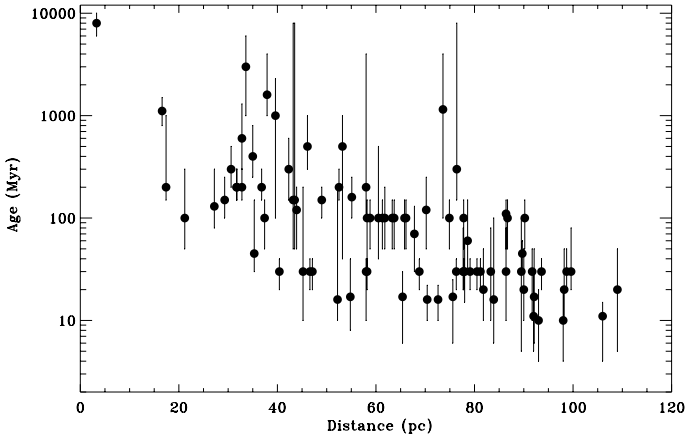

Fig. 12. Age vs. distance for the stars in the NaCo-LP sample.

(HIP 6177, Zurlo et al. 2013), other cases of old stars spuriously included in our sample are represented by the Li-rich giant HD 99409, by stars for which our determinations of age indicators are in contrast with the literature value (HIP 13008; HIP 114046), and by old interlopers in the kinematic space of young stars (HIP 71908, formerly classified as an Her-Lyr member).

Most of our target stars have not been previously observed in deep imaging, and in several cases, their ages have not been studied in detail. However, some of them were included independently in NICI imaging surveys (Wahhaj et al. 2013; Biller et al. 2013). For the seven stars in common, we obtained identical ages for one member of AB Dor MG (HIP 14684) and one of Her-Lyr (HD 139664). The objects HIP 99273 and TYC 8728-2262-1 were assigned to the β Pic MG in both cases, but there is a slight difference in the adopted group age. For HIP 11360, the star is classified as a β Pic member in NICI papers, while we adopt membership in the Tucana association, based on our revised system RV. For HD 61005, we adopt membership in Argus (40 Myr) while Wahhaj et al. (2013) adopt an age of 100 Myr without assigning membership to any known group. Finally, HIP 71908 is included in the Her-Lyr membership in Biller et al. (2013), while we claim it is a significantly older star with similar kinematics. While we are convinced of our adopted choices, this comparison is a further indication of the challenges represented by the age determination of young stars.

10. Discussion and conclusions

We have performed a characterization of the targets of the NaCo-LP to probe the occurrence of exoplanets and brown dwarfs in wide orbits. With this aim, we acquired spectroscopic data using FEROS, HARPS, and CORALIE and retrieved additional spectroscopic data from public archives. From these spectra, we determined radial and projected rotational velocities, lithium equivalent widths, effective temperatures, and chromospheric emission of the targets. We also analyzed photometric time series available from ASAS and Super-WASP archives to derive rotational periods and investigate the stellar variability phenomena. These data were used to investigate basic properties of the targets of our deep-imaging planet search program. These basic properties included ages, distances, masses, and multiplicity. Such information is needed for a proper interpretation of the direct imaging results, which are presented in the companion paper by Chauvin et al. (2015).

Histograms showing the distribution of age, distance, mass, and metallicity are in Fig. 11. The irregular behavior of the age distribution is due to members of MGs, which cluster at the same age in the histogram. The median age of the targets is 100 Myr. Few targets have estimated ages below 20 Myr and even fewer have ages older than 500 Myr, which represent old interlopers for which our original selection criteria failed to remove. The presence of older interlopers is due to a variety of causes related to age estimation, as discussed in Sect. 9.4. The median distance of the stars in our sample is 63.7 pc. Considering that the region closest to the star is saturated or hidden by the coronagraph in our imaging observations (Chauvin et al. 2015), our survey is then typically sensitive to projected separations down to about 20 AU. Stellar age and distance from the Sun are correlated, as shown in Fig. 12. This correlation is the result of the low space density of very young stars in the solar neighborhood and of several nearby young stars being previously observed in other direct imaging surveys.

The average metallicity of stars in the NaCo-LP sample is close to solar (median value [Fe/H] = –0.03) with a dispersion that is significantly smaller than that of old nearby stars studied in RV surveys, which include both moderately metal-poor stars and metal-rich stars (Fischer & Valenti 2005; Sousa et al. 2008). Furthermore, the stars with the lowest and highest metallicity in our sample are typically among the oldest ones, thus carrying limited weight in terms of detection limits of planetary companions. Therefore, the exploration of any correlation between the frequency of giant planets in wide orbits and metallicity appears to be challenging for the direct imaging technique.

The median stellar mass is 1.01 $M_{\odot}$ with 94% of the stars having masses between 0.70 and 1.50 $M_{\odot}$. Therefore, our sample is tuned to the study of the occurrence of planets in wide orbit around solar-type stars and complements the results of RV surveys, which are mostly focused in the same range of stellar masses. Young, low mass stars are virtually excluded by our adopted magnitude limits, while few early type stars with confirmed young ages were known at the time of our sample selection. However, dedicated imaging surveys devoted to the search for planets around early-type stars were performed in recent years (Janson et al. 2011; Vigan et al. 2012), while other authors focused their attention on low-mass stars (Delorme et al. 2012). Appropriate merging of these samples and of those of other surveys, which are mostly focused on solar-type stars (e.g., Lafrenière et al. 2007), will allow a preliminary evaluation of the frequency of planets in wide orbits. We will address this issue in the forthcoming paper by Vigan et al. (2014). The soon-to-come new generation instruments, such as SPHERE and GPI, will allow an extension of these results to lower planetary masses and closer separations to the star and thus provide, when coupled with RV results, a complete view of the occurrence of giant planets over a wide range of separations.

Acknowledgements. Based on observations collected at La Silla and Paranal Observatory, ESO (Chile): Programs 70.D-0081A, 072.D-0021, 072.C-0393, 074.D-0016, 074.A-9002, 074.A-9020, 076.C-0578, 076.A-9013, 077.C-0138, 077.D-0525, 081.A-9005, 082.A-9007, 083.A-9003, 083.A-9011, 083.A-9013, 084.A-9004, 084.A-9011 (FEROS), 072.C-0488, 074.C-0037, 075.C-0689, 076.C-0010, 077.C-0012, 077.D-0085, 077.C-0295, 079.C-0046, 079.C-0170, 080.D-0151, 080.C-0712, 080.C-0664, 081.D-0008, 081.C-0779, 082.C-0390, 184.C-0815 (HARPS), 184.C-0157 (NaCo). Based on data obtained from the ESO Science Archive Facility. This research has made use of the SIMBAD database and Vizier services, operated at CDS, Strasbourg, France and of the Washington Double Star Catalog maintained at the U.S. Naval Observatory. We have used data from the WASP public archive in this research. The WASP consortium comprises of the University of Cambridge, Keele University, University of Leicester, The Open University, The Queen's University Belfast, St. Andrews University and the Isaac Newton Group. Funding for WASP comes from the

consortium universities and from the UK's Science and Technology Facilities Council. We thank the SACY team for providing reduced spectra of NaCo-LP targets from their archive. We thank the SOPHIE Consortium for providing unpublished activity measurements. We thank L. Pastori for providing the CES spectra of HD 16699 A and B. We thank B. Mason for providing astrometric data for individual objects collected in the Washington Double Star Catalog. We acknowledge partial support from PRIN-INAF 2010 "Planetary systems at young ages and the interactions with their active host stars". JC was supported by the US National Science Foundation under Award No. 1009203.

References

Aarnio, A. N., Weinberger, A. J., Stassun, K. G., Mamajek, E. E., & James, D. J. 2008, AJ, 136, 2483
Absil, O., & Mawet, D. 2010, A&ARv, 18, 317
Alcala, J. M., Terranegra, L., Wichmann, R., et al. 1996, A&AS, 119, 7
Alcalá, J. M., Covino, E., Torres, G., et al. 2000, A&A, 353, 186
Ammler-von Eiff, M., & Reiners, A. 2012, A&A, 542, A116
Anderson, E., & Francis, C. 2012, Astron. Lett., 38, 331
Baade, D., & Kjeldsen, H. 1997, A&A, 323, 429
Baines, E. K., White, R. J., Huber, D., et al. 2012, ApJ, 761, 57
Baliunas, S. L., Donahue, R. A., Soon, W. H., et al. 1995, ApJ, 438, 269
Baraffe, I., Chabrier, G., Barman, T. S., Allard, F., & Hauschildt, P. H. 2003, A&A, 402, 701
Barbier-Brossat, M., & Figon, P. 2000, A&AS, 142, 217
Barenfeld, S. A., Bubar, E. J., Mamajek, E. E., & Young, P. A. 2013, ApJ, 766, 6
Barnes, S. A. 2007, ApJ, 669, 1167
Barrado y Navascués, D., Stauffer, J. R., & Jayawardhana, R. 2004, ApJ, 614, 386
Bensby, T., Feltzing, S., & Lundström, I. 2003, A&A, 410, 527
Bernhard, K., & Bernhard, C. 2010, Open Europ. J. Variable Stars, 128, 1
Bernhard, K., Bernhard, C., & Bernhard, M. 2009, Open Europ. J. Variable Stars, 98, 1
Beuzit, J.-L., Boccaletti, A., Feldt, M., et al. 2010, in Pathways Towards Habitable Planets, eds. V. Coudé Du Foresto, D. M. Gelino, & I. Ribas, ASP Conf. Ser., 430, 231
Biazzo, K., Randich, S., & Palla, F. 2011, A&A, 525, A35
Biazzo, K., D'Orazi, V., Desidera, S., et al. 2012, MNRAS, 427, 2905
Biller, B. A., Liu, M. C., Wahhaj, Z., et al. 2013, ApJ, 777, 160
Binks, A. S., & Jeffries, R. D. 2014, MNRAS, 438, L11
Boisse, I., Eggenberger, A., Santos, N. C., et al. 2010, A&A, 523, A88
Boss, A. P. 1997, Science, 276, 1836
Brandner, W., Alcala, J. M., Kunkel, M., Moneti, A., & Zinnecker, H. 1996, A&A, 307, 121
Bressan, A., Marigo, P., Girardi, L., et al. 2012, MNRAS, 427, 127
Bruntt, H., North, J. R., Cunha, M., et al. 2008, MNRAS, 386, 2039
Bruntt, H., Kurtz, D. W., Cunha, M. S., et al. 2009, MNRAS, 396, 1189
Bubar, E. J., Schaeuble, M., King, J. R., Mamajek, E. E., & Stauffer, J. R. 2011, AJ, 142, 180
Buenzli, E., Thalmann, C., Vigan, A., et al. 2010, A&A, 524, L1
Burrows, A., Marley, M., Hubbard, W. B., et al. 1997, ApJ, 491, 856
Butters, O. W., West, R. G., Anderson, D. R., et al. 2010, A&A, 520, L10
Carlberg, J. K., Smith, V. V., Cunha, K., Majewski, S. R., & Rood, R. T. 2010, ApJ, 723, L103
Carlberg, J. K., Cunha, K., Smith, V. V., & Majewski, S. R. 2012, ApJ, 757, 109
Carpenter, J. M., Mamajek, E. E., Hillenbrand, L. A., & Meyer, M. R. 2009, ApJ, 705, 1646
Casagrande, L., Portinari, L., & Flynn, C. 2006, MNRAS, 373, 13
Casagrande, L., Ramírez, I., Meléndez, J., Bessell, M., & Asplund, M. 2010, A&A, 512, A54
Casagrande, L., Schönrich, R., Asplund, M., et al. 2011, A&A, 530, A138
Chauvin, G., Thomson, M., Dumas, C., et al. 2003, A&A, 404, 157
Chauvin, G., Lagrange, A.-M., Dumas, C., et al. 2004, A&A, 425, L29
Chauvin, G., Lagrange, A.-M., Zuckerman, B., et al. 2005, A&A, 438, L29
Chauvin, G., Lagrange, A.-M., Bonavita, M., et al. 2010, A&A, 509, A52
Chauvin, G., Vigan, A., Bonnefoy, M., et al. 2015, A&A, 573, A127
Chen, C. H., Mamajek, E. E., Bitner, M. A., et al. 2011, ApJ, 738, 122
Churcher, L., Wyatt, M., & Smith, R. 2011, MNRAS, 410, 2
Cincunegui, C., Díaz, R. F., & Mauas, P. J. D. 2007, A&A, 469, 309
Currie, T., Burrows, A., Itoh, Y., et al. 2011, ApJ, 729, 128
Currie, T., Daemgen, S., Debes, J., et al. 2014, ApJ, 780, L30
Cutispoto, G., Pastori, L., Tagliaferri, G., Messina, S., & Pallavicini, R. 1999, A&AS, 138, 87
Cutispoto, G., Pastori, L., Pasquini, L., et al. 2002, A&A, 384, 491
Cutispoto, G., Tagliaferri, G., de Medeiros, J. R., et al. 2003, A&A, 397, 987
da Silva, L., Girardi, L., Pasquini, L., et al. 2006, A&A, 458, 609
da Silva, L., Torres, C. A. O., de La Reza, R., et al. 2009, A&A, 508, 833
Dall, T. H., Foellmi, C., Pritchard, J., et al. 2007, A&A, 470, 1201
de la Reza, R., & Drake, N. A. 2012, in ASP Conf. Ser. 464, eds. A. C. Carciofi, & T. Rivinius, 51
de La Reza, R., Torres, C. A. O., & Busko, I. C. 1981, MNRAS, 194, 829
De Silva, G. M., D'Orazi, V., Melo, C., et al. 2013, MNRAS, 431, 1005
Debes, J. H., Weinberger, A. J., & Song, I. 2008, ApJ, 684, L41
Delorme, P., Lagrange, A. M., Chauvin, G., et al. 2012, A&A, 539, A72
Demory, B.-O., Ségransan, D., Forveille, T., et al. 2009, A&A, 505, 205
Desidera, S., Gratton, R. G., Lucatello, S., Claudi, R. U., & Dall, T. H. 2006, A&A, 454, 553
Desidera, S., Covino, E., Messina, S., et al. 2011, A&A, 529, A54
Dobbie, P. D., Lodieu, N., & Sharp, R. G. 2010, MNRAS, 409, 1002
D'Orazi, V., Randich, S., Flaccomio, E., et al. 2009, A&A, 501, 973
D'Orazi, V., Biazzo, K., Desidera, S., et al. 2012, MNRAS, 423, 2789
Dotter, A., Chaboyer, B., Jevremović, D., et al. 2008, ApJS, 178, 89
Drake, N. A., de la Reza, R., da Silva, L., & Lambert, D. L. 2002, AJ, 123, 2703
Duchêne, G., & Kraus, A. 2013, ARA&A, 51, 269
Dupuy, T. J., & Liu, M. C. 2012, ApJS, 201, 19
Esposito, M., Covino, E., Alcalá, J. M., Guenther, E. W., & Schisano, E. 2007, MNRAS, 376, 1805
Esposito, S., Riccardi, A., Pinna, E., et al. 2011, in SPIE Conf. Ser., 8149, 02
Esposito, S., Mesa, D., Skemer, A., et al. 2013, A&A, 549, A52
Favata, F., Barbera, M., Micela, G., & Sciortino, S. 1995, A&A, 295, 147
Fehrenbach, C., & Duflot, M. 1974, A&AS, 13, 173
Fischer, D. A., & Valenti, J. 2005, ApJ, 622, 1102
Flower, P. J. 1996, ApJ, 469, 355
Frasca, A., Biazzo, K., Catalano, S., et al. 2005, A&A, 432, 647
Fuhrmann, K. 2004, Astron. Nachr., 325, 3
Gagné, J., Lafrenière, D., Doyon, R., Malo, L., & Artigau, É. 2014, ApJ, 783, 121
Galland, F., Lagrange, A.-M., Udry, S., et al. 2005, A&A, 443, 337
Galli, P. A. B., Bertout, C., Teixeira, R., & Ducourant, C. 2013, A&A, 558, A77
Gálvez, M. C., Montes, D., Fernández-Figueroa, M. J., de Castro, E., & Cornide, M. 2005, in 13th Cambridge Workshop on Cool Stars, Stellar Systems and the Sun, eds. F. Favata, G. A. J. Hussain, & B. Battrick, ESA SP, 560, 567
Gálvez, M. C., Montes, D., Fernández-Figueroa, M. J., & López-Santiago, J. 2006, Ap&SS, 304, 59
García-Alvarez, D., Lanza, A. F., Messina, S., et al. 2011, A&A, 533, A30
Glebocki, R., & Gnacinski, P. 2005, VizieR Online Data Catalog: III/244
Gontcharov, G. A. 2006, Astron. Lett., 32, 759
Gray, R. O., Corbally, C. J., Garrison, R. F., et al. 2006, AJ, 132, 161
Grenier, S., Baylac, M.-O., Rolland, L., et al. 1999, A&AS, 137, 451
Guenther, E. W., & Esposito, E. 2007 [arXiv:astro-ph/0701293]
Guillout, P., Klutsch, A., Frasca, A., et al. 2009, A&A, 504, 829
Guirado, J. C., Marcaide, J. M., Martí-Vidal, I., et al. 2011, A&A, 533, A106
Hale, A. 1994, AJ, 107, 306
Handler, G. 1995, Inform. Bull. Variable Stars, 4188, 1
Henry, T. J., Soderblom, D. R., Donahue, R. A., & Baliunas, S. L. 1996, AJ, 111, 439
Hines, D. C., Schneider, G., Hollenbach, D., et al. 2007, ApJ, 671, L165
Hinz, P. M., Bippert-Plymate, T., Breuninger, A., et al. 2008, in SPIE Conf. Ser., 7013, 28
Hinz, P. M., Rodigas, T. J., Kenworthy, M. A., et al. 2010, ApJ, 716, 417
Høg, E., Fabricius, C., Makarov, V. V., et al. 2000, A&A, 355, L27
Horne, J. H., & Baliunas, S. L. 1986, ApJ, 302, 757
Houk, N. 1982, Michigan Catalogue of Two-dimensional Spectral Types for the HD stars, 3
Hünsch, M., Schmitt, J. H. M. M., Sterzik, M. F., & Voges, W. 1999, A&AS, 135, 319
James, D. J., Melo, C., Santos, N. C., & Bouvier, J. 2006, A&A, 446, 971
Janson, M., Brandner, W., Lenzen, R., et al. 2007, A&A, 462, 615
Janson, M., Bonavita, M., Klahr, H., et al. 2011, ApJ, 736, 89
Jenkins, J. S., Jones, H. R. A., Tinney, C. G., et al. 2006, MNRAS, 372, 163
Jenkins, J. S., Murgas, F., Rojo, P., et al. 2011, A&A, 531, A8
Johnson, D. R. H., & Soderblom, D. R. 1987, AJ, 93, 864
Kalas, P., Graham, J. R., Clampin, M. C., & Fitzgerald, M. P. 2006, ApJ, 637, L57
Kalas, P., Fitzgerald, M. P., & Graham, J. R. 2007, ApJ, 661, L85
Kastner, J. H., Crigger, L., Rich, M., & Weintraub, D. A. 2003, ApJ, 585, 878
Kaufer, A., Stahl, O., Tubbesing, S., et al. 1999, The Messenger, 95, 8
King, J. R., Villarreal, A. R., Soderblom, D. R., Gulliver, A. F., & Adelman, S. J. 2003, AJ, 125, 1980
Kiraga, M. 2012, Acta Astron., 62, 67
Koen, C., & Eyer, L. 2002, MNRAS, 331, 45
Köhler, R., Kunkel, M., Leinert, C., & Zinnecker, H. 2000, A&A, 356, 541
Kraus, A. L., & Hillenbrand, L. A. 2007, ApJ, 662, 413

Kraus, A. L., Shkolnik, E. L., Allers, K. N., & Liu, M. C. 2014, AJ, 147, 146
Kuzuhara, M., Tamura, M., Kudo, T., et al. 2013, ApJ, 774, 11
Lafrenière, D., Doyon, R., Marois, C., et al. 2007, ApJ, 670, 1367
Lagrange, A.-M., Desort, M., Galland, F., Udry, S., & Mayor, M. 2009, A&A, 495, 335
Lagrange, A.-M., Bonnefoy, M., Chauvin, G., et al. 2010, Science, 329, 57
Lamm, M. H., Bailer-Jones, C. A. L., Mundt, R., Herbst, W., & Scholz, A. 2004, A&A, 417, 557
Lépine, S., & Bongiorno, B. 2007, AJ, 133, 889
López-Santiago, J., Montes, D., Crespo-Chacón, I., & Fernández-Figueroa, M. J. 2006, ApJ, 643, 1160
Lovis, C., Dumusque, X., Santos, N. C., et al. 2011, A&A, unpublished [arXiv:1107.5325]
Luhman, K. L., Stauffer, J. R., & Mamajek, E. E. 2005, ApJ, 628, L69
Macintosh, B. A., Graham, J. R., Palmer, D. W., et al. 2008, in SPIE Conf. Ser., 7015, 18
Makarov, V. V. 2007, ApJ, 658, 480
Makarov, V. V., & Kaplan, G. H. 2005, AJ, 129, 2420
Malkov, O. Y., Oblak, E., Snegireva, A. E., & Torra, J. 2005, VizieR Online Data Catalog, J/A+A/446/785
Malo, L., Doyon, R., Lafrenière, D., et al. 2013, ApJ, 762, 88
Mamajek, E. E. 2004, Ph.D. Thesis, Steward Observatory, The University of Arizona, Tucson, AZ, USA
Mamajek, E. E. 2005, ApJ, 634, 1385
Mamajek, E. E., & Hillenbrand, L. A. 2008, ApJ, 687, 1264
Mamajek, E. E., Meyer, M. R., & Liebert, J. 2002, AJ, 124, 1670
Marmier, M. 2012, Ph.D. Thesis, University of Geneva
Marois, C., Lafrenière, D., Doyon, R., Macintosh, B., & Nadeau, D. 2006, ApJ, 641, 556
Marois, C., Macintosh, B., Barman, T., et al. 2008, Science, 322, 1348
Marois, C., Zuckerman, B., Konopacky, Q. M., Macintosh, B., & Barman, T. 2010, Nature, 468, 1080
Martí, J., Paredes, J. M., Garrido, J. L., & Luque-Escamilla, P. 2004, A&A, 423, 1073
Martin, D. C., Fanson, J., Schiminovich, D., et al. 2005, ApJ, 619, L1
Martinache, F., & Guyon, O. 2009, in SPIE Conf. Ser., 7440
Masana, E., Jordi, C., & Ribas, I. 2006, A&A, 450, 735
Masciadri, E., Mundt, R., Henning, T., Alvarez, C., & Barrado y Navascués, D. 2005, ApJ, 625, 1004
Mason, B. D., Wycoff, G. L., Hartkopf, W. I., Douglass, G. G., & Worley, C. E. 2013, VizieR Online Data Catalog, 1, 2026
Mayor, M., Pepe, F., Queloz, D., et al. 2003, The Messenger, 114, 20
Mayor, M., Marmier, M., Lovis, C., et al. 2011, A&A, submitted [arXiv:1109.2497]
Mentuch, E., Brandeker, A., van Kerkwijk, M. H., Jayawardhana, R., & Hauschildt, P. H. 2008, ApJ, 689, 1127
Messina, S., Desidera, S., Turatto, M., Lanzafame, A. C., & Guinan, E. F. 2010, A&A, 520, A15
Messina, S., Desidera, S., Lanzafame, A. C., Turatto, M., & Guinan, E. F. 2011, A&A, 532, A10
Meyer, M. R., Hillenbrand, L. A., Backman, D., et al. 2006, PASP, 118, 1690
Meyer, M. R., Carpenter, J. M., Mamajek, E. E., et al. 2008, ApJ, 673, L181
Montes, D., López-Santiago, J., Gálvez, M. C., et al. 2001, MNRAS, 328, 45
Moór, A., Ábrahám, P., Derekas, A., et al. 2006, ApJ, 644, 525
Moór, A., Pascucci, I., Kóspál, Á., et al. 2011, ApJS, 193, 4
Moór, A., Szabó, G. M., Kiss, L. L., et al. 2013, MNRAS, 435, 1376
Morale, F., Micela, G., Favata, F., & Sciortino, S. 1996, A&AS, 119, 403
Mordasini, C., Alibert, Y., & Benz, W. 2009, A&A, 501, 1139
Mordasini, C., Alibert, Y., Klahr, H., & Henning, T. 2012, A&A, 547, A111
Mouillet, D., Beuzit, J. L., Desidera, S., et al. 2010, in In the Spirit of Lyot 2010, University of Davis Diderot
Nakajima, T., & Morino, J.-I. 2012, AJ, 143, 2
Neuhaeuser, R., Sterzik, M. F., Schmitt, J. H. M. M., Wichmann, R., & Krautter, J. 1995, A&A, 297, 391
Neves, V., Bonfils, X., Santos, N. C., et al. 2013, A&A, 551, A36
Nidever, D. L., Marcy, G. W., Butler, R. P., Fischer, D. A., & Vogt, S. S. 2002, ApJS, 141, 503
Nielsen, E. L., & Close, L. M. 2010, ApJ, 717, 878
Nordström, B., Mayor, M., Andersen, J., et al. 2004, A&A, 418, 989
Norris, J. 1987, AJ, 93, 616
Norton, A. J., Wheatley, P. J., West, R. G., et al. 2007, A&A, 467, 785
Noyes, R. W., Hartmann, L. W., Baliunas, S. L., Duncan, D. K., & Vaughan, A. H. 1984, ApJ, 279, 763
Ortega, V. G., de la Reza, R., Jilinski, E., & Bazzanella, B. 2002, ApJ, 575, L75
Padgett, D. L. 1996, ApJ, 471, 847
Pallavicini, R., Randich, S., & Giampapa, M. S. 1992, A&A, 253, 185
Paulson, D. B., & Yelda, S. 2006, PASP, 118, 706
Paunzen, E., Schnell, A., & Maitzen, H. M. 2005, A&A, 444, 941
Pecaut, M. J., & Mamajek, E. E. 2013, ApJS, 208, 9
Pecaut, M. J., Mamajek, E. E., & Bubar, E. J. 2012, ApJ, 746, 154
Pepe, F., Mayor, M., Galland, F., et al. 2002, A&A, 388, 632
Perryman, M. A. C., Lindegren, L., Kovalevsky, J., et al. 1997, A&A, 323, L49
Perryman, M. A. C., Brown, A. G. A., Lebreton, Y., et al. 1998, A&A, 331, 81
Pizzolato, N., Maggio, A., Micela, G., Sciortino, S., & Ventura, P. 2003, A&A, 397, 147
Platais, I., Melo, C., Mermilliod, J.-C., et al. 2007, A&A, 461, 509
Pojmanski, G. 1997, Acta Astron., 47, 467
Pojmański, G. 2001, in Small Telescope Astronomy on Global Scales, eds. B. Paczynski, W.-P. Chen, & C. Lemme, IAU Colloq. 183, ASP Conf. Ser., 246, 53
Pojmanski, G. 2002, Acta Astron., 52, 397
Pollacco, D. L., Skillen, I., Collier Cameron, A., et al. 2006, PASP, 118, 1407
Preibisch, T., & Mamajek, E. 2008, The Nearest OB Association: Scorpius-Centaurus (Sco OB2), ed. B. Reipurth, 235
Preibisch, T., Brown, A. G. A., Bridges, T., Guenther, E., & Zinnecker, H. 2002, AJ, 124, 404
Press, W. H., Teukolsky, S. A., Vetterling, W. T., & Flannery, B. P. 1992, Numerical recipes in FORTRAN, The art of scientific computing, eds. W. H., Press, S. A., Teukolsky, W. T., Vetterling, & B. P., Flannery (Cambridge: University Press)
Quast, G. R., Torres, C. A. O., de La Reza, R., da Silva, L., & Drake, N. 2001, in Young Stars Near Earth: Progress and Prospects, eds. R. Jayawardhana, & T. Greene, ASP Conf. Ser., 244, 49
Rameau, J., Chauvin, G., Lagrange, A.-M., et al. 2013, ApJ, 772, L15
Reid, N. 2003, MNRAS, 342, 837
Reiners, A. 2006, A&A, 446, 267
Reiners, A., & Royer, F. 2004, A&A, 415, 325
Rhee, J. H., Song, I., Zuckerman, B., & McElwain, M. 2007, ApJ, 660, 1556
Roberts, D. H., Lehar, J., & Dreher, J. W. 1987, AJ, 93, 968
Rocha-Pinto, H. J., Castilho, B. V., & Maciel, W. J. 2002, A&A, 384, 912
Rodigas, T. J., Hinz, P. M., Leisenring, J., et al. 2012, ApJ, 752, 57
Royer, F., Gerbaldi, M., Faraggiana, R., & Gómez, A. E. 2002, A&A, 381, 105
Royer, F., Zorec, J., & Gómez, A. E. 2007, A&A, 463, 671
Saar, S. H., Nordstrom, B., & Andersen, J. 1990, A&A, 235, 291
Santos, N. C., Mayor, M., Naef, D., et al. 2002, A&A, 392, 215
Santos, N. C., Melo, C., James, D. J., et al. 2008, A&A, 480, 889
Saxton, R. D., Read, A. M., Esquej, P., et al. 2008, A&A, 480, 611
Scargle, J. D. 1982, ApJ, 263, 835
Schisano, E., Covino, E., Alcalá, J. M., et al. 2009, A&A, 501, 1013
Scholz, A., Coffey, J., Brandeker, A., & Jayawardhana, R. 2007, ApJ, 662, 1254
Schröder, C., Reiners, A., & Schmitt, J. H. M. M. 2009, A&A, 493, 1099
Siebert, A., Williams, M. E. K., Siviero, A., et al. 2011, AJ, 141, 187
Siess, L., & Livio, M. 1999, MNRAS, 308, 1133
Soderblom, D. R. 2010, ARA&A, 48, 581
Soderblom, D., Hillenbrand, L., Jeffries, R., Mamajek, S., & Naylor, T. 2013, in Protostars and Planets VI (University of Arizona Press), accepted [arXiv:1311.7024]
Song, I., Bessell, M. S., & Zuckerman, B. 2002, A&A, 385, 862
Song, I., Zuckerman, B., & Bessell, M. S. 2003, ApJ, 599, 342
Song, I., Zuckerman, B., & Bessell, M. S. 2012, AJ, 144, 8
Soubiran, C., Le Campion, J.-F., Cayrel de Strobel, G., & Caillo, A. 2010, A&A, 515, A111
Sousa, S. G., Santos, N. C., Israelian, G., Mayor, M., & Monteiro, M. J. P. F. G. 2007, A&A, 469, 783
Sousa, S. G., Santos, N. C., Mayor, M., et al. 2008, A&A, 487, 373
Sousa, S. G., Alapini, A., Israelian, G., & Santos, N. C. 2010, A&A, 512, A13
Stauffer, J. R., Schultz, G., & Kirkpatrick, J. D. 1998, ApJ, 499, L199
Stelzer, B., Neuhäuser, R., & Hambaryan, V. 2000, A&A, 356, 949
Strassmeier, K., Washuettl, A., Granzer, T., Scheck, M., & Weber, M. 2000, A&AS, 142, 275
Strassmeier, K. G., Weber, M., Granzer, T., & Järvinen, S. 2012, Astron. Nachr., 333, 663
Sudol, J. J., & Haghighipour, N. 2012, ApJ, 755, 38
Tamuz, O., Mazeh, T., & Zucker, S. 2005, MNRAS, 356, 1466
Tognelli, E., Prada Moroni, P. G., & Degl'Innocenti, S. 2011, A&A, 533, A109
Tokovinin, A. 2011, AJ, 141, 52
Tokovinin, A., Hartung, M., & Hayward, T. L. 2010, AJ, 140, 510
Torres, G. 2010, AJ, 140, 1158
Torres, C. A. O., da Silva, L., Quast, G. R., de la Reza, R., & Jilinski, E. 2000, AJ, 120, 1410
Torres, C. A. O., Quast, G. R., da Silva, L., et al. 2006, A&A, 460, 695
Torres, C. A. O., Quast, G. R., Melo, C. H. F., & Sterzik, M. F. 2008, Young Nearby Loose Associations (Bo Reipurth), 757
Udry, S., Mayor, M., Naef, D., et al. 2000, A&A, 356, 590

van Leeuwen, F. 2007, A&A, 474, 653
Viana Almeida, P., Santos, N. C., Melo, C., et al. 2009, A&A, 501, 965
Vigan, A., Patience, J., Marois, C., et al. 2012, A&A, 544, A9
Voges, W., Aschenbach, B., Boller, T., et al. 1999, A&A, 349, 389
Voges, W., Aschenbach, B., Boller, T., et al. 2000, IAU Circ., 7432, 1
Vorobyov, E. I., Zakhozhay, O. V., & Dunham, M. M. 2013, MNRAS, 433, 3256
Wahhaj, Z., Liu, M. C., Nielsen, E. L., et al. 2013, ApJ, 773, 179
Waite, I. A., Carter, B. D., Marsden, S. C., & Mengel, M. W. 2005, PASA, 22, 29
Waite, I. A., Marsden, S. C., Carter, B. D., et al. 2011, PASA, 28, 323
Weinberger, A. J., Anglada-Escudé, G., & Boss, A. P. 2013, ApJ, 762, 118
Weise, P., Launhardt, R., Setiawan, J., & Henning, T. 2010, A&A, 517, A88
White, R. J., Gabor, J. M., & Hillenbrand, L. A. 2007, AJ, 133, 2524
Wichmann, R., Covino, E., Alcalá, J. M., et al. 1999, MNRAS, 307, 909
Wichmann, R., Schmitt, J. H. M. M., & Hubrig, S. 2003, A&A, 399, 983
Woolf, V. M., & Wallerstein, G. 2005, MNRAS, 356, 963
Wright, J. T., Marcy, G. W., Butler, R. P., & Vogt, S. S. 2004, ApJS, 152, 261
Wright, N. J., Drake, J. J., Mamajek, E. E., & Henry, G. W. 2011, ApJ, 743, 48
Yao, B.-A., & Tong, J.-H. 1989, Inform. Bull. Variable Stars, 3334, 1
Zorec, J., & Royer, F. 2012, A&A, 537, A120
Zuckerman, B., & Song, I. 2004, ARA&A, 42, 685
Zuckerman, B., Song, I., Bessell, M. S., & Webb, R. A. 2001, ApJ, 562, L87
Zuckerman, B., Song, I., & Bessell, M. S. 2004, ApJ, 613, L65
Zuckerman, B., Bessell, M. S., Song, I., & Kim, S. 2006, ApJ, 649, L115
Zuckerman, B., Rhee, J. H., Song, I., & Bessell, M. S. 2011, ApJ, 732, 61
Zurlo, A., Vigan, A., Hagelberg, J., et al. 2013, A&A, 554, A21

Pages 20 to 45 are available in the electronic edition of the journal at http://www.aanda.org

Table 1. Measured parameters of NACO-LP targets on FEROS spectra.

Name	HJD −2 450 000	HRV km s^{-1}	$v \sin i$ km s^{-1}	$T_{\rm eff}$ K	EW (Li) mÅ	S-index	log $R_{\rm HK}$	Remarks
TYC 5839 0596 1a	5106.75256	+51.5 ± 1.5	18.0 ± 2.0			2.135	–3.990	deblended
TYC 5839 0596 1b	5106.75256	+21.3 ± 1.5	17.0 ± 2.0					deblended
HD 4944	5056.95069	+1.5 ± 0.5	8.0 ± 2.0	5609 ± 105	37	0.257	–4.572	A
		∼19						B
HD 15115	5399.87305	+2.9 ± 4.1			99	0.199	–4.748	
HD 15115	5399.87922	+1.9 ± 2.8			90	0.194	–4.769	
HD 16699	5106.82452	+15.5 ± 0.5	22.0 ± 2.0	5979 ± 85	46	0.305	–4.443	
HIP 13008	5198.57549	+1.5 ± 1.0	fast–rot			0.228	–4.642	
HD 19668	3331.69115	+14.1 ± 0.5	5.5 ± 0.6	5463 ± 20	175	0.502	–4.370	
HD 19668	3981.86578	+14.0 ± 0.4	5.6 ± 0.8	5478 ± 38	180	0.489	–4.383	
TYC 8060 1673 1	5100.82602	+14.1 ± 0.4	9.7 ± 1.2	4882 ± 28	223	1.790	–4.212	
TYC 8060 1673 1	5100.83814	+14.1 ± 0.4	9.7 ± 1.2	4869 ± 27	225	1.829	–4.203	
HIP 19775	5109.79537	+20.4 ± 0.5	13.1 ± 0.8	5840 ± 45	170	0.433	–4.261	
HIP 23316	5204.73415	22.5 ± 0.1	7.7 ± 2.1	5552 ± 33	225	0.659	–4.108	
HD 32981	4787.64545	+25.5 ± 0.0	4.8 ± 0.6	5975 ± 30	127	0.366	–4.357	
BD−09 1108	4787.66125	+20.5 ± 0.8	15.7 ± 1.1	5660 ± 45	205	0.595	–4.151	
HIP 25434								Desidera et al. (2006)
HIP 25436								Desidera et al. (2006)
HD 269620	5203.69027	18.6 ± 0.5	20.2 ± 2.6	5811 ± 105	212	0.482	–4.232	
TYC 5346 0132 1	5198.74360	+24.0 ± 1.5		5324 ± 87	280	0.937	–3.992	
HD 44748	5203.72205	+24.5 ± 0.4	9.2 ± 0.8	5657 ± 37	186	0.445	–4.296	
TYC 9181 0466 1	3807.58722	+15.6 ± 0.7	11.9 ± 1.2	5682 ± 45	214	0.538	–4.181	
TYC 9181 0466 1	3815.59140	+16.1 ± 0.6	11.6 ± 0.9	5670 ± 40	205	0.535	–4.184	
HD 49855	4167.58778	+20.1 ± 0.4	11.6 ± 1.1	5444 ± 36	237	0.621	–4.154	
HIP 35564	5109.83766	+24.0 ± 2.0	fastrot			0.218	–4.667	
HIP 36312	4908.52828	+17.1 ± 2.3			130	0.276	–4.515	
HIP 36414	4782.87637	+24.7 ± 1.3	31.5 ± 3.3	5753 ± 110	72	0.288	–4.490	
HIP 37563	3809.65732	+17.1 ± 0.4	14.3 ± 1.0	5801 ± 56	130	0.356	–4.405	
HD 63581	3338.82012	+18.1 ± 0.1	5.1 ± 0.8	5428 ± 22	116	0.505	–4.338	
HD 63608	3777.62320	+16.9 ± 0.3	3.0 ± 1.0	5375 ± 20	64	0.465	–4.384	
HIP 47646	4783.86693	+51.0 ± 1.0	15.0 ± 1.5	6615 ± 115	–	0.179	–4.830	
TWA 21	3807.65310	+18.0 ± 0.1	8.7 ± 1.3	4898 ± 21	364	1.777	–4.039	
TYC 7188 0575 1	5254.70678	+44.7 ± 2.0				3.786	–3.885	
HD 296790	4944.71070	+8.8 ± 0.8	31.5 ± 6.5	5400 ± 50	190	0.845	–4.129	
TYC 7743-1091-1	3926.5215	+21.9 ± 0.1		4931 ± 59	113.4			
HIP 58240	5254.76079	+5.9 ± 0.1	4.0 ± 0.5	5835 ± 24	115	0.365	–4.415	
HIP 58241	5254.75374	+6.9 ± 0.5	8.2 ± 0.8	5710 ± 22	114	0.394	–4.350	
HD 104467	3069.79015	+11.4 ± 0.7	26.8 ± 2.1	5730 ± 100	230	0.498	–4.244	
TYC 9231 1566 1	5254.83929	+13.5 ± 0.1	12.5 ± 0.8	5530 ± 40	270	0.645	–4.118	$E(B-V) = 0.08$
TYC 8979 1683 1	4942.79040	+12.1 ± 2.6		5650 ± 145	290	0.868	–4.059	
TYC 9245 0617 1	3420.79277	+13.2 ± 2.4	28.2 ± 6.2	5083 ± 70	391	1.597	–3.873	$E(B-V) = 0.09$
TYC 9245 0617 1	3421.77760	+14.1 ± 0.5	26.7 ± 2.2	5090 ± 70	410	1.595	–3.874	
TYC 9245 0617 1	3421.88252	+14.7 ± 0.7	28.8 ± 2.0	5114 ± 62	415			
TYC 9245 0617 1	3422.76198	+12.2 ± 0.6	26.2 ± 3.1	5059 ± 65	410	1.592	–3.874	
TYC 9245 0617 1	4582.77483	+9.6 ± 0.9	26.0 ± 1.7	5071 ± 65	393	1.441	–3.919	
HD 113553	3447.88101	+1.3 ± 0.1	10.6 ± 0.9	5760 ± 32	145	0.416	–4.347	
HD 113553	3447.86976	+1.3 ± 0.1	10.6 ± 1.0	5729 ± 25	141	0.415	–4.347	
TYC 7796 2110 1	5256.82087	+21.6 ± 9.6			339	0.881	–4.183	fast-rot/SB
HD 124831	3909.59212	+11.5 ± 0.8		5324 ± 92	200	0.534	–4.137	
HIP 70351	4940.77047	–8.6 ± 0.2	12.3 ± 0.7	5624 ± 50	164	0.460	–4.301	
GJ 560 A	3423.83863	+6.2 ± 0.2	14.5 ± 1.8	6067 ± 172				
GJ 560 B	3423.82772	+6.6 ± 0.4	3.0 ± 1.2	4761 ± 35		0.672	–4.705	
HD 129181	4496.86468	+4.8 ± 4.6			135	0.374	–4.360	
HD 129181	4496.87658	+2.8 ± 4.0			130	0.379	–4.352	
HIP 78747	4940.86043	–8.2 ± 0.5	24.0 ± 3.0	6005 ± 55	23	0.175	–4.861	
HIP 80758	4940.86585	+6.0 ± 0.1	10.8 ± 1.0	5328 ± 28	262	0.878	–4.065	
TYC 6815-0874-1						0.491	–4.321	
CD-25 11942	3909.79462	–1.5 ± 5.4		5300 ± 150	240	0.879	–4.184	$E(B-V) = 0.08$; fast-rot. SB2?
TYC 8728 2262 1	4941.87270	–0.2 ± 0.9		5245 ± 110	325	1.228	–3.992	
TYC 7401 2446 1	5106.60454	–15.0 ± 0.1	4.3 ± 0.7	5311 ± 18	155	0.618	–4.289	
TYC 6893 1391 1	5052.76453	–13.9 ± 0.5	3.7 ± 1.0	5005 ± 25	121	0.780	–4.334	
BD-14 5534						0.401	–4.360	
HD 189285	3906.84485	–19.5 ± 0.0	8.3 ± 0.9	5545 ± 35	141	0.455	–4.325	
HD 189285	4782.52813	–19.6 ± 0.2	8.3 ± 0.7	5620 ± 23	135	0.449	–4.331	

Table 1. continued.

Name	HJD –2 450 000	HRV km s^{-1}	$v \sin i$ km s^{-1}	$T_{\rm eff}$ K	EW (Li) mÅ	S-index	$\log R_{\rm HK}$	Remarks
HD 189245	5052.80066	–10.0 ± 2.0				0.303	–4.442	ultrafast-rot
TYC 5164 0567 1	3906.85805	–16.5 ± 0.0	7.8 ± 0.9	5140 ± 20	280	0.916	–4.333	
TYC 5164 0567 1	4783.49700	–16.5 ± 0.1	7.7 ± 0.9	5197 ± 25	260	0.821	–4.382	
HD 191089	3102.88426	–6.4 ± 1.7		5629 ± 165	91	0.200	–4.735	fast-rot.
HD 191089	3102.8					0.201	–4.733	
HD 199058	3908.85303	–18.7 ± 0.7	13.2 ± 0.6	5680 ± 60	160	0.392	–4.345	
HD 199058	4783.51539	–18.7 ± 0.7	14.5 ± 0.5	5752 ± 41	160	0.377	–4.367	
TYC 1090 0543 1	3908.85620	–19.5 ± 0.0	17.3 ± 1.4	4775 ± 45	115	2.650	–3.975	
TYC 5206 0915 1	5068.62201	+0.9 ± 0.6	22.9 ± 1.6	5170 ± 65	40	1.115	–4.011	
HD 203019	3904.90932	+23.9 ± 0.2	5.3 ± 1.0	5661 ± 22	–	0.429	–4.337	
HIP 105612	5054.77872	–2.7 ± 0.5	3.0 ± 1.0	5647 ± 25	29	0.327	–4.491	
CD-40 14901	4788.51865	–11.0 ± 0.5	15.0 ± 1.5	5653 ± 51	164	0.502	–4.239	
HD 217987	4784.54545	+7.5 ± 0.5	2.7 ± 0.5		0			
HD 220054	4778.57584	+7.3 ± 1.7			221	0.568	–4.167	
HIP 116063	5004.94059	+3.1 ± 0.0	2.6 ± 0.9	5963 ± 30	110	0.311	–4.465	

Table 2. Measurements of spectroscopic parameters from CORALIE RV survey.

ID1	ID2	N	RV km s^{-1}	$v \sin i$ km s^{-1}	$\log R_{\rm HK}$	Remarks
HIP 6177	HD 8049			3.52	–4.252	RV trend, Zurlo et al. (2013)
HIP 14684	HD 19668	4	14.65	6.29	–4.38	
HIP 37923	HD 63608	5	17.73	2.67	–4.372	
HIP 79958	HD 146464	3	1.74		–4.445	
HIP 105384	HD 203019	10	24.43	5.86	–4.356	
HIP 105612	HD 202732	3	–1.7	3.28	–4.476	

Table 3. Measurements of spectroscopic parameters from dedicated CORALIE observations.

ID1	JD -2 450 000	RV km s^{-1}	$FWHM$ km s^{-1}	S/N	Remarks
TYC 8128-1946-1	5927.6395	17.0 ± 0.5	...	94	individual lines, $v \sin i \sim 50$ km s^{-1}
HIP 36312	5931.8242	16.62 ± 0.07	40.1	43	pipeline
TYC 7796-2110-1	5931.8261	1.3 ± 4.5	...	15	individual lines, $v \sin i \sim 90$ km s^{-1}
TYC 7188-0575-1	5931.8654	–38.75 ± 0.05	42.9	32	manual recorrelation
HIP 25436	6360.6450	21.8 ± 3.8	...	32	individual lines, $v \sin i \sim 110$ km s^{-1}
HIP 25434	6360.6380	24.2 ± 1.5	...	17	individual lines, $v \sin i \sim 50$ km s^{-1}
TYC 7188-0575-1	6357.7972	–24.71 ± 0.08	39.1	14	manual recorrelation
HIP 35564	6357.7330	13.7 ± 1.1	...	108	individual lines, $v \sin i \sim 60$ km s^{-1}
HIP 72399	6357.7867	30.31 ± 0.05	15.1	17	pipeline
	6357.8246	33.24 ± 0.06	16.7	16	pipeline
HIP 72400	6360.7397	1.35 ± 0.02	8.1	23	pipeline
HIP 13008	6509.9063	0.6 ± 1.6	...	27	individual lines, $v \sin i \sim 80$ km s^{-1}
TYC 5606-0915-1	6508.6744	17.47 ± 0.06	31.0	21	pipeline

Table 4. Measurements of spectroscopic parameters from HARPS spectra.

ID1	N	JD start –2 450 000	JD end –2 450 000	RV (km s^{-1})	rms RV (km s^{-1})	$v \sin i$ (km s^{-1})	$FWHM$ (km s^{-1})	$\log R_{HK}$	EW(Li) (mÅ)	T_{eff} (K)	Remarks
HIP 6177	1	3263.	–	42.00	–	7.19	–		0	5045 ± 17	Zurlo et al. (2013)
HIP 11360	8	4439.68	4479.58	0.81	2.13		~20		95		pipeline
					0.12						SAFIR
HIP 14684	12	3311.79	3805.53	14.72	0.05		10.304		179	5451 ± 7	
HIP 32235	17	2948.87	3805.62	20.72	0.13	17.38	18.124	–4.169	239	5493 ± 11	
HIP 36948	12	5343.45	5347.47	22.64	0.04		12.830		173	5493 ± 15	
TWA 21	24	3402.83	4877.76	18.05	0.17		13.805	–4.06	364	4929 ± 4	
TYC 9245-0617-1	1	4594.78	–	11.49	–				438	5052 ± 111	
HIP 71908	15			7.07	0.15		19.459		–		subset of data
HIP 72399	1	3409.89	–	–11.71	–	14.15		–4.148	0	4903 ± 32	
HIP 76829	8	4542.72	4546.72	–7.08	0.63		~23		0		pipeline
					0.03						SAFIR
HIP 79958	1	3828.80	–	1.74	–		29.978		117	4838 ± 44	
HIP 98470	33	3622.54	5726.84	–10.27	2.02				90		pipeline
					0.09	100					SAFIR, subset of data, Lagrange et al. (2009)
HIP 114046	77	2985.57	4392.68	9.00	0.01		3.184		0		

Notes. The mean measurement of individual spectra is listed when more than one spectrum is available. For early-type stars we list both the absolute RV obtained with the HARPS pipeline and the RV dispersion of the differential RV obtained with the SAFIR code.

Table 6. Wide binaries in the NaCo-LP sample.

NaCo LP Target	Companion	Sep. (arcsec)	Sep. (AU)	avg_μ (mas/yr)	Δ_μ (mas/yr)	ΔV (mag)	fr_μ	Δ_X	$\lvert\Delta RV\rvert$ (km s^{-1})	N_{comp}
HIP 8038	HIP 8039	15.0	435	51.7	7.0	1.88	0.14	2.7	0.75	3
TYC 8484-1507-1	HIP 12326	8.7	535	87.1	7.9	0.51	0.09	0.7	0.00	4
TYC 8484-1507-1	HIP 12361	213.2	12557	88.4	6.7	1.58	0.072	3.0	1.10	–
HIP 25434	HIP 25436	12.0	976	27.1	3.7	0.80	0.14	6.2	0.60	3
HIP 35564	HD 57853	9.2	275	151.6	47.9	0.58	0.37	0.9	3.20	5
TYC 8128-1946-1	HIP 36312	81.7	6853	51.9	3.6	1.05	0.07	4.4	2.20	2
HIP 37923	HIP 37918	23.1	836	166.2	15.4	0.08	0.09	0.5	0.10	2
HIP 46634	HIP 46637	14.0	508	202.7	5.3	0.18	0.03	0.02	1.33	3
HIP 47646	HIP 47645	16.5	1161	123.2	3.2	2.78	0.03	0.3	–	2
HIP 58240	HIP 58241	18.6	649	174.9	34.5	0.03	0.2	0.5	0.90	2
HIP 71908	SAO 252852	15.8	263	302.6	0.7	5.22	0.0024	0.03	0.50	2
HIP 72399	HIP 72400	11.0	609	142.7	12.2	1.06	0.09	0.4	4.50	3
TYC 6786-0811-1	HIP 77235	50.5	3588	64.5	10.0	2.38	0.15	3.3	3.30	2–5?
HD 199058	TYC 1090-0543-1	245.1	16200	68.0	3.3	2.92	0.05	4.0	0.70	3
TYC 9339-2158-1	HIP 116063	36.3	1109	220.4	4.2	1.89	0.02	0.2	0.50	2

Notes. We list the name of the star observed with NaCo, the name of the wide companion, the projected separations in arcsec and in AU, the average proper motion of the components, the proper motion difference, the magnitude difference ΔV, the fractional proper motion difference, the Δ_X index, the absolute value of the RV difference and the number of components. For high-multiplicity systems, additional remarks are listed. Note on high-multiplicity systems: HIP 8038: close visual binary (VB); TYC 8484-1507-1: close VB and SB2 (likely same companion); HIP 12361: wide companion to TYC 8484-1507-1 and HIP 12326 triple system; HIP 25436: spectroscopic and astrometric binary; HIP 35564: SB; HD 57853: SB3; HIP 46637: SB; HIP 72399: SB; TYC 6786-0811-1: close VB; HIP 77235: triple system but physical link to TYC 6786-0811-1 needs confirmation; HD 199058: close VB. See Appendix B for further details and references.

Table 8. Properties of young moving groups (MGs).

MG	U km s^{-1}	V km s^{-1}	W km s^{-1}	Ref.	Age best	Age min	Age max	Ref.	N
TW Hydrae Association	–9.87 ± 4.15	–18.06 ± 1.44	–4.52 ± 2.80	Mal13	8	6	12	ZS04	0
β Pictoris Moving Group	–10.94 ± 2.06	–16.25 ± 1.30	–9.27 ± 1.54	Mal13	16	10	22	Des14	3
Tucana/Horologium Association	–9.88 ± 1.51	–20.70 ± 1.87	–0.90 ± 1.31	Mal13	30	20	40	Tor08	5+3?
Columba Association	–12.24 ± 1.03	–21.32 ± 1.18	–5.58 ± 1.89	Mal13	30	20	40	Tor08	5+1?
Carina Association	–10.50 ± 0.99	–22.36 ± 0.55	–5.84 ± 0.14	Mal13	30	20	40	Tor08	1
Argus Association	–21.78 ± 1.32	–12.08 ± 1.97	–4.52 ± 0.50	Mal13	45	30	55	Des14	2
AB Doradus Moving Group	–7.12 ± 1.39	–27.31 ± 1.31	–13.81 ± 2.16	Mal13	100	50	150	Des14	8+1?
Octans Association	–14.5 ± 0.9	–3.6 ± 1.6	–11.2 ± 1.4	Tor08	20	10	30	Tor08	0
ϵ Chamaeleon	–11.0 ± 1.2	–19.9 ± 1.2	–10.4 ± 1.6	Tor08	6	4	8	Tor08	2
η Chamaeleon	–12.0 ± 1.0	–19.0 ± 1.0	–10.0 ± 1.0	ZS04	8	6	10	ZS04	0
Cha-Near Association	–11.0 ± 1.0	–16.0 ± 1.0	–8.0 ± 1.0	ZS04	10	6	15	ZS04	0
Carina-Near Moving Group	–25.9 ± 1.0	–18.1 ± 1.0	–2.3 ± 1.0	Zuk06	200	150	300	Zuk06	4+1?
Ursa Majoris Moving Group	14.0 ± 1.0	1.0 ± 1.0	–9.0 ± 1.0	ZS04	500	400	600	Kin03	0
Hercules-Lyra Association	–13.2 ± 2.5	–20.6 ± 1.6	–11.9 ± 1.0	LoS06	200	150	300	LoS06	1
Corona Australis Association	–3.8 ± 1.2	–14.3 ± 1.7	–8.3 ± 2.0	Qua01	10	6	20	Qua01	3?
IC 2391 Open Cluster	–20.6 ± 2.0	–15.7 ± 2.0	–9.1 ± 2.0	Mon01	45	30	55	Des14	0
Hyades Open Cluster	–40.0 ± 2.0	–17.0 ± 2.0	–3.0 ± 2.0	ZS04	625	575	675	Per98	0
Pleiades Open Cluster	–12.0 ± 2.0	–21.0 ± 2.0	–11.0 ± 2.0	ZS04	125	110	140	Sta98	0
Upper Scorpius Association	–6.4 ± 0.5	–15.9 ± 0.7	–7.4 ± 0.2	Che11	11	5	14	Pec12	2?
Upper Centaurus Lupus Ass.	–5.1 ± 0.6	–19.7 ± 0.4	–4.6 ± 0.3	Che11	16	10	18	Pec12	1?
Lower Centaurus Crux Ass.	–7.8 ± 0.5	–20.7 ± 0.6	–6.0 ± 0.3	Che11	17	10	19	Pec12	3?

Notes. We list the MG name and the U, V, and W space velocity with corresponding literature source. We give the most probable age, minimum and maximum values, and the associated literature source. The final column gives the number of members in the NaCo-LP sample (wide companions not observed with NaCo are not included).

References. Mal13: Malo et al. (2013); Tor08: Torres et al. (2008); ZS04: Zuckerman & Song (2004); Mon01: Montes et al. (2001); Zuk06: Zuckerman et al. (2006); Kin03: King et al. (2003); LoS06: López-Santiago et al. (2006); Qua01: Quast et al. (2001); Per98: Perryman et al. (1998); Sta98: Stauffer et al. (1998); Che11: Chen et al. (2011); Pec12: Pecaut et al. (2012); Des14: this paper.

Appendix A: Literature compilation

The compilation of literature values for several stellar parameters (RV, $v \sin i$, EW of Li 6707.8 Å resonance line, $\log R_{\rm HK}$, $T_{\rm eff}$) is shown in Table A.1.

Table A.1. Summary of measurements of spectroscopic parameters available in the literature.

Star	JD –2 450 000	RV (km s^{-1})	$v \sin i$ (km s^{-1})	EW Li (mÅ)	S	log R_{HK}	T_{eff} (K)	Reference	Remarks
TYC 5839-0596-1		20.0	36.5 ± 3.7	100				SACY	N = 1, SB2, Halpha emission
TYC 5839-0596-1a	5106.75	+51.5 ± 1.5	18.0 ± 2.0		2.135	–3.990		Des14	FEROS, deblended
TYC 5839-0596-1b	5106.75	+21.3 ± 1.5	17.0 ± 2.0					Des14	FEROS, deblended
TYC 0603-0461-1		–12.9		160				SACY	N = 1 Halpha emission
HIP 3924		10.7	28	138				Wic03	
			33.5 ± 1.9	132 ± 5				Wei10	
	5056.95	+1.5 ± 0.5	8.0 ± 2.0	37	0.257	–4.572	5609 ± 105	Des14	FEROS,A component
	5056.95	~19						Des14	FEROS, B component
	5056.95	~9						Des14	approx. center of mass RV
HIP 6177									see Zurlo et al. (2013)
HIP 8038		8.7	5.0	80				SACY	N = 1
HIP 8039		9.5	5.0	80				SACY	N = 1
					0.459	–4.457	5151	Gra06	
		9.4 ± 0.3	5.0					Nor04	N = 3, rms RV 0.6 km s^{-1}
HIP 10602		10.4 ± 1.3						BaB00	N = 8
			240	0			15665	DaS09	
							12470 ± 560	Sou10	
HIP 11360				40				Deb08	
		8.8 ± 3.0						Moo06	
							6755 ± 71	Mas06	
	5399.87	2.9 ± 4.1		99	0.199	–4.748		Des14	FEROS
	5399.88	1.9 ± 2.8		90	0.194	–4.769		Des14	FEROS
	4439–4479	0.8 ± 0.8		95				Des14	HARPS N = 8
HIP 12326		16.0 ± 0.2	22.3 ± 0.4	50				SACY	N = 3; rms RV 0.3 km s^{-1}
		15.9	22	55			6200	Tor00	
	–44.21	16.1 ± 0.7	21 ± 2					Cut99	components exchanged
	–42.24	16.4 ± 2.6						Cut99	components exchanged
	–40.21	15.6 ± 2.1						Cut99	components exchanged
		16.1						Mon01	
			20	58			6200	Fav95	
		16.2 ± 0.2	20	40				Moo11	
	5106.82	15.5 ± 0.5	22.0 ± 2.0	46	0.305	–4.443	5979 ± 85	Des14	FEROS
TYC 8484-1507-1		16.8 ± 0.9	6.0 ± 0.2	250				SACY	N = 3 rms RV = 1.6 km s^{-1}, SB?
		15.9	8	255			5600	Tor00	
	–44.24	16.4 ± 0.7	11 ± 3					Cut99	components exchanged
	–42.22	16.2 ± 0.9						Cut99	components exchanged
	–40.19	15.9 ± 1.1						Cut99	components exchanged
			<8	193			5610	Fav95	
		15.8 ± 0.3		220				Moo11	
HIP 12361		17.3 ± 8.5	100					Moo11	
HIP 12394		13.6 ± 0.9						XHIP	
			96 ± 8					Roy02	
			98				10575 ± 198	Pau05	
							10471	Zor12	
			99.5 ± 18.6					Rei04	
HIP 13008		3.2 ± 2.0						Nor04	
		3.2 ± 2.0						BaB00	N = 3, RV var
		2.4 ± 0.7						Gon06	N = 2 rms 0.8 km s^{-1}
							6678 ± 76	Mas06	
					0.428	–4.161	6721	Gra06	
		2.12 ± 0.73						Gre99	N = 1, Suspected SB
	5198.58	1.5 ± 1.0			0.228	–4.642		Des14	FEROS
	6509.91	0.6 ± 1.6	80					Des14	CORALIE

References. Des14: this paper; SACY: Torres et al. (2006); Aar08: Aarnio et al. (2008); Alc96: Alcala et al. (1996); Alc00: Alcalá et al. (2000); Amm12: Ammler-von Eiff & Reiners (2012); Baa97: Baade & Kjeldsen (1997); BaB00: Barbier-Brossat & Figon (2000); Bia12: Biazzo et al. (2012); Bub11: Bubar et al. (2011); Cin07: Cincunegui et al. (2007); Cut99: Cutispoto et al. (1999); Cut02: Cutispoto et al. (2002); Cut03: Cutispoto et al. (2003); DaS09: da Silva et al. (2009); Deb08: Debes et al. (2008); Des06: Desidera et al. (2006); DOr12: D'Orazi et al. (2012); Fav95: Favata et al. (1995); Feh74: Fehrenbach & Duflot (1974); Gal05: Gálvez et al. (2005); Gal06: Gálvez et al. (2006); Gle05: Glebocki & Gnacinski (2005); Gon06: Gontcharov (2006); Gra06: Gray et al. (2006); Gre99: Grenier et al. (1999); Gui09: Guillout et al. (2009); Hen96: Henry et al. (1996); Jen06: Jenkins et al. (2006); Jen11: Jenkins et al. (2011); Lag08: Lagrange et al. (2009); LoS06: López-Santiago et al. (2006); Mam02: Mamajek et al. (2002); Mam04: Mamajek (2004); Mas06: Masana et al. (2006); Men08: Mentuch et al. (2008); Mon01: Montes et al. (2001) Moo06: Moór et al. (2006); Moo11: Moór et al. (2011); Moo13: Moór et al. (2013); Nid02: Nidever et al. (2002); Nor04: Nordström et al. (2004); Pau05: Paunzen et al. (2005); Pau06: Paulson & Yelda (2006); RAVE3: Siebert et al. (2011); Rei03: Reid (2003); Rei04: Reiners & Royer (2004); Rei06: Reiners (2006); Rhe07: Rhee et al. (2007); RoP02: Rocha-Pinto et al. (2002); Roy02: Royer et al. (2002); Roy07: Royer et al. (2007); Saa90: Saar et al. (1990); Sch07: Scholz et al. (2007); Sch09: Schröder et al. (2009); Son02: Song et al. (2002); Son03: Song et al. (2003); Son12: Song et al. (2012); Sou10: Soubiran et al. (2010); Str00: Strassmeier et al. (2000); Str12: Strassmeier et al. (2012); Tor00: Torres et al. (2000); ViA09: Viana Almeida et al. (2009); VSOP: Dall et al. (2007); Wai05: Waite et al. (2005); Wai11: Waite et al. (2011); Wei10: Weise et al. (2010); Whi07: White et al. (2007); Wic99: Wichmann et al. (1999); Wic03: Wichmann et al. (2003); Woo05: Woolf & Wallerstein (2005); Wri04: Wright et al. (2004); XHIP: Anderson & Francis (2012); Zor12: Zorec & Royer (2012); Zuk06: Zuckerman et al. (2006).

Table A.1. continued.

Star	JD –2 450 000	RV (km s^{-1})	$v \sin i$ (km s^{-1})	EW Li (mÅ)	S	log R_{HK}	T_{eff} (K)	Reference	Remarks
HIP 14684			7.1 ± 1.1	165 ± 5				Wei10	
			7	191			5383	DaS09	
		14.2 ± 1.8	6.2 /6.4		0.476	–4.40		Jen11	FEROS
		14.46 ± 0.70	10.0	178	0.444	–4.40 ± 0.11		Whi07	
			7.0				5500 ±	Pau06	
		14.6 ± 0.7						Mon01	
					0.476	–4.38		Wri04	$N = 5$
								Str00	
	3331.69	14.1 ± 0.5	5.5 ± 0.6	175	0.502	–4.370	5463 ± 20	Des14	FEROS
	3981.87	14.0 ± 0.4	5.6 ± 0.8	180	0.489	–4.383	5478 ± 38	Des14	FEROS
		14.65	6.29			–4.38		Des14	CORALIE, $N = 4$
	3311–3805	14.71		179			5451 ± 7	Des14	HARPS,$N = 12$
TYC 8060-1673-1		15.3		229				SACY	$N = 2$, rms RV 0.5 km s^{-1}
							4487	DaS09	
			10				4777 ± 70	ViA09	
	5100.83	14.1 ± 0.4	9.7 ± 1.2	224	1.810	–4.208	4876 ± 28	Des14	FEROS $N = 2$ (same night)
HIP 19775		20.8	13.9 ± 0.1	183				SACY	$N = 3$, rms RV 0.3 km s^{-1}
							6140	DaS09	
			13				5910	ViA09	
		20.2 ± 0.3	14					Nor04	$N = 2$, rms RV 0.3 km s^{-1}
	5109.79	20.4 ± 0.5	13.1 ± 0.8	170	0.433	–4.261	5840 ± 45	Des14	FEROS
HIP 23316		23.5	7.9 ± 1.2	210				SACY	$N = 1$
			8	210			5721	DaS09	
			7				5716 ± 50	ViA09	
	5204.73	22.5 ± 0.1	7.7 ± 2.1	225	0.659	–4.108	5552 ± 33	Des14	FEROS
HD 32981			6	140			5995	DaS09	
			5.0 ± 2.0				6200	DOr12	
	4787.65	25.00 ± 0.00	4.8 ± 0.6		0.366	–4.357	5975	Des14	FEROS
BD-09 1108			18.0	245			5645 ±	DaS09	
	4787.66	20.50 ± 0.80	15.7 ± 1.1	205	0.595	–4.151	5660 ± 45	Des14	FEROS
HIP 25434	2721.03	24.94 ± 0.33	40		0.39	–4.30		Des06	
	2721.03			183				Des14	FEROS, same spec as Des06
	Jul.–Aug. 09	23.6 ± 1.8		158 ± 10				Moo13	
	6360.64	24.2 ± 1.5	50					Des14	CORALIE
HIP 25436	2721.01	32.17 ± 1.30	112		0.25	–4.57		Des06	
	2721.01			107				Des14	FEROS, same spec as Des06
	Jul.–Aug. 09	22.6 ± 6.7		<41				Moo13	
	6360.65	21.8 ± 3.8	110					Des14	CORALIE
TYC 9162-698-1		18.7	22.3 ± 3.1	226				SACY	$N = 7$, rms RV 1.0 km s^{-1}
		14 ± 7						Feh74	
	5203.69	18.6 ± 0.5	20.2 ± 2.6	212	0.482	–4.232	5811 ± 105	Des14	FEROS
TYC 5346-132-1		24.5 ± 1.5	30	290 ± 10				Alc00	
		26.2 ± 1.0	29					Alc00	
				350				Alc96	
	5198.74	24.0 ± 1.5		280	0.937	–3.992	5324 ± 87	Des14	FEROS
HIP 30261		24.8		200				SACY	$N = 1$
		25.1 ± 0.3	8.0					Nor04	$N = 1$
							5666 ± 51	Mas06	
	5203.72	24.5 ± 0.4	9.2 ± 0.8	186	0.445	–4.296	5757 ± 37	Des14	FEROS
TYC 7617-549-1		25.0 ±	11.6 ± 1.2	310				SACY	$N = 1$
TYC 9181-0466-1		16.4 ± 0.1	13.5 ± 3.3	210				SACY	$N = 4$
			11.6 ± 0.9	198 ± 3				Wei10	
	3807.59	15.6 ± 0.7	11.9 ± 1.2	214	0.538	–4.181	5682 ± 45	Des14	FEROS
	3815.59	16.1 ± 0.6	11.6 ± 0.9	205	0.535	–4.184	5670 ± 40	Des14	FEROS
HIP 32235		20.7 ± 0.1	12.4 ± 0.3	233				SACY	$N = 3$
	4167.59	20.1 ± 0.4	11.6 ± 1.1	237	0.621	–4.154	5444 ± 36	Des14	FEROS
	2948–3805	20.72	17.38	239		–4.169	5493 ± 11	Des14	HARPS $N = 17$
HIP 35564		17.3 ± 1.5						Nor04	$N = 1$
	2721.99	26.85 ± 0.79	68		0.23	–4.64		Des06	$N = 1$
	Jan. 2006	18.6 ± 2.0						Zuk06	$N = 1$
		22.54 ± 0.68						Gre99	$N = 1$
					0.354	–4.31	6603	Gra06	
		21.40 ± 0.60						XHIP	
			65.6 ± 3.3				6366	Amm12	
	5109.84	24.0 ± 2.0			0.218	–4.667		Des14	FEROS
	6357.73	13.7 ± 1.1	~60					Des14	CORALIE
HD 57853		15.5 ± 3.9	20					Nord04	
	2721.99	0.32 ± 0.18	19.5		0.29	–4.49		Des06	SB2
					0.333			Gra06	
		17.6 ± 0.7	22.0 ± 1.5					Saa90	orbit

Table A.1. continued.

Star	JD –2 450 000	RV (km s^{-1})	$v \sin i$ (km s^{-1})	EW Li (mÅ)	S	log R_{HK}	T_{eff} (K)	Reference	Remarks
TYC 8128-1946-1		21.10	52 ± 5.2	250				SACY	
	5927.64	17.0 ± 0.5	50					Des14	CORALIE
HIP 36312						–4.46		Jen11	
	4908.53	+17.1 ± 2.3		130	0.276	–4.515		Des14	FEROS
	5931.82	16.6 ± 0.1						Des14	CORALIE
HIP 36414		29.0 ± 5.0	25					Nor04	N = 10 rms RV 1.2 km s^{-1}
		28.0 ± 2.0		80				Zuc06	
							6130 ± 56	Mas06	
	4782.88	24.7 ± 1.3	31.5 ± 3.3	72	0.288	–4.490	5753 ± 110	Des14	FEROS
HIP 36948									see Desidera et al. (2011)
	5343–5347	22.64		173			5493 ± 15	Des14	HARPS, N = 12
HIP 37563		17.5 ± 0.2	14					Nor04	N = 6 rms RV 0.5 km s^{-1}
		17 ± 1		135				Zuc06	
			14.4 ± 1.0	122 ± 1				Wei10	
			15	145				Cut0203	
					0.347	–4.422	5860	Gra06	
					0.427	–4.30		Hen96	N = 1
		17.1	15	147/142				Wic03	
		16.4	15	127.2				Wai05	EwLi corr.
		18	14					Wai05	
	3809.66	17.1 ± 0.4	14.3 ± 1.0	130	0.356	–4.405	5801 ± 56	Des14	FEROS
HIP 37918		19.1	6.3 ± 1.2	120				SACY	N = 1
		17.2 ± 0.4	6					Nor04	N = 12 rms RV 1.2 km s^{-1}
		17 ± 1		110				Zuc06	
	2721.08	17.65 ± 0.11	6.0		0.59	–4.27		Des06	
								Gra06	
			6.0 ± 2.0				5550	DOr12	
	3338.82	18.1 ± 0.1	5.1 ± 0.8	116	0.505	–4.338	5428 ± 22	Des14	FEROS
HIP 37923		17.9	3.2 ± 1.2	70				SACY	N = 1
		17.3 ± 0.2	4					Nor04	N = 7 rms RV 0.5 km s^{-1}
		17 ± 1		76				Zuc06	
	2721.10	17.70 ± 0.11	3.2		0.53	–4.31		Des06	
								Gra06	
			3.0 ± 2.0				5450	DOr12	
	3777.62	+16.9 ± 0.3	3.0 ± 1.0	64	0.465	–4.384	5375 ± 20	Des14	FEROS
		17.73	2.67			–4.372		Des14	CORALIE, N = 5
TYC 8927-3620-1		15.9	99.9 ± 9.9	300				SACY	N = 1
HIP 46634		27.3 ± 0.2	4					Nor04	N = 2 rms RV 0.1 km s^{-1} comp. exchanged
				25				Cut99	
								Str00	
		27.1 ± 0.4						Mon01	
		27.07 ± 0.04						Gal05	multi-epoch, RV constant
		27.93 ± 0.05	<3	33 ± 6			5140 ± 35	Str12	N = 96 DT=1129, single
						–4.40		Des14	SOPHIE
HIP 46637		15.9 ± 25.7	13					Nor04	N = 2 rms RV 36.3 km s^{-1} comp. exchanged
								Wic03	
								Cut02	
								Str00	
		~28		131				Gal06	
		29.26 ± 0.3	12.5 ± 0.5	109 ± 7			5150 ± 65	Str12	SB, center of mass RV
HIP47646		49.9 ± 0.4	16					Nor04	N = 2
	4783.87	51.0 ± 0.1			0.179	–4.830		Des14	FEROS
HIP47645					0.513	–4.30		Gra06	
TWA 21		17.7	9.4 ± 1.2	365				SACY	N = 1
		17.5 ± 0.8		290				Son03	
			6.0 ± 1.0					Sch07	
				369 ± 20			4689 ± 14	Men08	N = 5
			9.0				4923 ± 119	ViA09	
			8.2 ± 1.0	357 ± 3				Wei10	
	3807.65	18.0 ± 0.1	8.7 ± 1.3	364	1.777	–4.039	4898 ± 21	Des14	FEROS (N = 1)
	3402–4596	18.0 ± 0.1		364	1.69	–4.06	4929 ± 4	Des14	HARPS (N = 24)
TYC 7188-575-1		+42.9 ± 2.1	25	50				Son02	
	5254.70	+44.7 ± 2.0			3.786	–3.885		Des14	FEROS
	5931.87	–38.75 ±						Des14	CORALIE
	6357.80	–24.71 ±						Des14	CORALIE
TYC 6069-1214-1		19.4		240				SACY	N = 1
TYC 7722-0207-1		10.4	27.2 ± 2.7	200				SACY	N = 1
		10.6	15	130				Rei03	
	4944.71	8.8 ± 0.8	31.5 ± 6.5	190	0.845	–4.129	5400 ± 50	Des14	FEROS

Table A.1. continued.

Star	JD –2 450 000	RV (km s^{-1})	$v \sin i$ (km s^{-1})	EW Li (mÅ)	S	log R_{HK}	T_{eff} (K)	Reference	Remarks
TYC 7743-1091-1		17.4	17	114/82				Wic03	
	3926.52		17.6 ± 1.1	95 ± 1				Wei10	
	3926.52	+21.9 ± 0.1		113.4 ± 2.0			4931 ± 59	Des14	FEROS
HIP 58240					0.354	–4.43		Hen96	
					0.325	–4.482	5749	Gra06	
		5.8	5.2 ± 1.2	110				SACY	$N = 1$
		6.2 ± 0.2	5					Nor04	N-4, rms RV 0.2 km s^{-1}
		6.0 ± 0.4		111				Zuc06	
			5.0 ± 2.0				5900	DOr12	
	5254.76	+5.9 ± 0.1	4.0 ± 0.5	115	0.365	–4.15	5835 ± 24	Des14	FEROS
HIP 58241					0.398	–4.34		Hen96	
					0.388	–4.359	5784	Gra06	
		6.9	9.0 ± 1.2	110				SACY	$N = 1$
		6.9 ± 0.1	7					Nor04	$N = 8$, rms RV 0.4 km s^{-1}
		6.7 ± 0.3		110				Zuc06	
			9.0 ± 2.0					DOr12	
							5800	Bia12	
	5254.75	6.9 ± 0.5	8.2±0.8	114	0.394	–4.350	5710 ± 22	Des14	FEROS
TYC 9231-1566-1		14.2	13.1 ± 1.2	280				SACY	$N = 1$
			13	280			5344	DaS09	
			12				4979 ± 40	ViA09	
				140			5781	Mam02	
							5763 ± 132	Bub11	
	5254.84	13.5 ± 0.1	12.5 ± 0.8	270	0.645	–4.118	5530 ± 40	Des14	FEROS
TYC 8979-1683-1		13.3	31.9 ± 3.2	290				SACY	$N = 1$
	4942.79	12.1 ± 2.6		290	0.868	–4.059	5650 ± 145	Des14	FEROS
		13.9 ± 1.9		260				Son12	$N = 3$
TYC 8989-0583-1		10.8	47.0 ± 4.7	350				SACY	$N = 1$
		10.50 ± 3.0		260				Son12	$N = 3$
TYC 9245-0617-1		12.8	24.3 ± 2.4	400				SACY	$N = 1$
			24	400			4917	DaS09	
				370			5176	Mam02	
			20.0 ± 3.0					Gle05	
			26.0 ± 1.5	400 ± 6				Wei10	
	3420.79	13.2 ± 2.4	28.2 ± 6.2	391	1.597	–3.873	5083 ± 70	Des14	FEROS
	3421.78	14.1 ± 0.5	26.7 ± 2.2	410	1.595	–3.874	5090 ± 70	Des14	FEROS
	3421.88	14.7 ± 0.7	28.8 ± 2.0	415			5114 ± 62	Des14	FEROS
	3422.76	12.2 ± 0.6	26.2 ± 3.1	410	1.592	–3.874	5059 ± 65	Des14	FEROS
	4582.77	9.6 ± 0.9	26.0 ± 1.7	393	1.441	–3.919	5071 ± 65	Des14	FEROS
	4594.78	11.5		438			5052 ± 111	Des14	HARPS, $N = 1$
		11.1 ± 1.5		350				Son12	$N = 3$
HIP 63862		1.1	10.9 ± 1.2	140.0				SACY	$N = 1$
		1.1 ± 0.2	11					Nor04	$N = 5$
			11.6 ± 0.9	139 ± 1				Wei10	
		2	10					Wai05	
			12	155				Cut02-03	
		1.1	11	154				Wic03	EWLi=145 corrected
					0.460	–4.30		Hen96	$N = 1$
	3447.88	1.3 ± 0.1	10.6 ± 0.9	145	0.416	–4.347	5760 ± 32	Des14	FEROS
	3447.87	1.3 ± 0.1	10.6 ± 1.0	141	0.415	–4.347	5729 ± 25	Des14	FEROS
TYC 7796-2110-1		25.0	113.0 ± 11.3	400:				SACY	$N = 1$
				315				Son12	$N = 1$
	5256.82	21.6 ± 9.6	fast	339	0.881	–4.183		Des14	FEROS
	5931.83	1.3 ± 4.5	~90					Des14	CORALIE
TYC 9010-1272-1		10.2	38 ± 3.8	210				SACY	$N = 2$, rms RV 0.5 km s^{-1}, SB2?
		43.4 ± 4.9	8					Nor04	$N = 5$ rms RV 11 km s^{-1}
	3909.59	11.5 ± 0.8		200	0.534	–4.137	5324 ± 92	Des14	FEROS, SB2
HIP 70351		–8.3	16.9 ± 1.2	170				SACY	$N = 1$
	4940.77	–8.6 ± 1.2	12.3 ± 0.7	164	0.460	–4.301	5624 ± 50	Des14	FEROS
α Cir	3423.84	6.2 ± 0.2	14.5 ± 1.8					Des14	FEROS
		7.07						Des14	HARPS, $N = 15$ subset of data
GJ 560B		7.0 ± 4.0						LoS06	
	3423.83	6.6 ± 0.4	3.0 ± 1.2	0	0.672	–4.705	4761 ± 35	Des14	FEROS
HIP 71933		8.7						SACY	$N = 1$, SB?
		12.1 ± 0.4	2.0					Nor04	$N = 1$, discr. $v \sin i$
		4.0	75	139 ± 7				Wai11	
	4496.86	3.8 ± xxx		132	0.377	–4.356		Des14	$N = 2$, same night
HIP 72399		–25.9		0				SACY	$N = 1$
					2.076	–4.114		Gra06	
	3409.89	–11.71	14.15	0		–4.148	4903 ± 32	Des14	HARPS $N = 1$
	6357.79	30.31 ± 0.05						Des14	CORALIE

Table A.1. continued.

Star	JD –2 450 000	RV (km s^{-1})	$v \sin i$ (km s^{-1})	EW Li (mÅ)	S	log R_{HK}	T_{eff} (K)	Reference	Remarks
	6357.82	33.24 ± 0.06						Des14	CORALIE
HIP 72400		0.3		0				SACY	N = 1
					1.176			Gra06	
	6360.74	1.35 ± 0.01						Des14	CORALIE
TYC 7835-2569-1		3.3	17.0	150				SACY	N = 1
		–10.0 ± 5.0	17					Nor04	N = 2, rms 2.1 km s^{-1}, SB
		1.9	16.0	157				Wic99	
HIP 76829		–5.4 ± 1.8						Nor04	
		–5.4 ± 2.0						Mon01	
							6649	Gra06	
			71.6 ± 3.6				6681	Rei06	
					0.234			Sch09	
	4542–4546	–7.1		0				Des14	HARPS N = 8
TYC 6781-0415-1		–6.7		410				SACY	N = 1
		–3.0 ± 2.1	29	409/429			5410	Aar08	
HIP 77235		–20.7 ± 1.8						XIP	
			68					Roy07	
TYC 6786-0811-1		–24.0		180.0				SACY	N = 1
HIP 78747			23.7 ± 1.2					Rei03	
		–6.2 ± 3.7						BaB00	
					0.322	–4.328	6743	Gra06	
			23.7		0.179		6606	Sch09	
	4940.86	–8.2 ± 0.5	24.0 ± 3.0	23	0.175	–4.861	6005 ± 55	Des14	FEROS
TYC 6209-0769-1		3.0		140				SACY	N = 1
HIP 79958		2.0	16.8 ± 1.2	110				SACY	N = 1
		1.8 ± 0.4	17					Nor04	N = 2 rms 0.4 km s^{-1}
					1.725	–4.147	4607	Gra06	
		1.68						VSOP	from VSOP web site
	3828.80	1.74		117	1.912		4838 ± 44	Des14	HARPS
		1.74				–4.45		Des14	CORALIE, N = 3
HIP 80290		–5.0	37.0 ± 3.7	200				SACY	N = 1
HIP 80758		6.9	11.1 ± 1.2	280				SACY	N = 1
		6.3 ± 0.3	11					Nor04	N = 2 rms 0.3 km s^{-1}
	4940.87	6.0 ± 0.1	10.8 ± 1.0	262	0.878	–4.065	5328 ± 28	Des14	FEROS
TYC 6818-1336-1		–2.4	71.0 ± 7.1	150				SACY	N = 1
		–4.3 ± 1.6	56		180/198		6440	Aar08	US ?
TYC 6815-0874-1		0.8	90.0 ± 2.8	270				SACY	N = 2 rms 0.2 SB2?
TYC 6815-0084-1		–4.4 ±	57.0 ±	310.0				SACY	N = 2 SB2?
		–6.5 ± 1.5	53 ±	307/324			5250	Aar08	Upper Sco? dist>100pc
	3909.79	–1.5 ± 5.4	fast	240	0.879	–4.087	5300 ± 150	Des14	
TYC 7362-0724-1		–3.1	36.7 ± 3.7	270				SACY	N = 1
TYC 8728-2262-1		1.6	35.3 ± 1.4	360				SACY	N = 4rms 1.4 km s^{-1}
			35	360			5036	DaS09	
	4941.87	–0.2 ± 0.9		325	1.228	–3.992	5245 ± 110	Des14	FEROS
		–0.5 ± 3.7		310				Son12	N = 2
HIP 86672		–6.2 ± 1.0	17					Nor04	N = 2 rms RV 1.4 km s^{-1}
		–5.8	15.5 ± 0.2	260				SACY	N = 4 rms RV 1.3 km s^{-1}
		–5.7 ± 2.5					6470	RAVE3	
HIP 89829		–7.0	114.7 ± 2.5	290				SACY	N = 3 rms RV 2.6 km s^{-1}
			115	290			5645	DaS09	
		–4.7	114	211 ± 13				Wai11	
HIP 93375		–5.7		140				SACY	N = 1
		–5.8 ± 0.5	17					Nor04	N = 2 rms RV 0.3 km s^{-1}
			17	140			6254	DaS09	
	2005-08-28	–6.6 ± 2.2					6383	RAVE3	
	2005-08-28	–6.2 ± 2.2					6577	RAVE3	
							6073 ± 60	Mas06	
HIP 94235				165				SACY	N = 4 rms RV 1.1 km s^{-1}
		8.1 ± 0.6	24					Nor04	N = 4 rms RV 1.1 km s^{-1}
			24	165			6102	DaS09	
			24	165				Cut02	
							6010 ± 53	Mas06	
TYC 6893-1391-1		–12.7	4.5 ± 1.2	125				SACY	N = 1
					0.780	–4.334		Des14	FEROS
TYC 5736-0649-1		–7.0	206.0 ± 20.6	250				SACY	N = 3, rms RV 3.5 km s^{-1}, SB?
					0.401	-4.360		Des14	FEROS
HD 189285			9.0	140			5630	DaS09	
			8.0 ± 2.0				5800	DOr12	
	3906.84	–19.5 ± 0.1	8.3 ± 0.9	141	0.455	–4.325	5545 ± 35	Des14	FEROS
	4782.53	–19.6 ± 0.2	8.3 ± 0.7	135	0.449	–4.331	5620 ± 23	Des14	FEROS

Table A.1. continued.

Star	JD –2 450 000	RV (km s^{-1})	$v \sin i$ (km s^{-1})	EW Li (mÅ)	S	log R_{HK}	T_{eff} (K)	Reference	Remarks
HIP 98470			100					Lag08	rms RV 86 m/s
			72.6		0.339	-4.309	6259	Sch09	
		–13.2 ± 3.7						Nor04	N = 2, rms RV 2.5 km s^{-1}
			72.6 ± 3.6				6259	Rei06	
					0.470	–4.164	6333	Gra06	
		–8.20 ± 5.0						Mon01	
		–8.20						BaB00	
			86					Baa97	flagged as SB
							6399 ± 67	Mas06	
	5052.80	–10.0 ± 2.0			0.303	–4.442		Des14	FEROS
	3622-5726	–10.27		90				Des14	HARPS, N = 33
TYC 5164-0567-1			8.00	290			5083	DaS09	
	3906.86	–16.50 ± 0.00	7.8 ± 0.9	280	0.916	–4.333	5140 ± 20	Des14	FEROS
	4783.50	–16.50 ± 0.10	7.7 ± 0.9	260	0.821	–4.382	5197 ± 25	Des14	FEROS
HIP 99273		–5.8 ± 2.2	45					Nor04	N = 2, rms RV 3.1 km s^{-1}
			37.7		0.247	–4.603		Sch09	
		–7.8 ± 2.2	37.0 ± 1.6	58	0.257 ± 0.091	–4.49 ± 0.24		Whi07	
				95 ± 6				Mam04	
			45	95			6521	DaS09	
							6600	Rhe07	
							6473 ± 68	Mas06	
			48.8 ± 3.0	101 ± 5				Wei10	
	3102.88	–6.4 ± 1.7	fast	91	0.200	–4.734		Des14	FEROS
HD 199058			14.00	160			5894	DaS09	
		–19.09 ± 0.99	11.00	160.5			5721	Gui09	
	2480.51	–19.00 ± 1.31						Gui09	
	2481.44	–19.18 ± 1.49						Gui09	
	3908.85	–18.70 ± 0.70	13.20 ± 0.6	160	0.392	–4.345	5680 ± 60	Des14	
	4783.52	–18.70 ± 0.70	14.50 ± 0.5	160	0.377	–4.367	5752 ± 41	Des14	
TYC 1090-0543-1			18.0	120			4589	DaS09	
	3908.86	–19.5 ± 0.0	17.3	115	2.650	–3.975	4775 ± 45	Des14	
TYC 5206-0915-1		–23.3		40				SACY	N = 1
	5068.62	0.9 ± 0.6	22.9 ± 1.6	40	1.115	–4.011	5170 ± 65	Des14	FEROS
	6508.67	17.47 ± 0.1						Des14	CORALIE
HIP 105384		24.1	6.5 ± 1.2	0				SACY	N = 1
		24.0 ± 0.1	6					Nor04	6 rms 0.3 km s^{-1}
					0.409	–4.36		Hen96	N = 1
					0.361	–4.436	5696	Gra06	N = 1
					0.49			Cin07	N = 4
							5774 ± 51	Mas06	
		23.9	7	0				Wai05	N = 2
	3904.91	+23.9 ± 0.2	5.3 ± 1.0	0	0.429	–4.337	5661 ± 22	Des14	FEROS
		24.43	5.9			–4.356		Des14	N = 10, CORALIE
HIP 105612		–2.8	~5	7.6				Wai05	N = 2
		–2.1 ± 0.2	3					Nor04	N = 5, rms RV 0.3 km s^{-1}
					0.384	–4.40		Hen96	N = 1
					0.274	–4.602	5566	Gra06	N = 1
							5694 ± 44	Mas06	
	5054.78	–2.7 ± 0.5	3.0 ± 1.0	29	0.327	–4.491	5647 ± 25	Des14	FEROS
		–1.7	3.3			–4.48		Des14	N = 3, CORALIE
HIP 107684		3.6	10.4 ± 1.2	190				SACY	N = 2 rms RV 0.5 km s^{-1}
			10	190			5759	DaS09	
			9				5714 ± 52	ViA09	
			11.2 ± 0.9	190 ± 1				Wei10	
HIP 108422		1.1	128.2 ± 1.7	294				SACY	N = 11, rms RV 2.1 km s^{-1}
			139.8 ± 9.4					Sch07	
				261 ± 20			5541 ± 27	Men08	
TYC 8004-0083-1		–9.1	15.1 ± 1.2	175				SACY	N = 1
			14.9 ± 1.0	175				Wei10	
	4788.52	–11.0 ± 0.5	15.0 ± 1.5	164	0.502	–4.239	5653 ± 51	Des14	FEROS
HIP 114046		8.81						Nid02	
		7.50		50				SACY	N = 4, rms RV 0.1 km s^{-1}
		7.5 ± 0.2	1.0					Nor04	=4, rms RV 0.1 km s^{-1}
						1.070		Wri04	
						1.081	–5.01	Jen06	HK outside cal range
							3680 ± 130	Woo005	
	4784.55	+7.5 ± 0.5	2.7 ± 0.5	0				Des14	FEROS
	2985–4392	+9.0						Des14	HARPS, N = 77
TYC 9338-2016-1		9.5	29.9 ± 0.5	259				SACY	N = 9, rms RV 0.8 km s^{-1}
		5.5 ± 1.9					5973	RAVE3	

Table A.1. continued.

Star	JD −2 450 000	RV (km s^{-1})	$v \sin i$ (km s^{-1})	EW Li (mÅ)	S	log R_{HK}	T_{eff} (K)	Reference	Remarks
			31.8 ± 1.9	259 ± 4				Wei10	
	4778.58	7.3 ± 1.7		221	0.568	-4.167		Des14	FEROS
TYC 9529-0340-1		9.2	73.9 ± 1.4	276				SACY	N = 11 rms RV = 2.0 km s^{-1}
			74	276			5481	DaS09	
TYC 9339-2158-1		4.3	4.1 ± 1.2	30				SACY	N = 1
		3.6 ± 0.2	4					Nor04	N = 4, rms 0.2 km s^{-1}
HIP 116063		3.9	3.4 ± 1.2	110				SACY	N = 1
		3.6 ± 0.2	4					Nor04	N = 5, rms RV 0.3 km s^{-1}
					0.284	-4.51		Hen96	
					0.277		5911	Gra06	
	1384.75	2					5910	RoP02	
	5004.94	3.1 ± 0.1	2.6 ± 0.9	110	0.311	-4.465	5963 ± 30	Des14	FEROS
TYC 6406-0180-1		–9.7	5.5 ± 1.2	30				SACY	N = 1
HIP 116910		11.1	31.1 ± 3.1	230				SACY	N = 4 rms 1.7 km s^{-1}
							5567	DaS09	

Appendix B: Notes on individual objects

TYC 5839-0596-1: (ASAS 001208−1550.5) The star is flagged as SB2 in SACY and we confirm this classification. Kiraga (2012) reports a photometric rotation period P = 2.532 d based on the ASAS photometry. We find two significant photometric periods, P = 1.644 d and P = 2.53 d, of comparable powers in almost all the seasonal Lomb-Scargle and Clean periodograms. The longer period is more consistent with $v \sin i$ = 18 km s^{-1} and with the radius of a K0IV PMS subgiant. The period P = 1.644 d is an alias, specifically a beat period between the star's rotation period and the ∼1 d data sampling. This is a result of the rotation of the Earth and the fixed longitude of the observation site. The star has also a very large X-ray luminosity ($\log L_X/L_{bol}$ = −3.0). While we do not have the orbital period of the SB2, the similar $v \sin i$ of the two components suggests that this is a tidally locked system. The star also shows a moderately large lithium abundance, which is compatible with an age similar to the Pleiades. We are unable to conclude whether this is a true young binary or if the system is a RS CVn variable with a relatively large lithium abundance (see, e.g., Pallavicini et al. 1992). The photometric distance was obtained by assuming equal magnitudes for the components.

TYC 0603-0461-1 = BD +07 85: (ASAS 003858+0829.0) New close visual binary from the NaCo-LP; ΔH = 0.10 mag at a projected separation of 74 mas, corresponding to 4.3 AU at the photometric distance after correction for binarity. It is kinematically consistent with the nearby, young population. We find three photometric periods: P = 3.60 d, P = 0.566 d, and P = 1.381 d. Although they are all significant, their relative power changes from season to season. We have no $v \sin i$ measurements, which with the R = 1.026 $R_\odot$ stellar radius, could allow us to fix an upper value to the rotation period. The period P = 1.381 d is the most significant period also revealed by the Clean analysis and may be the stellar rotation period. However, the other periods cannot be ruled out. Considering the binarity and the small magnitude difference between the components, the multiple periodicities reported in the photometric analysis might be due to the different components.

HIP 3924 = HD 4944: (ASAS 005024−6404.1; 1SWASP+J005024.31-640404.0) Our FEROS spectra indicate the presence of an additional component, which is more evident in the red part of the spectrum. Binarity is further supported by the RV difference of about 9 km s^{-1} between our RV and that measured by Wichmann et al. (2003). Therefore, the star is classified as SB2. We measured an RV difference of about 18 km s^{-1} between the components with a line depth for the secondary that is about 30% that of the primary at 6450 Å. Our projected rotational velocity and Li EW are significantly different from those reported in the literature by Wichmann et al. (2003) and Weise et al. (2010). The first discrepancy might be due to a different RV separation between the components at the time of observation. For Li EW, our FEROS spectrum indicates that the two components have a similar lithium line depth. We find various significant photometric periodicities. Only one, P = 9.3 d, is consistent with $v \sin i$ = 8 km s^{-1} and the stellar radius. It is found in the complete ASAS series as well as in one segment. As the primary is classified as F7, it is possible that the photometric period belongs to the secondary. No period is derived from the HIPPARCOS photometric data. Lithium and log R_{HK} indicators are consistent with an age comparable to the Hyades, while X-ray emission yields younger ages than the other indicators. These discrepancies may be linked to the blending of the components. The target's kinematics are only consistent with IC 2391 and with the nearby, young population. We adopt an age of 500 Myr, with a lower limit at the age of the IC 2391 MG.

HIP 6177 = HD 8049: Moderately old star rejuvenated by stellar wind from the progenitor of its WD companion. The properties of the K dwarf and the WD companion and a description of the most probable evolution of the system are presented in Zurlo et al. (2013).

HIP 8038: New close binary from the NaCo-LP (ΔH = 2.5 mag at 0.44 arcsec). There is also a wide companion, *HIP 8039*, which is 1.9 mag brighter and at a projected separation of 14.97 arcsec. This star was not observed as part of the NaCo-LP. All the components are included in the aperture photometry of ASAS and SuperWASP (referred to as ASAS 014314−2136.7 and 1SWASP+J014314.17-213656.5, respectively). Each season exhibits its own most significant period, which differs from season to season in both ASAS and SuperWASP data. The most likely period in SuperWASP seems to be P = 1.668 d but with a scattered phase light curve. No clear periodicity comes out from the Clean analysis or from the HIPPARCOS photometry.

As the wide companion HIP 8039 is 1.9 mag brighter, the tentative rotation period most likely belongs to the brighter component. The target's kinematics and age are only consistent with the young, nearby population.

HIP 10602 = HD 14228 = ϕ Eri (ASAS 021631−5130.7) Proposed in Torres et al. (2008) and Malo et al. (2013) as a high probability member of Tuc/Hor. Our analysis confirms that it has consistent kinematics, at the ≤1.0 sigma level, with the Tuc/Hor association and Gagné et al. (2014) tools also yield a very high membership probability. Torres et al. investigated color-magnitude diagram placement and found it to be consistent with Tuc/Hor membership. The star is quoted as a binary in Zuckerman & Song (2004) but the identification and properties of the companion are not provided. The candidate at about 90 arcsec (*ϕ Eri B = CPD-52 284*) is not physically associated, as reported in the Washington Double Star (WDS) catalog (Mason et al. 2013). This early-type star exhibits non-periodic photometric variability.

HIP 11360 = HD 15115 (ASAS 022616+0617.6). This F-type star's membership to the β Pic MG was first proposed by Moór et al. (2006). Torres et al. (2008) concluded a possible membership (prob. 60%). Malo et al. (2013) instead propose that the star is a bona fide member of the Columba association. These estimates are based on the only RV measurement available in the literature previous to our work (8.8 ± 3.0 km s^{-1}; Moór et al. 2006). Our RV determination (1.7 ± 1.0 km s^{-1}), which includes eight HARPS and two FEROS spectra, has better accuracy and concludes a value quite different from the previously published one. Adopting our RV value, Malo et al. (2013) and Gagné et al. (2014) tools support a high membership probability (98%) for the Tuc/Hor association. The discrepancy between Moór et al. (2006) RV and our value is marginally significant (about two sigma). It might be due to the presence of a close companion. However, the high-precision differential RVs obtained with the SAFIR code applied to HARPS data show a dispersion of only 120 m/s over 40 days with intra-night RV and line bisector variations suggestive of pulsation occurrences. The age determination from indirect indicators is inconclusive, as expected for an F star. Both the young ages of the Tucana association and older ages, up to about 200 Myr, are compatible with the data. Verifying the true membership requires further investigation, including confirmation of the adopted RV value with longer baseline observations. The star exhibits non-periodic photometric variability. HIP 11360 hosts a debris disk that is unique for its large asymmetry, being detected out to 315 AU on the east side and more than 550 AU on the west side (Kalas et al. 2007). Rodigas et al. (2012) showed that the geometry is wavelength dependent and found indications of a gap in the disk at about 1 arcsec.

TYC 8484-1507-1 = HD 16699B This star is a new close visual binary from the NaCo-LP observations (sep. 0.06 arcsec = 3.6 AU, ΔH = 0.23 mag). SACY lists it as a possible SB. There is an additional component (*HIP 12326 = HD 16699*) at 8.7 arcsec, corresponding to a projected separation of 530 AU. According to Cutispoto et al. (1999), HD 16699 shows a composite spectrum, with one system of sharp lines and another system of broad lines superimposed. Since the RV is constant, this was interpreted as being due to a companion at moderately large separation. This would indicate a quadruple system. However, we note that the $v \sin i$ values of the two components in Cutispoto et al. (1999) are roughly exchanged with respect to other studies in the literature (Table A.1). An analysis of the CES spectra used in Cutispoto et al. (1999) indicates that the components were indeed exchanged in the original study. In light of this, the new companion seen in the NaCo-LP is likely the same one appearing in the composite spectra by Cutispoto et al. (1999). The separation of a few AU is compatible with the lack of a measurable RV variation, given the short time baseline of the observations. Indeed, our FEROS spectrum of the primary does shows no indication of additional components, while a check of the spectra in the Torres et al. (2006) database confirms the composite nature of the secondary's spectrum. The two components of TYC 8484-1507-1 have similar magnitudes but very different $v \sin i$ values, pointing to an intrinsically large difference between their rotational velocities, or to a strong misalignment of their rotation axes, which would be unusual for such a close binary (Hale 1994). The two stars are indistinguishable by the ASAS photometry (ASAS 023844−5257.0). The blended light curve shows variability but exhibits no significant periodicity. The target's kinematics match only the IC 2391 open cluster, with a correspondence of <2.0 sigma. The target's sky position is inconsistent with confirmed IC 2391 members, which all lie around RA = 8 h. However, the system could be an outlier of the kinematic association of young stars that Torres et al. (2008) proposes to comprise IC 2391 and Argus. The age indicators are somewhat puzzling. The secondary has a lithium line above that of Pleiades stars with similar colors (which would be consistent with the possible association with Argus) while that of the primary is below. Ca II H and K emission is also much stronger in the secondary (as was seen in SACY spectra). The system is not resolved in the ROSAT All Sky catalog, but XMM observations clearly indicate that the X-ray emission is concentrated on TYC 8484-1507-1 (the close visual pair seen with NaCo). These differences are not easy to reconcile. The composite nature of TYC 8484-1507-1 might somewhat alter some of the parameters. The very young isochrone age derived by Moór et al. (2011; 12 Myr) for TYC 8484-1507-1 is due to this. After correcting the photometry for the flux of the new visual component, the star lies close to the main sequence. Considering these uncertainties, we adopt an age of 100 Myr, with a lower limit of 40 Myr and an upper limit of 500 Myr. The system has an additional very wide (216 arcsec = 13 000 AU projected separation) common proper motion star, *HIP 12361 = HD 16743*. Moór et al. (2011) measured for this star a similar RV to those of HD 16699 A and B, and noted a fully consistent trigonometric parallax. It is then likely that the stars form a quadruple system. As expected for an early F star, HIP 12361 provides little additional contribution to the determination of the age of the system. Isochrone age analyses yield an upper limit to stellar age of about 1.7 Gyr. Finally, HIP 12361 hosts a debris disk (Moór et al. 2011).

HIP 12394 = HD 16978 = ϵ Hyi (ASAS 023932−6816.1) Early type star, proposed as a member of Tuc/Hor by Torres et al. (2008) and Malo et al. (2013). Our kinematics analysis shows that its motion does indeed match (<1.0 sigma) those of the Tuc/Hor group in U, V, and W velocities, and BANYAN II on-line tool further supports membership. The star meets the age requirement of Torres et al. A small X-ray luminosity is derived from ROSAT. The star exhibits non-periodic photometric variability.

HIP 13008 = HD 17438 = HR 827 Fast-rotating mid-F star. It is a possible binary, based on the HIPPARCOS acceleration and the difference between the HIPPARCOS and the historical

proper motion (Makarov & Kaplan 2005). The fast rotation does not allow an accurate RV measurement, but the existent RVs and line profile analysis present no compelling evidence for binarity. The star was originally flagged as young because of the high level of chromospheric activity reported by Gray et al. (2006). However, our own measurement indicates a significantly lower value ($\log R_{HK} = -4.64$). Similar discrepancies between Gray et al. (2006) and other sources are observed for other F-type stars in our sample (HIP 35564, HIP 78747). These discrepancies might be due to the larger width of the spectral region used by Gray et al. (2006) to derive the S-Index (3 Å vs. the usual 1 Å). This may induce spurious effects for F-type stars due to their shallow Ca II H and K absorptions. HIP 13008 exhibits non-periodic photometric variability. A slightly sub-solar metallicity was reported from Strömgren photometry (Casagrande et al. 2011). The isochrone age is 1.288 ± 0.912 Gyr. The target's kinematics are consistent with the young, nearby population. We adopt the isochronal age, which is consistent with our activity measurement and kinematics.

HIP 14684 = HD 19668 = IS Eri (ASAS 030942−0934.8) Malo et al. (2013) propose this star to be a bona fide member of the AB Dor MG. The target's kinematics match the AB Dor group within the 2.0 sigma threshold; the BANYAN II online tool yields high membership probability, and age indicators support this assignment. The rotation period $P = 5.46$ d was discovered by Messina et al. (2010) and subsequently confirmed by Wright et al. (2011). There is no X-ray counterpart in the ROSAT all sky catalog. The closest source in the ROSAT Faint Source Catalog has an integration time significantly lower than the typical ones. This may be an indication of some instrumental issues that caused the non-validation of a source, as found for HD 61005 in Desidera et al. (2011). Therefore, we do not list in Table 11 any upper limit on X-ray luminosity. The effective temperature resulting from the spectral type quoted in Simbad and HIPPARCOS catalog (G0) is more than 500 K warmer than our photometric and spectroscopic ones. This is likely due to a wrong spectral classification. We adopt the revised classification (G8/K0V) by Meyer et al. (2006).

TYC 8060-1673-1 = CD-46 1064 (ASAS 033049−4555.9) Proposed as a 100% probability member of Tuc/Hor by Torres et al. (2008). Our kinematic analysis shows that it matches both the Tuc/Hor and TW Hydrae associations at the 1.0 sigma level in U, V, and W. The star's sky position and XYZ galactic distances are inconsistent with other known members of TWA. All the age indicators are consistent with an age younger than 100 Myr. Malo et al. (2013) and Gagné et al. (2014) Bayesian analysis tools predict a very high probability of Tuc/Hor membership at a distance of 43.5 pc. This predicted distance for membership is consistent with the photometric distance of 40.4 pc. The rotation period $P = 3.74$ d was discovered by Messina et al. (2010) from ASAS data and was subsequently confirmed by SuperWASP data (Messina et al. 2011) and by Kiraga (2012).

HIP 19775 = HD 26980 (ASAS 041423−3819.0) Proposed as a bona fide member of Columba by Torres et al. (2008) and Malo et al. (2013). The kinematic analysis shows that its UVW motion matches Columba at the <2.0 sigma level, and the BANYAN II on-line tool yields high membership probability. The ages from various youth indicators are also consistent with the age of Columba. Messina et al. (2010) reported a rotation period $P = 2.53$ d based on ASAS data. From the analysis of SuperWASP data, Messina et al. (2011) found $P = 1.684$ d to be the most significant periodicity. Considering the $v \sin i = 13.9$ kms^{-1} and the stellar radius $R = 1.015\ R_{\odot}$, we infer rotation axis inclination values of $i = 43°$ and $i = 27°$, respectively. The observed maximum light curve amplitude up to $\Delta V = 0.07$ mag is compatible with both inclinations, although it is most consistent witih the larger $i = 43°$ value. This suggests $P = 2.53$ d as the more likely rotation period.

HIP 23316 = HD 32372 (ASAS 050052−4101.1; 1SWASP+ J050051.86-410106.7) Proposed as a high-probability member of Columba by Torres et al. (2008) and Malo et al. (2013). Our kinematic analysis shows that its UVW motion matches Columba at the <2.0 sigma level, reinforcing the membership assignment, which is also confirmed by the Gagné et al. (2014) on line tool. Also, the ages from various youth indicators are consistent with the age of Columba. The most significant period we find in the SuperWASP data is $P = 2.183$ d. Another significant period is $P = 1.8$ d, which is the 1-d beat period of the $P = 2.183$ d rotation period. The ASAS data analysis does not provide any conclusion on the rotation period. The highest peak of the HIPPARCOS data periodogram is at $P = 17.8$ d, which coincides with the maximum of the window function.

HD 32981 = BD-16 1042 = TYC 5901-1109-1 Proposed as a 100% probability member of AB Dor by Torres et al. (2008). The kinematic analysis shows that its UVW motion matches AB Dor at the <1.0 sigma level. The age of the star from various youth indicators is also broadly consistent with the age of the AB Dor group. Malo et al. (2013) Bayesian analysis tools predict a 97% probability of AB Dor membership at a distance of 79 pc while Gagné et al. (2014) return a very low membership probability, as most of the proposed AB Dor members. The predicted distance for membership is roughly consistent with the photometric distance of 86.7 pc. Messina et al. (2010) found a rotation period $P = 0.985$ d.

BD−09 1108: (ASAS 051537−0930.8) Proposed as an 85% probability member of Tuc/Hor by Torres et al. (2008). The kinematic analysis shows that its UVW motion matches Tuc/Hor at the <2.0 sigma level, reinforcing the membership assignment. The age of the star from various youth indicators is also consistent with the age of the Tuc/Hor association. Malo et al. (2013) Bayesian analysis tools predict a 17% probability of Tuc/Hor membership and a 78% probability of Columba membership at distances of 80.5 pc and 74.0 pc respectively. These predicted distances for membership are both smaller than the photometric distance of 93.6 pc. Instead, the Gagné et al. (2014) on line tool returns a very low membership probability on both associations when our photometric distance is included while a 54% membership probability for Columba at a distance of 67 pc. Messina et al. (2010) found a rotation period $P = 2.72$ d, which was subsequently confirmed by Kiraga (2012).

HIP 25434 = HD 274197 This is the secondary of a wide binary system with the star *HIP 25436 = HD 35996* being the primary. HIP 25436 is brighter by 0.8 mag in V band. The two components have a separation of about 12 arcsec. Using three epoch RV measurements (Desidera et al. 2006; Moór et al. 2013, and our CORALIE observations), we found that the primary is an SB. There is also additional evidence that one of the components is itself a binary. The slope of –0.070 deg/year for the position angle measured by HIPPARCOS is not compatible with the much smaller long term trend seen in the visual measurements (as derived by us from the individual measurements

in WDS, kindly provided by Dr. B. Mason). Furthermore, there are significant differences between the short term (3.25 yr baseline) proper motion measured by HIPPARCOS (van Leeuwen 2007) and the long term proper motion which includes old photographic plates (e.g. Tycho2, Høg et al. 2000). This supports an orbital period of a few years for the SB. In the ASAS photometry, the two components are indistinguishable from HIP 25434 (ASAS 052623−4322.6; 1SWASP+J052622.97-432236.2). We find a significant period $P = 5.34$ d in only one ASAS season and $P = 6.6$ d in the SuperWASP data (only 59 measurements available). These periods are "uncertain" and the component to which they belong is ambiguous. Considering the early spectral type of the primary, they are more likely due to photometric variations of the secondary, HIP 25434. However, they are both inconsistent with secondary's stellar radius and $v \sin i$, and would imply an age much older than that derived from other methods. Moór et al. (2013) propose membership to the Columba association. The space velocities and association to groups depend sensitively on the adopted proper motion. Using the HIPPARCOS proper motion, the kinematics are only consistent with the Nearby Young Population. Adopting the Tycho2 proper motion results in a high membership probability to the Columba association using the Malo et al. (2013) and Gagné et al. (2014) Bayesian analysis tools. Considering that the HIPPARCOS astrometry is likely biased by the astrometric motion of the additional component orbiting HIP 25436, the Tycho2 proper motion should be preferred. The age indicators are consistent with Columba membership.

TYC 9162-0698-1 = HD 269620 (ASAS 052927−6852.1) The star's kinematics match Tuc/Hor, Columba, and Carina at <2.0 sigma. The estimated age of the star is also broadly consistent with the ages of these groups, as all age indicators are within the distribution of known members. The Malo et al. (2013) Bayesian analysis predicts an 85% probability of the star being a member of Columba at a distance of 93.5 pc. This is close to the photometric distance estimate of 98.7 pc. Membership to the Columba association was also recently proposed by Moór et al. (2013). On the other hand, Gagné et al. (2014) BANYAN II web tool does not confirm this assignment, suggesting a possible membership to Carina (15%) or the field. The star is projected in front of the LMC. Kiraga (2012) finds a photometric rotation period $P = 2.613$. We also find the same period $P = 2.61$ d either from Lomb-Scargle or Clean analysis.

TYC 5346-0132-1 = BD-8 1195: (ASAS 053835−0856.7) Proposed as a member of Columba by Torres et al. (2008). At the <2.0 sigma level, its kinematics match TWA, Columba, and η Cha. However, the target's distance and position in the sky are inconsistent with TWA or η Cha membership. The age indicators are also more consistent with Columba than the other groups. Thus, the analysis reinforces the Columba membership assignment. The Malo et al. (2013) tools predict 100% probability of Columba membership at a distance of 80.5 pc. This predicted distance for membership is nearly equal to our photometric distance of 81.2 pc. The Gagné et al. (2014) on line tool yields a probability of 53.6%. ROSAT shows no X-ray counterparts within the adopted matching radius of 30 arcsec, but the bright X-ray source 1RXS J053835.1-085639 lies just above the threshold (angular distance of 32.5 arcsec from the optical source). The position of the X-ray source XMMSL1 J053834.6-085645 is 6 arcsec apart from TYC 5346-0132-1, suggesting that 1RXS J053835.1-085639 is associated to TYC 5346-0132-1. The photometric period $P = 1.983$ d is found by both the Lomb-Scargle and the Clean analysis at high confidence level and in good agreement with the earlier determination by Kiraga (2012).

HIP 30261 = HD 44748: (ASAS 062157−3430.7; 1SWASP+J062157.25-343043.7) This target's kinematics do not match at the <2.0 sigma level any of the investigated groups and associations. The kinematics are also not consistent with the nearby, young population. The star is estimated to be quite young (60 Myr) based on lithium and estimated to be slightly older than the Pleiades based on other indicators. With either a Scargle-Lomb or Clean analysis, the photometric period $P = 4.16$ d is found in almost all the ASAS seasons and all the SuperWASP data. The same rotation period was also found by Kiraga (2012).

TYC 7617-0549-1 = CD-40 2458: (ASAS 062607−4102.9) Proposed as a 70% probability member of Columba by Torres et al. (2008). At the <1.0 sigma level, its kinematics match both Columba and Carina. However, the target's X galactic distance is inconsistent with other Carina members, which have a relatively tight distribution. The age of the star is broadly consistent with the Columba association. Thus, the analysis reinforces the Columba membership assignment. The Malo et al. (2013) and Gagné et al. (2014) Bayesian analysis tools predict 100% probability of Columba membership at a distance of 77.5 pc. This predicted distance for membership is nearly equal to our photometric distance of 77.8 pc. Messina et al. (2010) found a rotation period $P = 4.13$ d in ASAS data and $P = 4.14$ d in SuperWASP data (Messina et al. 2011). This was subsequently confirmed by Kiraga (2012).

TYC 9181-0466-1 = HD 47875: (ASAS 063441-6953.1) New close visual binary from our program ($\Delta H = 1.5$ mag at 1.89 arcsec). All indicators are consistent with an age younger than 100 Myr, but there is no previously published association with MGs. The target's kinematics match Tuc/Hor and TWA at the <2.0 sigma level. However, its position on the sky and estimated age reject it as a TWA member. The Malo et al. (2013) Bayesian analysis predicts a 97% chance of it being a Tuc/Hor member at 65.5 pc, which is not so different from our photometric distance of 77.7 pc (including a correction for binarity). Thus, the star might be a previously unrecognized member of Tuc/Hor. However, the updated BANYAN II web tool does not support the Tuc-Hor membership. With both period search methods, we find $P = 2.77$ d to be the most significant period in most seasons. A second period $P = 1.56$ d has comparable power in several seasons. Considering $v \sin i = 13.5$ km s^{-1} and stellar radius $R = 1.075\ R_{\odot}$, we infer rotation axis inclination values of $i = 43°$ and $i = 22°$, respectively. The observed maximum light curve amplitude up to $\Delta V = 0.04$ mag is more compatible with the longer period $P = 2.77$ d.

HIP 32235 = HD 49855: (ASAS 064346−7158.6) Proposed as a bona fide member of Carina by Torres et al. (2008) and Malo et al. (2013). Its kinematics match both Columba and Carina at the <2.0 sigma level, and the membership to Carina was fully supported by Gagné et al. (2014) on-line tool. The target's YZ galactic distances differ slightly from what is expected for Columba. The age is consistent with both Columba and Carina. Thus, the analysis reinforces the Carina membership assignment. Messina et al. (2010) found a rotation period $P = 3.83$ d in ASAS data, which is subsequently confirmed by Kiraga (2012).

HIP 35564 = HD 57852 = HR 2813: (ASAS 072021−5218.7) Fast-rotating early-type star, proposed as a member of Carina-Near moving group by Zuckerman et al. (2006). The target's kinematics match the Carina-Near group at the <1.0 sigma level and show no indication of matching any other group. The age estimates are also consistent with the age of this group. Thus, the Zuckerman et al. membership assignment is confirmed. The RV measurements show a scatter of a few km s^{-1} when combining data from several sources, indicating it is an SB. The CCF shows a broad profile with no indication of additional components. The star also exhibits non-periodic photometric variability. It has a moderately wide (9 arcsec projected separation) companion *HD 57853 = HR 2814*, a late F star which is a spectroscopic triple (see Saar et al. 1990; Desidera et al. 2006). The total mass of the close triple was estimated to be about 2.4 $M_{\odot}$ (Saar et al. 1990). The system is therefore a hierarchical quintuple.

TYC 8128-1946-1 = CD-48 2972 (ASAS 072823−4908.4) Proposed as a 100% probability member of Argus by Torres et al. (2008). At the <1.0 sigma level, its kinematics match both the Argus association and IC 2391 cluster. The age diagnostics support a young age, compatible with Argus membership. The Malo et al. (2013) Bayesian analysis tools with our adopted parameters as input predict 100% probability of Argus membership at a distance of 76.5 pc. On the other hand, membership is rejected by the Gagné et al. (2014) online tool. The FEROS RV by SACY and our measurement made with CORALIE differ from one another by 3.1 km s^{-1}. Considering the large $v \sin i$ of the star, we consider it a possible SB. Additional measurements are needed for confirmation of binarity. Messina et al. (2011) report a rotation period P = 1.038 d, subsequently confirmed by Kiraga (2012). *HIP 36312 = HD 59659* is an F7 star at 81 arcsec from TYC 8128-1946-1. According to Torres et al. (2008), the proper motions and distances are compatible with a physical association, but no spectroscopy was available to them to confirm this. The RV measured by us on two epochs is consistent with that of TYC 8128-1946-1; the trigonometric distance of HIP 36312 is compatible with the photometric and kinematic ones for TYC 8128-1946-1. The star was not detected in X-ray but it is moderately active and lithium-rich. Taking these indicators' reduced age sensitivity for F stars into account, we consider the age to be compatible with that of TYC 8128-1946-1. Therefore, we classified the two objects as physically associated, adopting the trigonometric distance of HIP 36312 for TYC 8128-1946-1. We also added HIP 36312 to the list of probable members of the Argus association.

HIP 36414 = HD 59704 (ASAS 072931−3807.4) Proposed as a member of Carina-Near moving group by Zuckerman et al. (2006). However, the target's kinematics do not match the Carina-Near group at the <2.0 sigma level. On the other hand, the age of the star is consistent with 200 Myr or older. According to Tokovinin (2011) and Nordström et al. (2004), the star is an SB without an orbital solution (σ_{RV} = 1.2 km s^{-1}). Our somewhat discrepant FEROS RV (ΔRV = 2.6 km s^{-1} with respect to Nordström et al. 2004) further supports the presence of RV variability. We therefore classify this star as a likely SB, though additional measurements would be required for orbit determination. The system RV is also needed for a better assesment of MG membership. We also found non-periodic photometric variability. The star *CCDM J07295-3807B* at about 12 arcsec separation is not physically associated (Tokovinin 2011).

HIP 36948 = HD 61005 Proposed as a member of Argus by Desidera et al. (2011). At the <1.0 sigma level its kinematics match only the Argus association. The ages derived for this star are all ~100 Myr, slightly older than the ~40 yr age of the group but compatible with the Argus membership assignment. Malo et al. (2013) also propose this star as a bona fide member of Argus and this is further supported by the Gagné et al. (2014) online tool. In the Spitzer FEPS sample, this star exhibited the largest 24 μm excess with respect to the photosphere (Meyer et al. 2008). The star's disk was first resolved with HST (Hines et al. 2007), indicating the presence of two components: an external one shaped by interaction with the interstellar medium and an internal ring or disk. Observations in the H-band performed as part of our NaCo-LP (Buenzli et al. 2010) enabled the characterization of the inner ring, showing a significant offset of its center with respect to the star and also showing a rather sharp inner rim. These properties might be due to the perturbation by a planetary companion, undetected in the available observations.

HIP 37563 = HD 62850 Proposed as a member of Carina-Near moving group by Zuckerman et al. (2006). The target's kinematics match the Carina-Near group at the <1.0 sigma level and show no indication of matching any other group. Thus, the Zuckerman et al. membership assignment is confirmed. Our Lomb-Scargle and Clean analyses of the ASAS (ASAS 074236-5917.8) timeseries revealed two periods, P = 3.65 d and P = 1.37 d, in seven out of eight seasons and in the complete series. Considering the $v \sin i$ = 14 km s^{-1} and the stellar radius R = 1.055 $R_{\odot}$, we infer rotation axis inclination values of i = 75° and i = 21°, respectively. An observed maximum light curve amplitude never exceeding ΔV = 0.02 mag is observed. The photometric amplitude and longer period are fully compatible with the activity level and age of the star. The shorter period would make the star an outlier in Fig. 6, 7. We therefore adopt P = 3.65 d as the rotation period.

HIP 37923 = HD 63608 Together with its wide (23.1 arcsec projected separation) companion *HIP 37918 = HD 63581*, HIP 37923 was proposed as a member of the Carina-Near moving group by Zuckerman et al. (2006) and as a member of the IC 2391 cluster by Nakajima & Morino (2012). The target's kinematics match the Carina-Near group at the <1.0 sigma level in V and W velocities but match at 3.2 sigma in the U velocity; HIP 37918 matches at 2.1 sigma in the U velocity. However, the age of the components is consistent with that of the Carina-Near group. The kinematics do not match well with IC 2391. Thus, the membership assignment to Carina-Near is still likely, although not as robust as other proposed members. The difference in Li EW between the components is striking, considering the small difference in temperature.

TYC 8927-3620-1 = HD 77307 (ASAS 085849−6115.3) Fast-rotating star with large lithium abundance, indicating a young age of about 20 Myr. The star was resolved as a very close visual binary (sep 0.1 arcsec) in NaCo-LP (ΔH = 0.50 mag) with an additional bright star at 4.9 arcsec. The latter (*2MASS 08584794-6115161 = WDS 08588-6115B*) is also included in 2MASS and WDS catalogs, being only 0.5 mag fainter than the central star. There is also an additional object (*2MASS 08584777-6115335 = WDS 08588-6115C*) listed in WDS at 19 arcsec. It has a different proper motion from TYC 8927-3620-1 in the UCAC4 catalog and, therefore, is not physically associated. A subgiant

luminosity class is reported in SACY. The target's kinematics are only consistent with the young, nearby population. Using both period search methods, we find $P = 0.874$ d in all ASAS seasons. The same period is also found by Bernhard & Bernhard (2010) and Kiraga (2012) from ASAS data.

HIP 46634 = HD 82159B (ASAS 093035+1036.0) Member of a wide pair whose components have similar brightness ($\Delta V = 0.01$ mag). We could not identify the rotation period, as the most significant frequency changed from season to season. No significant period comes out from the HIPPARCOS data analysis. Strassmeier et al. (2012) classified it as a single star based on extensive RV monitoring. Nordström et al. (2004) instead flagged it as being RV variable (rms RV 36 km s^{-1}, $N = 2$). Taking also the measured $v \sin i$ into account, we speculate that the spectroscopic measurements of the two components were exchanged in Nordström et al. (2004). The companion, *HIP 46637 = GS Leo = HD 82159A*, is a close SB (period = 3.86 days Strassmeier et al. 2012). Strassmeier et al. (2012) report a HIP 46637 rotation period of 3.05 days. Its age indicators, along with the integrated X-ray luminosity, are altered by the fast rotation induced by the close companion. These indicators are therefore not considered for age dating of the system. We note the large difference in lithium EWs in spite of the very similar temperatures of the stars. The lithium EW of HIP 46634 and $\log R_{\rm HK}$ (the latter kindly provided by the SOPHIE Consortium) indicate an age intermediate between that of the Pleiades and Hyades. At the <2.0 sigma level, the kinematics do not match any of the investigated groups and associations. Its kinematics are similar to that of the Hyades. However, the solar metallicity derived by Strassmeier et al. (2012) argues against a physical link with this cluster. The G5 spectral type of HIP 46634 corresponds to an effective temperature warmer than 400 K than the photometric one. As the spectroscopic temperature by Strassmeier et al. (2012) is slightly cooler than the photometric one, we argue that the spectral classification needs to be revised.

HIP 47646 = HD 84199 (ASAS 094251−2257.9; 1SWASP+J094250.81-225755.7) is an F5V star that exhibits non-periodic photometric variability. A low level of chromospheric activity and low lithium content are derived from our FEROS spectra ($\log R_{\rm HK} = -4.83$). The kinematic parameters are distant from the loci of investigated groups and associations. This is consistent with a moderately old age. Taking isochrone fitting and Casagrande et al. (2011) metallicity into account yields an age of 1.156 ± 0.950 Gyr. However, the star exhibits common proper motion and astrometric agreement with the K2.5 star HIP 47645 (projected separation of about 1200 AU), which appears to be much younger, based on high chromospheric activity (Gray et al. 2006). The system's integrated X-ray emission ($\log L_{\rm X} = 29.25$) also supports the younger age. One way to reconcile all these observations would be to conclude that HIP 47645 is a tidally-locked SB, but no existing spectroscopic data confirms this hypothesis.

TWA 21 = HD 298936 Formerly listed by Song et al. (2003) as a candidate member of TWA and classified by Zuckerman & Song (2004) and Mamajek (2005) as a member, it was later rejected as a TWA member by Torres et al. (2008), based on the separation in the Z direction with respect to confirmed members. Viana Almeida et al. (2009) included it as a possible member of the Carina association (age 30 Myr). Our kinematic analysis, which includes the trigonometric parallax recently measured by Weinberger et al. (2013), shows that this star is consistent with both the TWA and Columba groups at the <2.0 sigma level. The match to Columba in *UVW* space is actually within 1.0 sigma. The Malo et al. (2013) Bayesian analysis tools predict a 99% probability of Columba membership and only 1% probability of TWA membership. On the other hand, BANYAN II web tool yields a very high membership probability to Carina MG. In contrast to these results, Weinberger et al. (2013) recently showed, using a kinematic trace-back study, that the kinematics of TWA 21 are consistent with the TWA group. The age from isochrone fitting is intermediate between the quoted ages for TWA and Columba. The most probable lithium age is around 15–20 Myr with the sequence of Carina, Columba, and Tucana representing an upper limit. Independently from any membership assignment, we adopt the isochrone age of 17 Myr. Messina et al. (2010) found a rotation period $P = 4.43$ d in ASAS data.

TYC 7188-575-1 (ASAS 102204−3233.4; 1SWASP+J102204.47-323326.9) The star is an SB with a peak-to-valley RV difference of 83 km s^{-1}. The four available RV measurements are spread out over year timeframes and do not allow an estimate of orbital period, which might conclude the possibility of a tidally-locked system. Our FEROS spectrum reveals a complex CCF profile, suggesting a possible SB2 system. However, the comparison with CORALIE spectra shows that the spectral lines have comparable width, while moving tens of km s^{-1} with respect to the FEROS spectrum. Therefore, the system may be triple or, more likely, the spectral lines are deformed by the presence of starspots, given the exceptionally high activity level (Balmer lines down to Hϵ were seen in emission). The star has the largest photometric variability (0.28 mag) in our sample. The X-ray emission is also very strong. The Lomb-Scargle and Clean analysis of ASAS and SuperWASP data reveal three major periodicities: $P = 4.27$ d, $P = 1.297$ d, and $P = 0.81$ d, in order of decreasing power. The longest period is listed in ACVS. However, it is not consistent with the $v \sin i = 25$ km s^{-1} and the stellar radius of a K0V star. Therefore, we adopt $P = 1.297$ d as the rotation period. The extremely high activity level might be due to the interaction between the two stellar components, especially if they have already left the main sequence (RS CVn-type variability). The presence of lithium (comparable to that of Pleiades stars of similar spectral type) would also be consistent with an RS CVn system, as these stars often show a moderate lithium content (Pallavicini et al. 1992), although of still debated origin. Adopting the mean RV from the available measurement and using the photometric distance, assuming a main sequence star, yield kinematic parameters that are compatible with the nearby, young population. However, the center of mass RV is needed for a better assessment.

TYC 6069-1214-1 = BD-19 3018 (ASAS 102737−2027.2; 1SWASP+J102737.33-202710.6) Only SACY spectroscopic data available. The most important photometric period is $P = 3.91$ d ($P = 4.14$ d in SuperWASP data). There also exists a second period, $P = 1.34$ d, in both ASAS and SuperWASP data, as reported by Kiraga (2012). However, the absence of known $v \sin i$ prevents us from distinguishing between the correct one and the alias. At <2.0 sigma, the target's kinematics match only the Carina association. The star's age from multiple youth indicators is intermediate between that of Carina association and of AB Dor MG, making the Carina membership unlikely.

TYC 7722-0207-1 = HD 296790 (ASAS 102204−3233.4; 1SWASP+J103243.90-444055.6) Classified as a possible TWA member by Reid (2003), but our analysis of kinematics and age indicators does not support it. The Lomb-Scargle and Clean analysis of the photometric time series reveal two periods, $P = 2.01$ d and $P = 1.975$ d, of comparable power in almost all seasons. Both may be real, arising from surface differential rotation. These periods are also consistent with the $v \sin i = 27.2$ km s^{-1}. A period $P = 4.29$ d is listed in ACVS and reported by Kiraga (2012). Such a value is not consistent with $v \sin i$ and the stellar radius.

TYC 7743-1091-1 = HD 99409: (ASAS 112558−4015.8; 1SWASP+J112558.28-401549.9) This is a late type star with a moderately strong lithium line, as measured by Wichmann et al. (2003); Weise et al. (2010). Luminosity class II-III is quoted in the Michigan Spectral Survey Catalog (Houk 1982). DDO photometry by Norris (1987) also supports luminosity class III and excludes a dwarf star. Our analysis of a FEROS archive spectrum confirms the giant status of the star. We derived $T_{\rm eff} = 4931 \pm 59$ using ARES. From this, we concluded $\log n({\rm Li}) \sim 1.9$ dex. The most important photometric period is $P = 39 \pm 7$ d, based on both our methods of period search. The star is found to be a hard X-ray source (HR1 $= 0.86 \pm 0.08$). The RVs from Wichmann et al. (2003) and the FEROS spectrum differ by 4.3 km s^{-1}, making it a suspected SB. HD 99409 is therefore not a bona fide young star but should be rather added to the census of lithium-rich giants. The moderately large $v \sin i$ (17 km s^{-1}), fast rotation (39 days), and strong X-ray emission are remarkable for a giant star. Similar features have been reported for other lithium-rich giants, and, indeed, the frequency of lithium-rich stars is much larger for fast-rotating giants than for normal giants (Drake et al. 2002). These features might be linked to planet engulfment phenomena (Siess & Livio 1999; Carlberg et al. 2010, 2012), but alternative mechanisms have also been proposed (de la Reza & Drake 2012). The kinematic parameters are inconsistent with all of the groups investigated.

HIP 58240 = HD 103742 (ASAS 115642−3216.1; 1SWASP+J115642.30-321605.3) With its wide companion *HIP 58241 = HD 103743* (ASAS 115644−3216.0; 1SWASP+J115643.77-321602.7), HIP 58240 was proposed by Zuckerman et al. (2006) to be a member of the Carina-Near moving group. The kinematics of HIP 52840 match the TWA, Argus, and Carina-Near moving group at the <2.0 sigma level. The age diagnostics measured for this target are inconsistent with the expected ages for the TWA and Argus associations. The kinematics of HIP 58241 match Argus, the Carina-Near moving group, the Hercules-Lyra association, and IC 2391 at the <2.0 sigma level. Considering both components and the age diagnostics, the membership to Carina-Near is likely. For both stars, we could derive the rotation period in neither ASAS nor SuperWASP data; each season showed its own significant periodicity. This may be linked to the blending of the components in ASAS and SuperWASP images. HIP 58241 is a nearly perfect Solar analog (except for multiplicity) at an age of 200 Myr (D'Orazi et al. 2012). This component was not observed in the NaCo-LP. Tokovinin et al. (2010) and Tokovinin (2011) identified an additional source at about 4 arcsec from HIP 52841. Its physical association to HIP 52841 requires confirmation. WDS lists an additional component, *CD-31 9365 C*, which is an unrelated F2 background star (Torres et al. 2006).

TYC 9231-1566-1 = HD 105923 (ASAS 121138−7110.6) New close visual binary ($\Delta H = 3.02$ mag at 1.98 arcsec). It was proposed by Torres et al. (2008) as an 80% probability member of the ϵ Cha association with a kinematic distance of 115 pc and by Mamajek et al. (2002) as a high probability member of LCC with a kinematic distance of 98.5 pc. Mamajek et al. (2002) estimated $A_V = 0.48 \pm 0.08$, while Messina et al. (2011) derived a significantly lower value ($E(B-V) = 0.03$, $A_V = 0.1$). This discrepancy originates from the two different spectral classifications in Mamajek et al. (2002) and Torres et al. (2006; G3IV vs. G8V respectively). Our spectroscopic effective temperature (5530 ± 40 K) supports an intermediate value, $E(B-V) = 0.08$. Adopting this latter value, we infer a photometric distance of 98 pc for an age of 10 Myr. The age indicators clearly point to a very young age, consistent with those of ϵ Cha and LCC. An age younger than β Pic MG is likely, thus favoring the ϵ Cha membership. However, considering the uncertainty in the distance and reddening, and the influence of the newly discovered binary companion, we consider 20 Myr to be an upper limit for the stellar age. Messina et al. (2011) report a rotation period of $P = 5.05$ d, which they classified as "confirmed". This was subsequently also confirmed by Kiraga (2012). The star has no significant RV variations.

TYC 8979-1683-1 = CD-62 657 (ASAS 122825−6321.0): Classified as an LCC member by Song et al. (2012) with a photometric distance of 73 pc. We derived a similar photometric distance of 75.6 pc, assuming no reddening. However, the discrepancy between the photometric (5306 K) and the spectroscopic (5650 ± 145 K) effective temperature, along with the spectral type (G7V), may indicate the presence of some amount of interstellar or circumstellar absorption ($E(B-V) \leq 0.10$ mag). This may increase the distance estimate up to about 80 pc, and would imply an even younger age from Li EW. Our analysis indicates that the target's kinematics match TWA, US, and Corana Australis at <2.0 sigma. The star's age from multiple youth indicators is also consistent with these young ages. The target's declination is further south than any known member of TWA, implying that a membership is unlikely. The star may belong to the outskirts of UCL or LCC, in the direction of the Sun, having a photometric distance, which is closer to the mean distances of the ScoCen subgroups. The most important period in the photometric time series is $P = 3.35$ d, which is the same as the one found by Kiraga (2012). However, it is inconsistent with $v \sin i = 31.9$ km s^{-1} and the stellar radius. Using both period search methods, we also find two other important periods of comparable power: $P = 1.42$ d and $P = 0.76$ d in all the seasons and in the complete series. Considering the stellar radius $R = 1.035\ R_\odot$, we infer rotation axis inclination values of $i = 60°$ and $i = 37°$, respectively. An observed maximum light curve amplitude up to $\Delta V = 0.11$ mag is observed, suggesting that the star's rotation period is likely $P = 1.42$ d.

TYC 8989-0583-1 = HD 112245 (ASAS 125609−6127.4) New close visual binary discovered in our program ($\Delta H = 2.6$ mag). Classified as an LCC member in Song et al. (2012) with a photometric distance of 68 pc (close to our adopted value of 65 pc). The target's kinematics match Tuc/Hor, TWA, and UCL at <2.0 sigma. The star's age from multiple youth indicators is consistent with it being very young and compatible with the ages of Tuc/Hor but likely is younger. The target's declination is further south than any known member of TWA, implying that it is likely not a member

of this association. The target's photometric distance is also only half of the distance expected for membership in one of the ScoCen subgroups. However, it could be part of the population of closer stars linked to these groups, as studied by Song et al. (2012). We do not have spectra for the derivation of spectroscopic temperature. From spectral type (K0Ve) and photometric temperature (4929 K), a small amount of absorption can not be excluded. The Lomb-Scargle analysis of the photometric timeseries indicated $P = 4.89$ d, $P = 1.25$ d, and $P = 0.83$ d as the most important periods. However, the two longer ones are inconsistent with $v \sin i = 47$ km s^{-1} and the stellar radius $R = 1.095\ R_{\odot}$. The Clean analysis shows $P = 1.25$ d and $P = 0.556$ d to be the most important. We adopt $P = 0.556$ d as the rotation period, which is also reported by Bernhard & Bernhard (2010).

TYC 9245-0617-1 = CD-69 1055 (ASAS 125826−7028.8) The star is a WTTS, as indicated by its strong lithium, filled-in Hα line, strong X-ray emission, and near-IR excess. Torres et al. (2008) proposed it as an 80% probability member of the ϵ Cha association, while Mamajek et al. (2002) and Song et al. (2012) proposed it to be a member of LCC. Kinematic distances of 101 pc and 85 pc were derived by Torres et al. (2008) and Mamajek et al. (2002), respectively, while Song et al. (2012) obtained a photometric distance of 75 pc. Mamajek et al. (2002) estimated $A_V = 0.46 \pm 0.12$ while Messina et al. (2011) derived a slightly lower value ($E(B-V) = 0.11$, $A_V = 0.34$). Our spectroscopic and photometric temperatures are equal for $E(B-V) = 0.09$. Adopting this latter value, we infer a photometric distance of 93 pc for an age of 10 Myr, which is supported by the Li EW of 410 mÅ. This is consistent with the Torres et al. (2008) kinematic estimate, and together with our kinematic analysis for this distance it supports the association with ϵ Cha. Messina et al. (2011) and Kiraga (2012) report a rotation period of $P = 2.007$ and $P = 1.989$ d, respectively. From the RV data, there is an indication of RV variability on timescales of a few years and amplitude of a few km s^{-1}. Considering the young age and the probable presence of circumstellar material, this might be due to variable obscuration from the circumstellar disk (see, e.g., Schisano et al. 2009, for the case of T Cha) and the presence of a companion. We, therefore, consider the star as a possible SB, but we keep it in the sample for the statistical analysis.

HIP 63862 = HD 113553 (ASAS 130517−5051.4) This target's kinematics do not match any of the groups and associations investigated at the <2.0 sigma level. Its kinematics are also not consistent with the nearby, young population. The star is estimated to be slightly older than 100 Myr. The most important period is $P = 4.5$ d, which is found in almost all seasons and confirms the period $P = 4.456$ d found by Kiraga (2012).

TYC 7796-2110-1 = CD-41 7947 (ASAS 133432−4209.5; 1SWASP+J133431.89-420930.7) was reported as a suspected SB2 in the SACY survey. The photospheric lines appear very broad in our FEROS spectrum; the target might be indeed an unresolved SB2 with fast-rotating (and very active) components. The CORALIE spectrum also shows a complex profile, but we can not confirm the SB2 status from these data (similar line width). Three-epoch RVs show large scatter; however considering the large measurement errors, this is not conclusive for a binary classification. The star was classified as an LCC member in Song et al. (2012) with a photometric distance of 93 pc, which is very similar to our adopted value of 92 pc. The rotation period $P = 1.022$ d is found in both ASAS and SuperWASP data by both period search methods. The target's kinematics and age are consistent with the young, nearby population at the <2 sigma level, and with UCL and LCC at the <3 sigma level. We noted a large difference in Li EW between SACY and Song et al. (2012) (400 vs. 315 mÅ, respectively). Age indicators are consistent with LCC, but the very fast rotation and possible binarity make the parameters uncertain.

TYC 9010-1272-1 = HD 124831 (ASAS 141805−6219.0) New close visual binary (projected separation 0.27 arcsec = 25 AU, $\Delta H = 1.01$ mag). The star is also listed as a possible SB2 in SACY. The analysis of our FEROS spectrum shows a strongly asymmetric CCF, which is likely due to an additional component. Significant RV variations are reported in the literature. Considering the RV difference between the components, ~20 km s^{-1} in our FEROS spectrum, and the line depth ratio of about 0.7, it is plausible that the newly discovered visual companion is not the main object responsible for the RV variations and spectral contamination. The system might therefore be triple. The period $P = 1.477$ d is the most important period found by either Lomb-Scargle or Clean analysis. This confirms the earlier determination by Kiraga (2012) and is consistent with $v \sin i = 38$ km s^{-1} and the stellar radius. The target kinematics match several groups subgroups at the <2.0 sigma level. Considering the star age, membership to Tuc/Hor or COL, seems plausible, but improved understanding of the multiplicity and of the system RV are needed.

HIP 70351 = HD 125485: (ASAS 142339−7248.5) Young star with an age of about 100 Myr, consistently derived from various indicators. The most important period in the photometric time series is $P = 3.58$ d, but the period $P = 1.385$ d is also present in both Lomb-Scargle and Clean periodograms. No period is found from Hipparcos data. The target's kinematics do not match any of the groups and associations investigated at the <2.0 sigma level. Its kinematics are also not consistent with the nearby, young population.

HIP 71908 = GJ 560A = α Cir (ASAS 144230−6458.5) roAp star. Isochrone fitting, carried out using the effective temperature by Bruntt et al. (2008), yields an age of 1.10 ± 0.17 Gyr. Bruntt et al. (2009) report a rotation period $P = 4.479$ d for the primary. No period is derived from ASAS nor from Hipparcos data. The wide companion *GJ 560B = SAO 252852* is included by López-Santiago et al. (2006) in the list of Her-Lyr members. HIP 71908 is also proposed by Nakajima & Morino (2012) as a member of β Pic MG. The kinematics of the star are consistent with the ϵ Cha moving group and Her-Lyr association at the <1.0 sigma level. BANYAN II web tool yields a very high membership probability to β Pic MG. However, the age measured by comparing isochrones in the HR diagram indicates that the primary has an age around 1 Gyr, making it much older than either of these groups. There are also no indications of young age for the secondary, as the system is not detected with ROSAT; the level of chromospheric activity is low and lithium is not detected in the spectrum. These age estimates rule out kinematic membership in either of these young associations, and the star is therefore likely an older field dwarf interloping in the kinematic space where young stars are concentrated. We adopt the isochrone age of the primary.

HIP 71933 = HD 129181 (ASAS 144244−4848.0) RV measurements from SACY, Nordström et al. (2004), Waite et al. (2011) and our FEROS spectrum show a rather large scatter (4 km s^{-1}), suggesting binarity. Indication of binarity comes also from the astrometric acceleration detected by

HIPPARCOS. The small $v \sin i$ quoted by Nordström et al. (2004) (2 km s^{-1}) is highly discrepant with the fast rotation reported by Waite et al. (2011) and with our own spectrum (70 km s^{-1}). The Nordström et al. (2004) RV measurement should therefore be taken with caution. The broad photospheric lines make the RV measurement rather uncertain, and an SB2 nature cannot be ruled out. However, the deformation of the line profile might also be due to spots. This issue was also discussed by Waite et al. (2011), who favor the star-spot interpretation. We therefore consider this star as only a possible binary. Our analysis of photometric data reveals marginal evidence of a period $P = 0.67$ d in two ASAS seasons and in the HIPPARCOS data. This star is very active and is also found to be a relatively hard X-ray source (HR1 $= 0.58 \pm 0.07$). The strong lithium EW is consistent with an age between about 30 and 150 Myr. The star is clearly above the main sequence on the color-magnitude diagram with an isochrone age of 16 ± 6 Myr. This is marginally inconsistent with the Li estimate, but the fast rotation makes the Li EW measurement uncertain. The kinematics are fully consistent with UCL when Tycho2 proper motion is adopted (1.9 sigma discrepancy with respect to VL07) and Nordström et al. (2004) RV is excluded. Isochrone age is also fully compatible with UCL but the distance is closer then that of most of its known members. We therefore conclude that this is a truly young star located in front of UCL. It is uncertain whether it is physically related to UCL and/or LCC. It may be a binary with a period of a few years, but this needs confirmation.

HIP 72399 = HD 130260 (ASAS 144810−3647.0; 1SWASP+J144809.66-364702.2) This is a very active K dwarf but without detectable lithium. Four RV determinations (one by SACY and the others ours from HARPS and CORALIE data) show that the star is an SB1. The two CORALIE spectra were taken with a time separation of about one hour and have an RV difference of about 3 km s^{-1}, indicating a short period for the binary orbit. Our analysis of ASAS data confirms the $P = 3.897$ d period reported by Kiraga (2012). We find the same period in the SuperWASP data as well. The K5V star *HIP 72400 = HD130260B* at 10 arcsec is a probable wide companion. It has similar proper motion and parallax, but a slightly different RV (which can be understood as being due to our poor sampling of the HIP 72399 binary orbit). Both components have rather large parallax errors. The X-ray emission of the two components is not spatially resolved by ROSAT, but the XMM source reported in Saxton et al. (2008) is much closer to the SB component, suggesting that it is the main X-ray emitter. The lack of lithium in the primary yields an age lower limit of about 300 Myr, which is not consistent with the estimates based on coronal and chromospheric emission and rotation period. The kinematics of HIP 72400 are slightly outside the box of very young stars but fully compatible with a moderately young age. Its slow rotation, as derived from the CORALIE spectrum, argues against a star as active as the primary. All these facts support the hypothesis that the high activity and fast rotation of HIP 72399 is due to tidal locking and not to a young age. However, we can not conclusively demonstrate this without a measurement of the binary's orbital period.

TYC 7835-2569-1 = HD 137059 (ASAS 152517−3845.4; 1SWASP+J152516.99-384526.0) Close visual binary (1.05 arcsec separation, $\Delta V = 0.3$ mag, $\Delta H = 0.1$ mag) first discovered by Brandner et al. (1996) and confirmed by NaCo-LP data. The star was found to be SB2 from CORAVEL spectra. Makarov (2007) classified it as a member of the Lupus association (age 5–27 Myr) with a kinematic distance of 89 pc, but the star is not included in the recent study of the Lupus star-forming region by Galli et al. (2013). Kinematic parameters are consistent with β Pic, Cha-Near, CrA and Upper Sco. However, the unresolved binary may imply that the RV measurements used in these analyses are very uncertain, making the kinematic analysis difficult to interpret. Furthermore, lithium EW and X-ray flux are below those of most members of the youngest associations, such as β Pic and Tuc-Hor. Rather, the fluxes are more compatible with an age older than those quoted in Makarov (2007) for Lupus and the ages of other groups mentioned above. The star is therefore most likely a moderately young star without associations to known groups. Our kinematic distance, using the AB Dor MG sequence as a reference, and including binary correction, is 70.2 pc. The SuperWASP data analysis gives a period $P = 3.69$ d. In contrast, the ASAS data analysis gives two periods, $P = 2.32$ d and $P = 1.75$ d. Considering the stellar radius $R = 1.009\ R_{\odot}$ and $v \sin i = 17$ km s^{-1}, we infer rotation axis inclination values of $i = 50°$ and $i = 36°$, respectively. The observed maximum light curve amplitude never exceeds $\Delta V = 0.04$ mag, suggesting that both rotation periods are possible. The present data do not allow us to be sure about the correct rotation period. The multiple photometric periods might belong to the different components, considering their similar brightnesses.

HIP 76829 = HD 139664 (ASAS 154111−4439.7) Proposed as a member of the Her-Lyra association by López-Santiago et al. (2006). The kinematics of the star are consistent with Her-Lyr at the <2.0 sigma level. Beside kinematics, additional indications of youth are provided by coronal and chromospheric emission and fast rotation, but the sensitivity of these diagnostics for mid-F stars is not so strong. No lithium was detected in our analysis of the HARPS spectra. The age of the star resulting from X-ray and Ca H and K is compatible with Her-Lyr membership. We find marginal evidence of a period $P = 0.719$ d, which is consistent with $v \sin i = 71.6$ km s^{-1} and the stellar radius. However, the measured period is very uncertain. HIP 76829 hosts a debris disk, which was spatially resolved by Kalas et al. (2006) using HST. The disk is oriented nearly edge-on. The emitting material is concentrated on a belt at a separation of about 83 AU.

TYC 6781-0415-1 = CD-24 12231 (ASAS 154131−2520.6; 1SWASP+J154131.21-252036.4) Very young star with a lithium age younger than 10 Myr (from $B - V$ color). Classified by Aarnio et al. (2008) as a probable member of US with a kinematic distance of 109 ± 11 pc. This star is found to be a hard X-ray (HR1 $= 0.94 \pm 0.03$; see Sect. 6.2) and radio (Martí et al. 2004) source. This is consistent with the very young age of US and the age derived from the lithium EW of the star. Martí et al. (2004) quotes the star as RV constant over four consecutive nights but does not provide RV values. Individual RVs from SACY and Aarnio et al. (2008) are also consistent with a single star. We note a highly discrepant effective temperature from $B - V$ and $V - K$ colors (5373 K vs. 4569 K); reddening cannot account for this. The temperature from $B - V$ is consistent with the G9IVe and G8e spectral classifications from SACY and Carpenter et al. (2009) respectively. The high level of activity implies high levels of photometric variability. This would result in significant errors when combining magnitudes taken several years apart. However, from ASAS data, the variability in V band

over 10 years is within 0.18 mag, and thus unable to explain the discrepancy. Alternatively, significant K band excess could be due to a circumstellar disk. Using only the $B - V$ color, since it is consistent with the spectral classification, we derive a photometric distance of 89 pc using the β Pic sequence (upper limit). We derive 106 pc for a 11 Myr age. Within the uncertainties, these distances are compatible with the kinematic distance by Aarnio et al. (2008). The kinematic analysis made with the longer distance supports the association with US. The ASAS data analysis gives two likely periods, $P = 1.05$ d and $P = 20$ d, whereas the SuperWASP data analysis gives a period $P = 1.05$ d as the most significant, although periods of 20d and longer are also present. The rotation period $P = 1.05$ d is compatible with the stellar radius and $v \sin i$. The rotation period $P = 1.05$ d is "uncertain".

TYC 6786-811-1 = HD 140722C (ASAS 154611−2804.4; 1SWASP+J154610.73-280423.3) The star was first resolved into a close visual binary (0.11 arcsec separation) by Köhler et al. (2000). The companion was also detected in our NaCo observations. This star is classified as a US-B (which corresponds to UCL) member (Köhler et al. 2000; Kraus & Hillenbrand 2007). No significant period is found either in ASAS or in SuperWASP photometric data. The tight triple system *HIP 77235 = HD 140722 = HR 5856* at 50 arcsec has similar proper motion and radial velocity. The discrepancy, slightly exceeding the quoted errors, may be due to the multiplicity of both the wide components. HIP 77235 is a close triple. AB components have a separation of 0.58 arscec with A further resolved into a closer pair with 0.20 arcsec projected separation. The integrated spectral type of the triple is F2IV. The trigonometric distance of HIP 77235 is 71.1 ± 5.5 pc, compatible with the photometric distance of TYC 6786-811-1 (which is 78.6 pc including the correction for binarity), and further supporting the physical association. However, the literature contains no indications of youth for the tight triple, and it was not detected in X ray by ROSAT. This may be due to the early spectral type of the components, which should all be F stars based on the magnitude differences with respect to the primary. In the end, we consider this target to be inconclusive. Age indicators (Li and X-ray emission) for HD 140722C support a young age (nominal ages of 60 Myr for Li and 120 Myr for X-ray), but not as young as the UCL age (16 Myr). The derived distance also seems to argue against a membership with the UCL group. Using the Hipparcos distance of the wide companion, the UVW velocities of the star is not consistent with any group, within 2.0 sigma. Thus, our kinematic and age analysis make UCL membership unlikely. The star might be an outlier in the kinematic distribution of most nearby young stars. However, an unresolved binarity could make the adopted RV measurements uncertain.

HIP 78747 = HD 143928 = HR 5975 (ASAS 160437−3751.8) Mid F star, originally classified by Gray et al. (2006) as young because of the high $\log R_{\rm HK}$. But much lower activity levels are reported in Schröder et al. (2009) and also measured in our FEROS spectrum. The star was also not detected by ROSAT. The isochrone age is 2.357 ± 0.627 Gyr, taking the subsolar metallicity by Casagrande et al. (2011) into account. No period is found either in ASAS or Hipparcos data. The target is likely an old star, but with young star kinematics. The companion listed in WDS and CCDM *(CD-37 10680B*, $V = 13.0$ at about 40 arcsec) is not physically associated.

TYC 6209-0769-1 = BD-19 4341 (ASAS 161414−1939.6) Moderately young star with an age similar to the Pleiades. We find two periods of comparable powers, $P = 2.14$ d and $P = 1.86$ d, using both a Lomb-Scargle and Clean analysis of the ASAS timeseries. The rotation period $P = 2.14$ d is "likely". The target's kinematics are consistent with the young, nearby population.

HIP 79958 = HD 146464 (ASAS 161916−5530.3) This is a moderately young star with an age similar to the Pleiades. The period $P = 2.325$ d that we find with both Lomb-Scargle and Clean was also reported by Koen & Eyer (2002) from Hipparcos data and by Kiraga (2012) from ASAS data. The rotation period derived from $\log R_{\rm HK}$ is much longer than the observed one (Fig. 7). As there are no additional plausible longer period periodicities in the photometric time-series, the discrepancy is likely due to one of the following: (1) the chance observation of low-activity phases on the 3-epoch CORALIE monitoring; or (2) errors in the transformation from S Index to $\log R_{\rm HK}$, as the color of the star is slightly outside the validity range of the Noyes et al. (1984) prescriptions. At the <2.0 sigma level, the target's kinematics and age are only consistent with the nearby, young population.

HIP 80290 = HD 147491 = V972 Sco (ASAS 162323−2622.3; 1SWASP+J162322.93-262216.3) Close visual binary observed with NACO (projected separation 3.3 arcsec; $\Delta H = 1.9$ mag). A source at similar position close to the star is reported in the 2MASS catalog (*2MASS 16232272-2622168*) but with a magnitude much brighter than our measurement. Yao & Tong (1989) classified it as a δ Scu variable. This classification was revised by Handler (1995); we confirm it is a BY Dra rotational variable. We find a period $P = 1.513$ d among ASAS, SuperWASP, and Hipparcos data, which agrees with the earlier determination by Kiraga (2012). The star is projected close to the globular cluster M4. The star's kinematics match Corona-Australis at the <2.0 sigma level. The estimated age of the star is quite young and it may have membership consistent with CrA. The star is also kinematically equivalent with the nearby, young population. The star *WDS J16234-2622B = 2MASS J16232242-2622230* at a projected separation of about 10 arcsec is likely not physically associated.

HIP 80758 = HD 148440 (ASAS 162920−3057.7; 1SWASP+J162920.16-305739.8) The young age (adopted value of 20 Myr) is derived consistently from various indicators, including isochrone fitting (19 ± 14 Myr). The target's kinematics is only consistent with the young, nearby population. We find $P = 3.38$ d from ASAS data and $P = 3.55$ d from SuperWASP data. No period is derived from Hipparcos data.

TYC 6818-1336-1 = HD 153439 (ASAS 170043−2725.3) This star was classified as a possible member of the Upper Scorpius association (Aarnio et al. 2008), with a kinematic distance of 130 ± 12 pc. There is a severe discrepancy on the star's spectral type: G0IV according to SACY and F5 according to the Michigan spectral atlas. The latter is adopted by Aarnio et al. (2008). This has a significant impact on the presence of reddening and, therefore, on the distance to the star. Considering the better agreement of photometric temperatures from $B - V$ and $V - K$ and the higher spectral resolution of SACY spectra, we adopt the unreddened case. The age of the system is also quite uncertain. The star is found to be a relatively hard X-ray source (HR1 = 0.46 ± 0.20), which supports a very young age. Lithium EWs from SACY and Aarnio et al. (2008) differ

by 30 mÅ . Taking these uncertainties into account, ages from 10 to 100 Myr are possible. The most important photometric period is $P = 1.13$ d, which is found in only three seasons. The rotation period $P = 1.13$ d is "uncertain" and does not contribute meaningful age constraints. Adopting an age of 30 Myr, we derive a photometric distance of 89.5 pc. However, if the star is younger than 15 Myr, then the distance would be farther than 100 pc (105 pc using β Pic sequence). The star's kinematics are only consistent with the young, nearby population and Corona-Australis association at the <2.0 sigma level.

TYC 6815-0874-1 = CD-25 11922 (ASAS 170433−2534.3) Fast-rotating star, flagged as a possible SB2 in SACY. There are two spectra from SACY; the line profile changed between the two epochs, but the line width is similar. We thus cannot claim conclusive inference that it is an SB2. From the ASAS photometric data, we find a period $P = 1.373$ d using both Lomb-Scargle and Clean analyses. In a comparison of spectral type vs. photometric effective temperature, there are indications of some amounts of reddening ($E(B-V) \sim 0.1$ mag). Taking the β Pic sequence as reference, we derive a distance of 109 pc. The possibility that the star is an SB2 adds uncertainty to the derivation of stellar properties from photometry. The target's kinematics and age are only consistent with the young, nearby population. The star position is at the edges of the US group. The *UVW* velocities all match those of the US group but only at the <3.6 sigma level. The nominal position of the X-ray source RXS J170428.0-253520, which is classified in SACY as the X-ray counterpart of TYC 6815-0874-1, is 93 arcsec apart from that of the optical source, but with a very large position error (41 arcsec). We also noted that the integration time in the ROSAT catalog is significantly smaller than the usual ones. Furthermore, the X-ray source is hard (HR1 $= 1.00 \pm 0.32$), which is unusual for the kind of stars we are investigating. Without additional X-ray observations, we are unable to conclude on the association of the ROSAT source with our target star.

TYC 6815-0084-1 = CD-25 11942 (ASAS 170601−2520.5) is also a fast-rotating suspected SB2 in SACY (no clear signature of binarity in our spectrum). TYC 6815-0084-1 is a possible member of Upper Scorpius association according to Aarnio et al. (2008) with a kinematic distance of 127 pc. Assuming a reddening $E(B-V) = 0.08$ from the comparison of spectral type and photometric temperatures and adopting as reference the sequence of β Pic MG, we obtain a photometric distance of 79 pc, which increases to 92 pc for a 11 Myr age. The lithium EW is compatible with a very young age (10–20 Myr) and then wth US membership. The space velocities are also compatible with US, and matching improves increasing distance to 110–130 pc. The sky position is only 0.7 deg outside the formal boundaries of US adopted in Preibisch & Mamajek (2008). We find more photometric periods that persist in different seasons and that are all close or shorter than 1 day, which is expected from the high $v \sin i = 57$ km s^{-1}. However, it is difficult to say which is the correct one. One likely period is $P = 1.243$ d, but also $P = 1.03$ d and $P = 0.507$ d may be the rotation periods. A very similar period (1.246d) is also listed in Kiraga (2012). The star has similar kinematic parameters to TYC 6815-0874-1, which is also in our sample. The projected separation of the two stars is about 21 arcmin, a value that is too large for a bound system (≥100 000 AU); however considering the similar ages, a common origin for the two stars cannot be excluded. The photometric distances are roughly consistent taking the uncertainties due to reddening, age, and possible binarity of both objects into account.

TYC 7362-0724-1 = HD 156097 (ASAS 171658−3109.1) G5V star with large lithium content. Only one SACY measurement is available. We find a photometric period of $P = 1.92$ d. The star's kinematics match Corona-Australis at the <2.0 sigma level. The estimated age of the star is quite young (about 20 Myr), and it could be consistent with CrA membership. The position on the sky is slightly outside the nominal edges of US and UCL; membership in the US or UCL groups can not be excluded.

TYC 8728-2262-1 = CD-54 7336 (ASAS 172955−5415.8) Proposed by Torres et al. (2008) as a 90% probability member of β Pic. At the <2.0 sigma level, its kinematics match β Pic, TWA, Chamaleon, and Corona Australis. The target's position on the sky is inconsistent with the TWA known member distribution. Ages derived from various methods are fully compatible with β Pic MG. Thus, the analysis reinforces the β Pic membership assignment. The Malo et al. (2013) Bayesian analysis tools predict 100% probability of β Pic membership at a distance of 71.5 pc. This predicted distance for membership is consistent with the photometric distance of 70.4 pc. The Gagné et al. (2014) online tool yield only a 19% membership probability. Instead Song et al. (2012) classified the star as a US star with a photometric distance of 72 pc. Messina et al. (2010) and Kiraga (2012) report a rotation period $P = 1.819$ d. However, the secondary period $P = 0.620$ d that is also found in five out of nine seasons may be more consistent with $v \sin i = 35.3$ km s^{-1} and the stellar radius. The rotation period $P = 0.620$ d is "uncertain".

HIP 86672 = HD 160682 = V2384 Oph (ASAS 174230–2844.9) Our analysis does not reveal evidence of eclipses, although Malkov et al. (2005) listed it in their catalog of eclipsing binaries. Malkov et al. (2005) neither give an orbital period nor find the secondary minimum, which makes their classification questionable. We derive the same period $P = 3.755$ d from either Lomb-Scargle or Clean analyses. This value is similar to the $P = 3.912$ d period found by Kiraga (2012) The star's kinematics match Corona-Australis at the <2.0 sigma level. The estimated age of the star is young (30 Myr) but is marginally inconsistent with the CrA's younger proposed age.

HIP 89829 = HD 168210 (ASAS 181952−2916.5) Ultrafast-rotating star ($v \sin i$ 114 km s^{-1}) that is proposed by Torres et al. (2008) and Malo et al. (2013) as a high-probability member of β Pic MG, while membership is rejected by BANYAN II. At the <2.0 sigma level, its kinematics match β Pic. The large lithium EW and high levels of activity and photometric variability are consistent with the β Pic MG membership assignment. Isochrone fitting further supports the pre-MS status (age of 15 ± 3 Myr). The star resides in a field that is very crowded with fainter stars. We derive the same period $P = 0.571$ d from either Lomb-Scargle or Clean analyses. This period is also reported by Kiraga (2012) and in ACVS. No period is found in the HIPPARCOS data. According to Waite et al. (2011), the star is likely single, with line profile variations most likely due to star spots.

HIP 93375 (ASAS 190106−2842.8) Proposed by Torres et al. (2008) as a high-probability member of AB Dor. The target's age from various youth indicators is about 100 Myr, which agrees with the range expected for AB Dor members. Thus, the analysis reinforces the AB Dor membership assignment.

Malo et al. (2013) Bayesian analysis tools predict a 91% probability of AB Dor membership at a distance of 63.5 pc. This predicted distance for membership is consistent with the measured distance of 70.4 pc. On the other hand, the membership is formally rejected by the Gagné et al. (2014) online tool. We find no rotation period in either the ASAS data or the HIPPARCOS data. There is another star, *WDS J19011-2843B = CD-28 15269B*, at 11 arcsec projected separation. TYCHO2 and UCAC give no proper motion measurements for the possible secondary. However, the variations in projected separation, as listed in WDS (from 10.0 to 11.1 arcsec in 23 years), seem to argue against a physical association. When blinking images from different epochs, the candidate secondary also does not appear to exhibit co-movement with the primary.

HIP 94235 = HD 178085 (ASAS 191057−6016.0) New close visual binary (ΔH = 3.8 mag at 0.51 arcsec). Proposed by Torres et al. (2008) and Malo et al. (2013) as a bona fide member of AB Dor, while the Gagné et al. (2014) online tool yields a membership probability of 33%. At the <1.0 sigma level, its kinematics are only consistent with AB Dor. Age indicators are consistent with youth, reinforcing the AB Dor membership assignment. Messina et al. (2010) report a rotation period P = 2.24 d, which is subsequently confirmed by Kiraga (2012). The most important periods derived from a HIPPARCOS photometric data analysis are P = 4.28 d and P = 2.38 d. Considering the $v \sin i$ = 24 km s^{-1} and the stellar radius R = 1.085 $R_{\odot}$, we infer that the only consistent period is P = 2.24 d.

TYC 6893-1391-1 = CD-25 14224 (ASAS 193919−2539.0; 1SWASP+J193918.66-253901.3) Early K-dwarf for which age indicators yield an age slightly older than the Pleiades. Applying both Lomb-Scargle and Clean analyses to ASAS and SuperWASP data, we find a period P = 7.49 d, which confirms the period determination by Kiraga (2012). The target's kinematics are only consistent with the young, nearby population.

TYC 5736-0649-1 = BD-14 5534 (ASAS 194536−1427.9) This star has extremely high $v \sin i$ for a G6V star (206 km s^{-1}). The only period consistent with $v \sin i$ and the stellar radius is P = 0.2516 d. Kiraga (2012) reports a double period P = 0.5077 d, which is too long for the measured $v \sin i$. The star is found to be a relatively hard X-ray source (HR1 = 0.61 ± 0.25). The target's kinematics and age are only consistent with the Corona Australis association. The star was flagged in SACY as a possible SB, having an RV rms of 3.5 km s^{-1}. However, the very large $v \sin i$ makes the RV error large. H and K flux is typically underestimated with such a large $v \sin i$. In our FEROS spectrum, an extra absorption is seen in the core of the Na D doublet. As it has a RV similar to that of the star and is characterized by a single-component very narrow line profile, we favor a circumstellar origin.

HD 189285 = BD-04 4987 = TYC 5155-1500-1 (ASAS 195924−0432.1) Proposed as a 90% probability member of AB Dor by Torres et al. (2008). At the <2.0 sigma level, its kinematics match only AB Dor. The target's age is also consistent with expectations for the AB Dor group, although it does appear slightly older. The analysis is therefore consistent with the AB Dor membership assignment. It should be noted that the Malo et al. (2013) and Gagné et al. (2014) Bayesian analysis tools, using our adopted parameters as inputs, predict only a 6% and <1%, respectively, probability of AB Dor membership at a distance of 83.5 pc. Given the age of the star that results from age indicators, the AB Dor membership assignment is still possible. Messina et al. (2010) report a rotation period P = 4.85 d.

HIP 98470 = HD 189245 = HR 7631 Fast-rotating F star, proposed by Nakajima & Morino (2012) as a member of the AB Dor moving group. Its kinematics do match any of the considered groups at the <2.0 sigma level. A low membership probability to AB Dor (3.9%) is obtained using the Malo et al. (2013) Bayesian analysis tools. The target's age from lithium, X-ray and Ca H and K appears quite young, comparable to the loci of AB Dor MG and Pleiades. However, considering these methods' limited age sensitivity for F-type stars, an age as old as 200–300 Myr is also possible. Baade & Kjeldsen (1997) flagged the star as SB but without further details. In contrast, Lagrange et al. (2009) found an RV dispersion of only 86 m/s, for 18 epochs over 259 days. The other sparse RV measurements on longer time baselines are consistent with a constant RV within errors. The CCF from our FEROS spectrum does not show signatures of additional components. No period is found in either ASAS or SuperWASP photometric data. A tentative period P = 1.88 d is inferred from the HIPPARCOS photometric data.

TYC 5164-0567-1 = BD-03 4778 (ASAS 200449−0239.2) Proposed by Torres et al. (2008) as a 100% probability member of AB Dor. At the <1.0 sigma level, its kinematics match only AB Dor. The ages derived from various methods are also broadly consistent with the AB Dor group, but Li EW is larger than that of other members of similar color. Malo et al. (2013) Bayesian analysis tools predict a 98.5% probability of AB Dor membership at a distance of 66.0 pc. This predicted distance for membership is consistent with the photometric distance of 63.3 pc. On the other hand, the Gagné et al. (2014) online tool yields a very low membership probability. Messina et al. (2010) report a rotation period P = 4.68 d, which was later confirmed by Kiraga (2012).

HIP 99273 = HD 191089 (ASAS 200905−2613.4; 1SWASP+J200905.21-261326.5) Proposed by Moór et al. (2006), Torres et al. (2008), and Malo et al. (2013) as a bona-fide member of β Pic. At the <1.0 sigma level, its kinematics match only β Pic. The membership is also supported by Gagné et al. (2014) online tool. The age indicators are somewhat ambiguous, as expected for an F-type star. The Lithium EW measured on our FEROS spectrum is compatible with a β Pic age, but also with significantly older ages; chromospheric and coronal emission are rather low. No period is found in ASAS or SuperWASP data. A tentative period P = 0.488 d is derived from the HIPPARCOS data analysis, but this period is absent in the other datasets. We adopt β Pic membership and age, but allow for a maximum age of 200 Myr. Rhee et al. (2007) identify the star as SB, but without further details. The literature RVs show a modest scatter, which seems compatible with measurement errors, considering the early spectral type and the rotational velocity of the star. The star hosts a debris disk, with $T_{\rm dust}$ = 95 K, $R_{\rm dust}$ = 15 AU and $M_{\rm dust} = 3.4 \times 10^{-2}\ M_{\oplus}$ (Rhee et al. 2007). The disk was recently spatially resolved by Churcher et al. (2011).

HD 199058 (ASAS 205421+0902.4) New close visual binary (ΔH = 2.5 mag at 0.47 arcsec) identified by NaCo-LP observations. It also has a probable wide (245 arcsec projected separation) companion *TYC-1090-0543-1*, having very similar kinematic parameters and indicators supporting a young age. If a physical association is real, the projected separation is about 16000 AU. Both stars are included in the list of

AB Dor members by Torres et al. (2008). At the <2.0 sigma level, the kinematics of HD 199058 match also Tuc/Hor, Carina, and ϵ Cha. However, membership to Tuc/Hor or Carina is unlikely because of the star's northern declination. The star's sky position is inconsistent with ϵ Cha membership. The age indicators of both components are consistent with AB Dor membership. There is a discrepancy in the photometric distances of the two stars (55.0 pc for HD 199058, including binary correction, and 77.2 pc for TYC-1090-0543-1). It should be noted that Malo et al. (2013) Bayesian analysis tools predict only a 6% probability of AB Dor membership at a distance of 55.0 pc. This probability changes to >98% at 74 pc, a distance nearly identical to the photometric distance of TYC-1090-0543-1. On the other hand, Gagné et al. (2014) online tool yields a very low membership probability. We adopt the mean of the photometric distances of the two objects. Applying both Lomb-Scargle and Clean analyses in two seasons, we find an uncertain period $P = 3.47$ d for HD 199058.

TYC 5206-0915-1 = BD-07 5533 (ASAS 211834−0631.7) In ACVS, the star is listed with a period $P = 3.4447$ d and classified as a detached/semi-detached eclipsing binary. However, from our analysis of the photometric time-series we did not found convincing evidences for eclipses using this proposed period or their harmonics. Kiraga (2012) reports a period $P = 2.37$ d, which our analysis retrieves in all the seasons. From CCF in our FEROS spectrum, there are no indications of additional components. The large RV scatter (about 40 km s^{-1} peak-to-valley) from our FEROS and CORALIE spectra and SACY makes the star a short period spectroscopic binary (SB1). The fast rotational period and large activity levels may be due to youth or due to a tidally locked binary. Lithium EW is consistent with a star of age intermediate between Pleiades and Hyades, but the possibility that this is an RS CVn variable with detectable lithium cannot be ruled out. The target has very large uncertainties in *UVW* velocities because of a large spread in measured RVs. Until a systemic velocity can be established and used to calculate *UVW*, determining group membership is not possible. Overall, age determination remains highly uncertain until the orbital period of the binary can be established.

HIP 105384 = HD 203019 (ASAS 212047−3846.9; 1SWASP+J212046.59-384653.2) The lack of lithium in the spectrum of this star (from SACY) indicates an age older than the Hyades. Coronal and chromospheric activity (the latter based on several independent sources) instead suggest a younger age (about 250 Myr). RV monitoring indicates a single star and the CCF does not show additional components. Therefore, we are not considering a tidally locked binary. No rotation period is detected in our analysis, but the star exhibits non-periodic photometric variability. The kinematics do not match any of the groups and associations investigated at the <2.0 sigma level. The kinematics are also not consistent with the nearby, young population. An age of about 500 Myr might be roughly compatible with the various indicators, considering the observed scatter at fixed age.

HIP 105612 = HD 202732 (ASAS 212327−7529.6) Lithium and chromospheric activity indicate an age similar to the Hyades. X-ray emission suggests a slightly younger age. We find an uncertain period $P = 12.9$ d in the complete series and in two seasons. The resulting gyrochronology age from this period would be about 1100 Myr, older than the other indicators. The kinematics do not match any of the groups and associations investigated at the <2.0 sigma level and are also not consistent with the nearby, young population. The CCF does not show additional components and RV suggests a single star. Taking all these indications into account, we adopt an age of 700 Myr.

HIP 107684 = HD 207278 (ASAS 214849−3929.1) New close visual binary ($\Delta H = 2.8$ mag at 0.33 arcsec). Proposed by Torres et al. (2008) as a 100% probability member of the AB Dor moving group. At the <2.0 sigma level, its kinematics match only AB Dor. Its estimated age is also consistent with AB Dor membership. Malo et al. (2013) Bayesian analysis tools predict a 92% probability of AB Dor membership at a distance of 81.0 pc. This predicted distance for membership is consistent with the measured distance of 90.2 pc. On the other hand, the Gagné et al. (2014) online tool yields a very low membership probability. Messina et al. (2010, 2011) report a rotation period $P = 4.14$ d.

HIP 108422 = HD 208233 (ASAS 215751−6812.8) Close visual binary discovered by Chauvin et al. (2003); the physical association of the components was confirmed with our NaCo observations (Chauvin et al. 2015). The star was included as a member of the Tuc association by Zuckerman & Song (2004) but rejected by Torres et al. (2008). Malo et al. (2013) also propose this star as a bona fide member of Tuc/Hor and the analysis based on Gagné et al. (2014) confirms membership. The star is characterized by a very fast rotation, identified both spectroscopically and photometrically. We find the period $P = 0.4352$ d, which is also reported by Koen & Eyer (2002) from HIPPARCOS data analysis and by Kiraga (2012) from ASAS data analysis. In our analysis, the kinematics match only Tuc/Hor but at the >2.0 sigma level. However, the kinematics might somewhat altered by binarity. The estimated age from lithium is consistent with the ∼30 Myr age of Tuc/Hor. The star's isochrone age of 13 ± 3 Myr is formally even younger than the nominal Tuc/Hor group age. Taking all of these facts into consideration, we adopt a Tuc-Hor membership but acknowledge the possibility of an even younger age as suggested by the CMD position.

TYC 8004-0083-1 = CD-40 14901 (ASAS 224633−3928.8; 1SWASP+J224633.48-392845.2) All the age indicators point to a rather young star (best estimate of 90 Myr). However, the kinematics do not match any of the groups and associations investigated at the <2.0 sigma level. The kinematics are also not consistent with the nearby, young population. We find the period $P = 3.22$ d in all the ASAS and SuperWASP seasons. This period is also reported by Kiraga (2012).

HIP 114046 = HD 217987 = GJ 887 (ASAS 230552−3551.2) is the only M dwarf in our sample. It was included because of the tentative lithium detection in the SACY database ($EW = 50$ mÅ), which originally comes from de La Reza et al. (1981). However, our higher quality FEROS spectrum shows no lithium. The star is above the main sequence in the M_V vs. $B - V$ color-mag diagram, which would imply a pre-MS star, but the 2MASS magnitudes are most compatible with a main sequence star. Delorme et al. (2012) estimated an isochrone age of 100 Myr–10 Gyr from *VJHK* photometry. The stellar radius, as derived by Demory et al. (2009) using VLTI, is not anomalous in their mass-radius and luminosity-radius relationships. The star has rather low coronal and chromospheric activity. No rotation period is found in either ASAS (sparse data) or HIPPARCOS data. Using the kinematic population diagnostic by Bensby et al. (2003), we conclude a probable membership of the thick disk. We therefore adopt

a very old age for the star, 8 Gyr. We adopt the stellar mass and metallicity from Neves et al. (2013).

TYC 9338-2016-1= HD 220054 (ASAS 232153−6942.2) All age indicators are consistent with a young age (10–50 Myr). We find the period P = 1.875 d in ASAS and SuperWASP data. The same period was reported in ACVS by Bernhard et al. (2009), and by Kiraga (2012). RV measurements show some scatter (0.8 km s^{-1} rms in SACY); we consider it as a suspected SB. The star's kinematics match Tuc-Hor and TWA at the <2.0 sigma level. The star's estimated age is also quite young. Malo et al. (2013) Bayesian analysis tools predict a very low probability of being a true member of one of those groups at the photometric distance of 99.6 pc. The kinematics are consistent with the nearby, young population.

TYC 9529-0340-1 = CD-86 147 (ASAS 232749−8613.3) Proposed by Torres et al. (2008) as an 85% probability member of Tuc/Hor. At the <1.0 sigma level, its kinematics match only Tuc/Hor. The ages derived from various methods are also consistent with the Tuc/Hor association. The Malo et al. (2013) Bayesian analysis tools predict 100% probability of Tuc/Hor membership at a distance of 64.0 pc. This predicted distance for membership is consistent with the photometric distance of 68.8 pc. The Gagné et al. (2014) online tool yields a 74% membership probability. Messina et al. (2010) report a rotation period P = 2.31 d, which they note to be inconsistent with $v \sin i$ = 73.9 km s^{-1}. A new analysis, also made with the Clean method, reveals a period P = 0.7025 d, which confirms the rotation period P = 0.6975 d found by Kiraga (2012) and P = 0.7024 d found in ACVS.

TYC 9339-2158-1 = CD-69 2101 (ASAS 233101−6905.2) The star shares common proper motion, position, and radial velocity with *HIP 116063 = HD 221231*. Parallax of the companion is adopted for the system. No rotation period is found (likely due to the blending of the components). The age of the components from several diagnostics is estimated to be 300 Myr.

TYC 6406-0180-1 = HD 221545 Lithium EW and X-ray luminosity of this K0 star indicate an age of about 200 Myr. Kinematics derived assuming an MS status are consistent with a moderately young star. Non-typical of a star of this type, a period P = 36.271 d is reported by ACVS and confirmed by Kiraga (2012), who reports P = 36.34 d. Our analysis of ASAS data reveals two major power peaks in the seasonal periodograms, one at P = 36 d and another at P = 1.026 d. The first agrees with the mentioned literature values, whereas the latter, with a K-type MS stellar radius and the small $v \sin i$ value, would imply a very inclined (almost pole-on) star. In the latter case, we would not expect any light rotational modulation, whereas we find a light curve amplitude up to ΔV = 0.07 mag. We therefore consider the period P = 36 d as "confirmed". Such a rotation period being consistent with the measured $v \sin i$ = 5.5 km s^{-1} requires a stellar radius $R > 3\,R_\odot$. Large radii like this are found among subgiant K stars but not in the current V class assignation. The long rotation period is also unusual among active main-sequence stars, but typical of evolved stars. There is only one RV measurement in the literature. Therefore, limited inferences on binarity can be made. We adopt the main sequence age but allow for an age of 4 Gyr, which is obtained for an evolved star matching the stellar radius that is most consistent with the rotation period and $v \sin i$.

HIP 116910 = HD 222575 (ASAS 234154−3558.7) Proposed by Torres et al. (2008) and Malo et al. (2013) as a high-probability member of AB Dor. The Gagné et al. (2014) online tool yields a membership probability of 36%. At the <1.0 sigma level, the kinematics match only AB Dor. The ages derived from various methods are slightly younger than the proposed age of the AB Dor group; however since the kinematics only match this group and the star is surely young, the analysis reinforces the AB Dor membership assignment. Messina et al. (2011) report a rotation period P = 1.787 d, which was subsequently confirmed by Kiraga (2012).

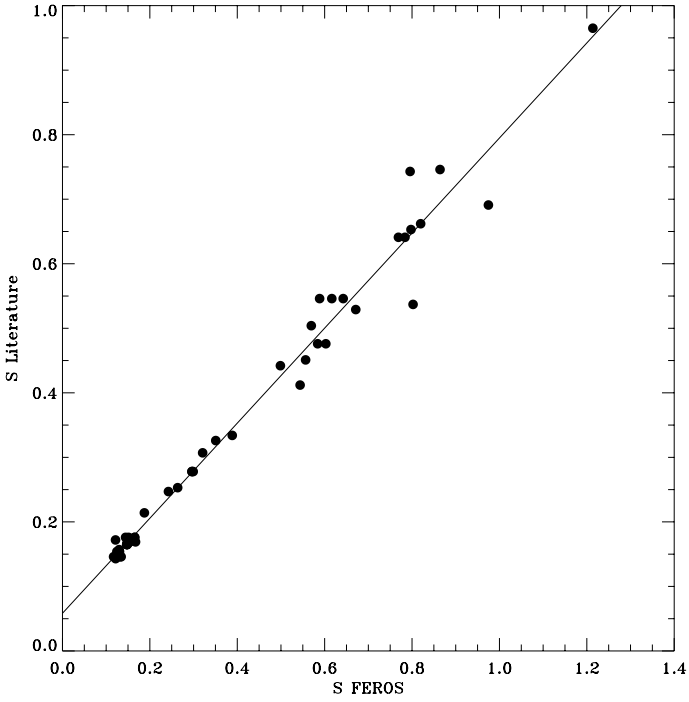

Fig. C.1. Calibration of the instrumental S index measured on FEROS spectra onto the standard Mt. Wilson scale.

Appendix C: *S* index calibration for FEROS

The instrumental S index was measured on FEROS spectra by integrating the flux over rectangular bandpasses that are 1 Å wide, as in Desidera et al. (2006). For a calibration onto the standard Mount Wilson scale, we used 73 spectra of 42 stars from the lists of Baliunas et al. (1995) and Wright et al. (2004). The relevant calibration stars were observed in the same nights as were our program stars and reduced in the same way. We determined that the inclusion of additional calibration stars from other sources, which are typically characterized by single-epoch measurements (e.g., Henry et al. 1996), increases the scatter of the calibration. A linear fit between FEROS instrumental S index and the literature calibrated S index was found to be fully adequate (Fig. C.1). The rms of residuals from the calibration is about 5%. To better understand the measurement errors, we plotted the absolute value of the difference between our calibrated S index and the literature ones in Fig. C.2. The stars with larger differences are those that are more active and have a small number of measurements in the calibration papers. This indicates that the intrinsic variability of chromospheric activity has a significant impact on our calibration. For the low-activity, low-variability star τ Ceti, the observed rms of the S index for 15 spectra is 0.0034 (2%). It should be further noted that the measured S index is underestimated for stars with

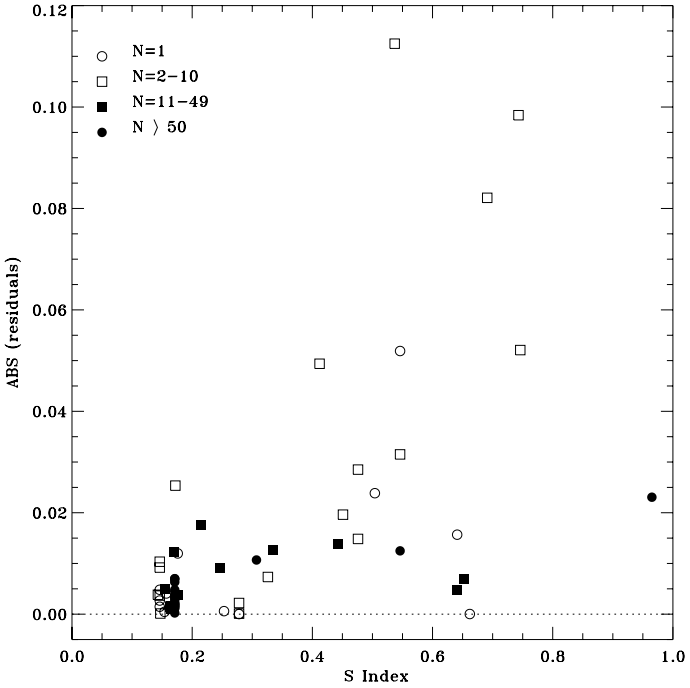

Fig. C.2. Absolute value of the difference between calibrated FEROS S index and literature values as a function of literature S index. Different symbols refer to stars with a different number of measurements available in the literature. The stars with the largest offsets all have small numbers of measurements in the literature, supporting the intrinsic variability of chromospheric emission as the main source of the observed scatter in the calibration.

$v \sin i > 40$ km s^{-1}, as part of the H and K emission lies outside the defined integration windows (Desidera et al. 2006). The calibrated S index was transformed into the chromospheric flux $\log R_{\rm HK}$ by following the prescriptions by Noyes et al. (1984).

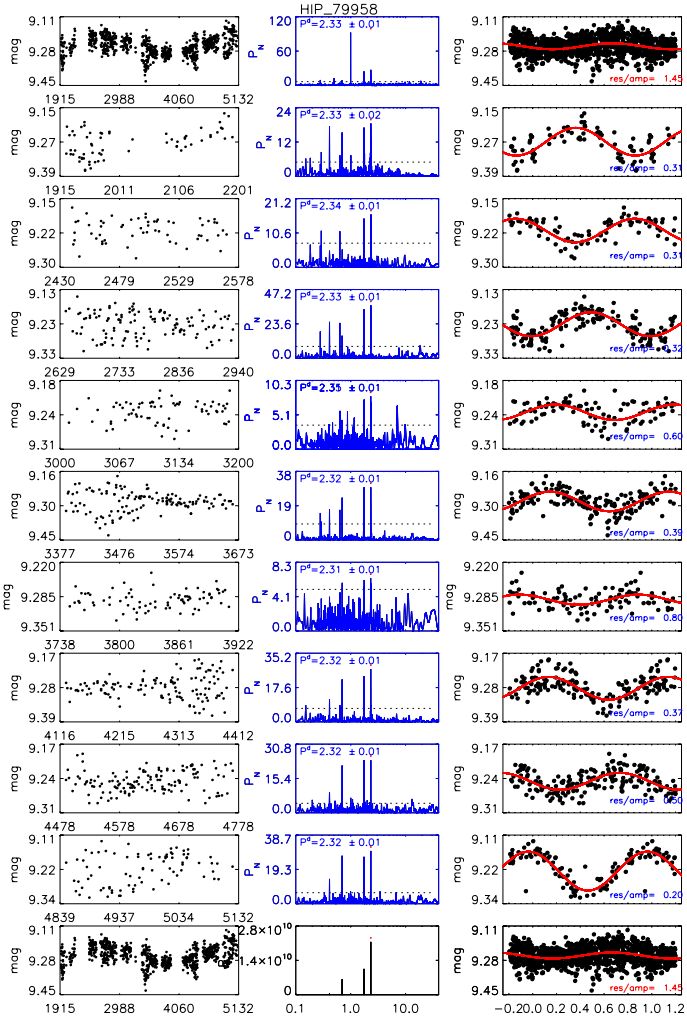

Fig. D.1. Example of photometric analysis for the target HIP 79958.

Appendix D: Details on rotation analysis

We present here some additional details on the result of our search for rotation periods. For the targets with newly determined rotation periods, or confirmed literature values, we list in Table D.1 the following: (1) the time interval spanned by each segment; (2) the number of V magnitude measurements; (3) the brightest V magnitude; (4) the light curve amplitude, which is measured as the amplitude of the sinusoid fit to the phased light curve; (5) the photometric accuracy; (6) the ratio of the average residuals from the fit on the light curve amplitude; (7) the rotation period; (8) the rotation uncertainty; (9) the normalized power of the periodogram peak, corresponding to the rotation period, and the power level corresponding to a 1% false alarm probability; and (10) the sequential number of the timeseries segment. The number 1 indicates the complete unsegmented timeseries.

Figure D.1 shows, as an example, the results of our period search for HIP 79958. In the left column, we plot the V magnitude time series (complete in the top left panel, and segmented in the other lower panels). In the middle column, we plot the Lomb-Scargle periodograms with an indication of the power level corresponding to the 1% FAP, and the peak corresponding to the rotation period. In the right column, we plot the phased light curve with the rotation period. The initial epoch is the same for all the light curves, whereas the rotation period is the one found in the corresponding season. In the seasons where no period is detected, we used the rotation period found from the whole time series analysis. In the bottom panels, we have multiplied all the periodograms and extracted the most significant periodicities. This represents a different approach to reveal peaks that are low power but persistent in each season. For all the targets that we newly determined, or confirmed, the rotation period, similar plots are available as online material.